



Hypersonic Aircraft Design

Student Authors: H. Alkamhawi, T. Greiner, G. Fuerst, S. Luich, B. Stonebraker, and T. Wray

Supervisor: Dr. G. M. Gregorek

Assistant: R. L. Reuss

Department of Aeronautical & Astronautical Engineering

Universities Space Research Association
Houston, Texas 77058

Subcontract Dated November 17, 1989
Final Report

May 1990

(NASA-CR-187008) HYPERSONIC AIRCRAFT DESIGN
Final Report (Ohio State Univ.) 174 p

CSCL 01C

N91-12661

528330

Unclas

63/05 0302472

123P

NASA-SUPPORT
11/05-CR
302472
P-174



Hypersonic Aircraft Design

Student Authors: H. Alkamhawi, T. Greiner, G. Fuerst, S. Luich,
B. Stonebraker, and T. Wray

Supervisor: Dr. G. M. Gregorek

Assistant: R. L. Reuss

Department of Aeronautical & Astronautical Engineering

Universities Space Research Association
Houston, Texas 77058

Subcontract Dated November 17, 1989
Final Report
RF Project 767919/722941

May 1990

Hypersonic Aircraft Design

AAE-416H

Professor Dr. Gerald M. Gregorek

Teaching Assistant: Robyn Reuss

Gold Team

Hani Alkarnhaw

Gerry Fuerst

Tom Greiner

Shawn Luich

Bob Stonebraker

Todd Wray

Abstract

This report outlines the preliminary design and characteristics of a hypersonic aircraft for a flight at Mach 10 using only scramjets for two minutes at 100,000 feet. There are many design problems that have to be addressed for such a highspeed flight. These include aerodynamic, thermal, logistical and structural problems.

This report contains ideas to deal with these problems that have been examined by our research team, the gold team. Aerodynamic calculations, logistical solutions are presented along with thermal and structural designs. Many ideas for hypersonic aircraft are based on theory and have limited experimental foundation.

The main objective of this project was to use our ideas and the theories of others to create an aircraft that will fly according to the mission requirements

TABLE OF CONTENTS

Abstract.....	i
Table of Contents.....	ii
List of Tables.....	iii
List of Figures.....	iv
Nomenclature.....	v
Introduction.....	vi
General Aircraft Design.....	1
Aircraft Design II.....	6
Weight Analysis.....	8
Rocket Boosters.....	10
Center of Gravity Location.....	12
Flight Profile I.....	14
Fuel Flight path (Energy state method).....	17
Inlet Design.....	22
Aerodynamics.....	27
Basic Stability Analysis.....	34
Landing Gear.....	36
Materials and Cooling Systems.....	39
Fuel Tank Insulation Thicknesses.....	45
Cost Analysis.....	49
Wind Tunnel Model.....	51
Conclusion.....	52
References.....	53
Tables.....	55
Figures.....	67
Appendix A.....	111
Appendix B.....	116
Appendix C.....	125
Appendix D.....	144
Appendix E.....	146

LIST OF TABLES

IN1	FLIGHT PATH.....	55
IN2	INLET AREA VERSUS MACH NUMBER AND ALTITUDE.....	56
IN3	RAMP LENGTHS VERSUS MACH NUMBER.....	57
IN4	THETA, BETA, EFFICIENCY FOR MACH NUMBER 1.4.....	58
IN5	THETA, BETA, EFFICIENCY FOR MACH NUMBER 2.0.....	58
IN6	THETA, BETA, EFFICIENCY FOR MACH NUMBER 3.0.....	58
IN7	THETA, BETA, EFFICIENCY FOR MACH NUMBER 4.0.....	59
IN8	THETA, BETA, EFFICIENCY FOR MACH NUMBER 5.0.....	59
IN9	THETA, BETA, EFFICIENCY FOR MACH NUMBER 6.0.....	59
AD1	COMPONENTS OF THE DRAG COEFFICIENT FOR THE WING AT DIFFERENT MACH NUMBERS.....	60
AD2	COMPONENTS OF THE DRAG COEFFICIENT FOR THE BODY AT DIFFERENT MACH NUMBERS.....	61
AD3	C_{D0} FOR THE DIFFERENT MACH NUMBERS.....	62
AD4	C_L FOR THE DIFFERENT MACH NUMBERS.....	63
AD5	C_L / RAD , C_L / RAD , AND K FOR THE DIFFERENT MACH NUMBERS.....	64
AD6	C_L , C_D , AND C_L / C_D FOR THE MISSION PROFILE.....	65
AD7	$C_{L_{\alpha}}$ VS. MACH NUMBER	66
AD8	K VS. MACH NUMBER	67
S1	C_{mcg} VS. ALPHA, C_L , C_D (M=0.8)	67
S2	C_{mcg} VS. ALPHA, C_L , C_D (M=2.0)	67
S3	C_{mcg} VS. ALPHA, C_L , C_D (M=10.0)	67

ORIGINAL PAGE IS
OF POOR QUALITY

000

LIST OF FIGURES

D1	AIRCRAFT DESIGN #1	67
D2	AIRCRAFT DESIGN #2.....	68
D3	AIRCRAFT DESIGN #3.....	69
D4	SCRAMJET DESIGN.....	70
D11 1	FINAL DESIGN	71
D11 2	CUTAWAY SHOWING NOZZLES	72
W61	WATTS WEIGHT STATEMENT	73
W62	GOLD WEIGHT ESTIMATE.....	75
RB1	AIRPLANE CONFIGURATION WITH ROCKET BOOSTERS.....	76
RB2	ROCKET BOOSTER FUEL ESTIMATE	77
FP1	FLIGHT PROFILE CALCULATIONS USING NEWTONS SECOND LAW	79
FP2	MAP OF FLIGHT PROFILE	79
ES1	NET THRUST VS. MACH NUMBER FOR TFRJ.	83
ES2	NET THRUST VS. MACH NUMBER FOR SCRAMJET.....	84
ES3	SFC VS. MACH NUMBER FOR SCRAMJET	85
ES4	ALTITUDE VS. MACH NUMBER	86
ES5	THRUST/DRAG VS. MACH NUMBER FOR FLIGHT PROFILE	87
IN1	INLET INSTALLED ON PLANE	88
IN2	INLET OPEN AND CLOSED POSITIONS.....	89
IN3	WEDGE PROFILE AT MACH=1.4,2,3.....	90
IN4	WEDGE PROFILE AT MACH=4,5,6.....	91
INS	INLET PRESSURE RECOVERY VERSUS MILITARY SPEEDS	92
AD1	C_D VS. ALPHA FOR DIFFERENT MACH NUMBERS	93
AD2	C_L VS. C_D FOR DIFFERENT MACH NUMBERS.....	94
AD3	C_{D0} VS. MACH #.....	95
AD4	C_D VS. MACH # FOR MISSION PROFILE.....	96
AD5	C_L VS. MACH # FOR MISSION PROFILE.....	97
AD6	L/D VS. MACH # FOR MISSION PROFILE.....	98
AD7	C_L VS. MACH #	99
AD8	K VS. MACH #	100
S1	C_{mcg} VS. ALPHA (M=0.8)	101
S2	C_{mcg} VS. ALPHA (M=2.0)	102
S3	C_{mcg} VS. ALPHA (M=10.0)	102
MS1	TEMPERATURE DISTRIBUTION	104
MS2	WHAT NEEDS TO BE COOLED	105
MS3	DRIVE COOLING	106
MS4	50-HZ COOLING	107

MS5	PANEL COOLING	108
MS6	N ₂ PURGE SYSTEM.....	109
MS7	CC ₂ PURGE SYSTEM.....	109
COST 1	TOTAL DEVELOPMENT AND EVALUATION	110

ORIGINAL PAGE IS
OF POOR QUALITY

NOMENCLATURE

AR	Aspect Ratio	
b	Span of Airplane	ft
C_D	A/C Drag coefficient	
C_{D0}	Coefficient of Drag at Zero lift	
C_{Df}	Skin Friction Drag Coefficient	
C_f	Friction Coefficient	
C_{Dw}	Wave Drag Coefficient	
C_{Dle}	Leading Edge Bluntness term	
C_{Db}	Base Pressure Drag Coefficient	
C_{Dp}	Subsonic Pressure Drag Coefficient	
C_{Dp}	Supersonic Wave Drag Coefficient	
C_{DN2}	Nose Wave Drag Coefficient	
C_{DA}	Body After Body Wave Drag Coefficient	
$C_{DA(NC)}$	Interference Drag Coefficient	
C_L	Lift Coefficient	
$C_{L\alpha}$	Lift Curve Slope	
C_{mac}	Moment Coefficient About Aerodynamic Center	

C_{mcg}	Moment Coefficient About C.G	
C_{m_α}	Slope Of C_m vs. α Curve	/deg
C_r	Root Chord	ft
C_T	Tip Chord	ft
d	Diameter of A/C	ft
dT	Time of Impulse	sec
e	Wing Efficiency Factor	
e'	Wing Planform Efficiency Factor	
oF	Temperature	degrees
f_N	Nose Fineness Ratio	
f_A	After-body Fineness Ratio	
h	Height of Landing Gear	ft
g	Gravitational Acceleration	ft/sec ²
K'	Inviscid Drag due to Lift	
K''	Viscous Drag due to Lift	
K	Drag due to Lift	
l	Length of Airplane	ft
LH_2	Liquid Hydrogen	

N	Maximum Landing Weight	lbs
ΔN	Subsonic Suction Parameter	
$M_{a.c}$	Mean Aerodynamic Center	ft
$X_{a.c}$	Location Of Aerodynamic Center	ft
r_{le}	Leading Edge Radius	in
S_{wet}	Wetted Area of Wing	ft ²
S_e	Exposed Planform Area	ft ²
S_B	Maximum Cross Sectional Area of Body	ft ²
t/c	Thickness to Chord Ratio	
T.F.R.J	Turbo Fan Ram Jet	
UK	Kinetic Friction Coefficient	
V	Landing Velocity	ft/sec
W	Landing weight of Airplane	lbs
X_{cg}	Location of Center of Gravity	ft
α	Angle of Attack	degrees
θ	Glide Angle	degrees

Λ_{le} Leading Edge Wing Sweep degrees

Λ_{Te} Trailing Edge Wing Sweep degrees


λ Taper Ratio

Introduction

The design group project chosen this year is to design a hypersonic aircraft which uses scramjets to accelerate from Mach 6 to Mach 10 and sustain that speed for two minutes. Initially the main difficulty was deciding on a propulsion system to propel the aircraft from the launched speed of Mach .8 to Mach 6 at 100,000 feet. The different propulsion systems being considered were solid rockets, liquid rockets, ramjets, and turbofan-ramjets. The final decision was that the aircraft would use one full scale turbofan-ramjet. Later it was decided to add two solid rocket boosters to save fuel and help the aircraft pass through the transonic region.

After the propulsion system was decided each member of the group was assigned a task such as: aerodynamics, aircraft design, stability and control, cooling systems, mission profile, and landing systems. The members researched their specific area of assignment and tried to get a physical understanding of how their system interacted with complete hypersonic aircraft.

After two weeks of research the group was ready to begin to set the aircraft configuration. The two possible choices available for the configuration were a waverider or conventional design. The conventional design was chosen due to its landing characteristics and the relative expense compared to a waverider. It was apparent from the start that the amount of fuel required to complete the mission greatly effected the relative size of the aircraft. Also the integration of the engine systems and their inlets affected the aircraft configuration. Each of the following sections of the report contribute to the final design of the hypersonic aircraft and is written by an individual member.



GENERAL AIRCRAFT DESIGN

An unmanned hypersonic researched vehicle was designed to test a SCRAMJET. This vehicle had to meet the following performance specifications:

- 1) The aircraft had to be carried to 40,000 ft. and launched from a carrier aircraft at $M=8$.
- 2) The aircraft will be capable of accelerating to $M=6$ and climbing to 100,000 ft. using its internal engines.
- 3) The aircraft will carry a prototype SCRAMJET engine that will be employed to accelerate the aircraft from $M=6$ to $M=10$ and is to maintain $M=10$ for 2 minutes of study level flight.
- 4) The aircraft will then decelerate and land back at its base, NASA Dryden Flight Test Center, CA.

The aircraft design process started by choosing the propulsion system to meet performance specification 2. Solid rockets were considered because of their simplicity, high thrust, and the fact that they can be dropped to reduced drag, but they were found to weigh too much of the total vehicle weight. Liquid rockets were considered because of their high thrust but the fuel and oxidizer would require too much volume. Ramjets were considered because of their simplicity and light weight but were found to be lacking performance in the subsonic and high drag transonic region. Finally, a General Electric hydrogen fueled augmented turbofanramjet was chosen.

The turbofanramjet was selected over the others for several reasons. It produces good thrust and efficiency within the Mach range of .8 to 6. It has an acceptable weight. It burns hydrogen, the same fuel as the scramjet. And in addition, the aircraft could have a powered landing.

The turbofanramjet was selected full scale; 22.1 ft. long, 6.92 ft. in dia., and 6100 lbs. in weight. The reason for selecting it full scale was to assure enough thrust around $M=1$ since this region would have the highest drag and the least thrust available.

Since the aircraft would burn liquid hydrogen, which has a very low density of 4.43 lb/ft^3 , most of the aircraft volume would be taken up by liquid hydrogen. Thus, in order to get a preliminary sizing of the aircraft, a rough estimate of total fuel consumption was needed. This was done by approximating the average vehicle weight at 45,000 lbs. Next an average lift to drag ratio of 2.5 was assumed. From this an average drag of 18,000 lbs was calculated. Next a preliminary altitude versus Mach number flight path was selected for the turbofanramjet using the General Electric data. From this an average thrust of 60,000 lbs., an average fuel flow rate of 60,000 lbs./hr., and a SFC of 1.0 was approximated. This resulted in an average accelerating force of 42,000 lbs. This then allowed the calculation of a flight time of 3 minutes from $M=.8$ at 40,000 ft. to $M=6$ at 100,000 ft., which meant 3000 lbs. of liquid hydrogen would be burned by the turbofanramjet. From $M=6$ to $M=10$ the SCRAMJETS would be turned on. An SFC of 2.0 and a thrust of 35,000 lbs. was assumed for the SCRAMJETS. The SCRAMJETS would then operate at $M=10$ for 2 minutes. From this the estimated SCRAMJET on time was calculated to be 7.48 minutes in which time they burned 7593 lbs. of liquid hydrogen. Thus the estimated total amount of hydrogen burned was 10593 lbs. This meant a fuel tank with

2391 ft³ was needed.

A conventional configuration was next selected because the aircraft was hypersonic research vehicle for a SCRAMJET which would only fly for short amounts of time covering a Mach range from 0 to 10 and would not be at any one Mach number for a long period of time. A conventional design would also keep the plane simple and within current technology.

A simple conventional design and the fact of wanting a slender low drag aircraft led to using one fuel tank placed in front of the turbofanramjet. Since some lift was wanted out of the fuel tank it was made slightly wider than it is high and is curved longer on the bottom. As a result the fuel tank was made 8 ft. wide , 6.5 ft. high , and 60 ft. long. This resulted in the fuel tank having 2450 ft.³ which met the fuel requirement. The plane, however, resulted in being 90 ft. long and resembled a missile with a SCRAMJET strap to the bottom (figure D1.).

After intial exact calculations were done on the plane in figure D1. it was found necessary to decrease the wing loading by one-half and add lifting surfaces to the front part of the aircraft in order to keep the nose up. This was done by increasing the wing span 10 ft. and strecthing the wing 40 ft. up the side of the fuselage (figure D2.). The wings extending up the side of the fuselage were blended into the body like that of an SR-71. This also allowed for more fuel storage. The exact SCRAMJET data from General Electric also caused a reconfiguration of the SCRAMJETS' location. Since the SCRAMJETS produced small net thrust of on the average of 6500 lbs at 100,000 ft. from M=6 to M=10. It was decided to use two of them. And since they required large exit areas of on the average of 35 ft² they were placed on either side of the fuselage and under the wing so as to get some inlet compression from under the wing. The exit nozzles expanded under and

over the wing and then expanded into the turbofanramjet nozzle to satisfy the necessary exit area requirements. The turbofanramjet nozzle was now made two dimensional and resembles a 6x7x10 rectangle. This was done in order to expand the SCRAMJET nozzles into the turbofanramjet nozzle. The full expanded SCRAMJET nozzle areas are shown in blue on figure D2. This expansion into the turbofanramjet nozzle also eliminated the base drag from the turbofanramjet nozzle when it was off. The base drag from the SCRAMJETS was eliminated by folding the nozzles into the side of the fuselage when not in use and expanding them outward when in use (figure D2.). The inlet to the turbofanramjet was placed on the bottom of the fuselage in order to assure a good compression surface for the inlet. The inlet to the turbofanramjet as well as the inlet to the SCRAMJETS will be closed off when not in use in order to reduce drag.

After more exact calculations on the design in figure D2, the design in figure D3 was arrived at. It was found necessary to add two more SCRAMJETS in order to achieve an acceleration quick enough to keep the flight time and distance reasonable, i.e., under 30 minutes and under 2000 miles. The two SCRAMJETS were added by just making the existing SCRAMJETS twice as wide (figure D3.). The SCRAMJETS expansion nozzle area is shown in blue on figure D3. A detailed view of a SCRAMJET itself in both the on and off stages is given in figure D4. The aircraft wings were also smoothed out to reduce drag (figure D3). The landing gear was also repositioned in order to reduce flexure stress on the ground. The front nose wheel is kept cool by the fuel tank. The avionics is positioned in the front of the plane.

This design (figure D3) resulted in aircraft 90 ft. long, 15 ft. high, fuselage width of 8 ft. and height of 6.5 ft. It has a wing that has a span of

40 ft., thickness to chord ratio of .05, an area of 850 ft.², aspect ratio of 1.88, and a wingloading of 42.68 lb/ft² empty and 56.20 lb/ft² full. The aircraft has a gross weight of 47,774 lbs. and a empty weight of 36,274 lbs.

The aircraft in figure D3, however, was larger than the French's carrier plane's limit by 5 feet, that is, their maximum plane length limit was 85 feet. This meant that this design had to be reduced by 5 feet. This could have been brought about in 2 ways.

The first way was to scale down the entire aircraft as it is now. At first a 50% scale down was studied. This evaluation discovered some important characteristics about drag, lift, weight, and volume in scaling down the aircraft. Since when the plane is scaled down the surface area and cross sectional area go down by the square. This reduces the drag by the square. The inlet and nozzle areas are reduced by the square. This reduces the mass flow rate by the square and thus the thrust is reduced by the square. Since the drag and thrust are both going down by the square it seems relatively simply to scale down the aircraft. The catch is that the volume is going down by the cube. This means the fuel volume is being reduced to a greater degree than the drag and thrust. This means that aircraft will run out of fuel before completing its mission. The good part about the volume going down by the cube, however, is that the structural weight also goes down by the cube.

The second way was to simply remove 5 feet of length from the aircraft's fuselage and readjust the plane accordingly.

AIRCRAFT DESIGN II

Gerry Fuerst

The final aircraft configuration was the result of a long evolution of aircraft designs. Originally, the plane resembled a missile that was powered by a turbofan-ramjet (TFRJ) and a scramjet. However, the length had to be shortened and the wing area increased. The nozzles of the scramjets had to be reworked in order to make them workable. The final design turned out to be that of a delta winged, tailless airplane (see figure DII 1).

The overall volume of the fuselage was dictated by the number of engines and the enormous fuel requirements. The plane uses one full-sized TFRJ to take it from Mach .8 to Mach 6. After Mach 6, the plane will use four full-sized scramjets to take it to Mach 10. Because of the large amount of fuel that is required to power these engines, the length of the plane was set at 85 feet (the maximum length that the French will allow).

The scramjets are located at the rear of the aircraft- two on each side of the TFRJ. When the 2-D nozzle of the TFRJ closes, it provides two vertical expansion surfaces for the scramjets (see figure DII 2). These expansion surfaces, along with pressure boundaries, will be used as the nozzles for the scramjets.

The aircraft has three separate inlets. A variable geometry inlet for the TFRJ is located on the bottom of the fuselage, and a mixed compression inlet is located on each side of the plane. These two mixed compression inlets supply air to the four scramjets. The scramjet inlets actually start about 18.5 feet upstream of the actual scramjet units. This is where the sides of the fuselage turn outward at a 6.5 degree angle. This turn in the fuselage produces an oblique shock that rests on the outer lip of the scramjets at Mach 10. This shock creates the initial compression of the air entering the scramjets.

The planform of the aircraft is basically a delta shape. Because of the fact that the aircraft will fly at Mach 10, the wing was designed with a high sweep angle and a low aspect ratio. The surface area of the wing is relatively small. However, this area could be even smaller for a plane flying at hypersonic speeds, but due to the fact that the plane must be landed, it was not reduced any further. The following parameters apply to the planform:

Wing Span, $b = 40$ ft

Root Chord, $C_r = 40$ ft

Tip Chord, $C_t = 5$ ft

Mean Aerodynamic Chord, $MAC = 27.037$ ft

Taper Ratio, $\lambda = 0.125$

Sweep Angle of Leading Edge, $\Lambda_{LE} = 69$ deg

Sweep Angle of Trailing Edge, $\Lambda_{TE} = 23$ deg

Exposed Surface Area, $S_e = 722.5$ ft²

Aspect Ratio, $A = 2.215$

Maximum Thickness Ratio, $t/c = 0.0370$

Zero Lift Angle of Attack, $\alpha_{oL} = 0$ deg

Aerodynamic Center, $X_{ac} = .5(MAC)$

The following parameters apply to the vertical stabilizer:

Surfac Area, $S_v = 120.75$ ft²

Root Chord, $C_{rv} = 27.5$ ft

Tip Chord, $C_{tv} = 7$ ft

Sweep Angle of Leading Edge, $\Lambda_{LE_v} = 73$ deg

Sweep Angle of Trailing Edge, $\Lambda_{TE_v} = 20$ deg

$X_{vs} = 17.69$ ft

$Z_{vs} = 6.435$ ft

Weight Analysis

Thomas Greiner

To better estimate the hypersonic aircraft weight for all of its flight systems an analysis was performed using a computer program developed by both the United States Air Force and the National Aeronautics and Space Administration . The initial program, P.D.W.A.P (Preliminary Design and Weights Analysis Program) requested basic preliminary design data such as fuel weight, number of crew men, type and number of engines to act as an initial data file for a larger more comprehensive weight program. The larger program called W.A.A.T.S, (Weight Analysis of Advanced Transportation Systems) bases its findings on a data base containing information on aircraft already in existence. Not only does the program provide weight estimates for the total aircraft and its subsystems but it also sizes the aircraft for fuel and flight regime.

When the program was run for the hypersonic aircraft, one problem that arose was that it did not allow for scramjet engines. Since there are four scramjets on the current design this could introduce substantial error, however given the engines provided by the program, the most reasonable choice was to describe the scramjets as ramjets. When the turbofan-ramjet onboard was entered into the program a highly exaggerated weight estimate for the inlet (over 200,000 pounds) was returned. This error was compensated for by considering the engine to be a ramjet and then adding to the weight of its inlet to adjust it to the actual weight of the turbofan-ramjet.

The data returned by the program indicated that the initial weight estimates were very reasonable. The take off weight computed by W.A.A.T.S was 44,133 pounds, see figure weight1 while the group used 48,000 pounds , see figure weight2. That eight percent difference is acceptable, however the computer program underestimated for the thermal protection sytems so the higher number will still be used. The computed

height of the aircraft matched the 8 feet that is used in the current design while the calculated span is 32 feet while the aircraft's current span is 40 feet.

Overall the W.A.A.T.S. program computed a very similar weight estimate for the aircraft and its subsystems reaffirming the initial estimates used by the design team.

Rocket Boosters

Thomas Greiner

Since the main driving force in sizing the hypersonic aircraft was the need to hold large volumes of liquid hydrogen, solid rocket boosters were considered for the main propulsion system that would be used to accelerate the aircraft from the launch speed of Mach .8 to the Scramjet operating speed of Mach 10. The solid rocket was considered because of the high thrust and accelerations which would not be a concern to the unmanned aircraft, also the booster could be jettisoned after its use. Preliminary calculations indicated that the rocket weight would be 75,000 pounds which was almost twice the aircraft weight. The idea of using rockets as the main propulsion system proved to heavy.

A full scale turbofan-ramjet,(T.F.R.J.) was chosen to accelerate the aircraft fom Mach .8 to Mach 6 but a problem arose because the engine's burning of liquid hydrogen increased the aircraft's size.

Another problem that occured was the efficency of the T.F.R.J. inlet to produce a reasonable pressure recovery at the low Mach numbers. Estimates made by the U.S.A.F. showed that a loss in thrust of 30% would occur through the transonic region, where the aircraft drag increases sharply. There is some concern whether the engines could produce enough thrust to push the aircraft through the sound barrier and that it would take more fuel to do so because of the lower accelerations.

These problems were great concerns that needed to be corrected without penalizing the design by increasing its size to add more liquid hydrogen. One solution was to put the aircraft into a dive and use gravity to gain speed after seperation from the carrier aircraft. This method could work but it would take more fuel to climb back to the original altitude.

Another solution was to use strap on booster packs to accelerate through the transonic region. These boosters would be used from Mach .8 to Mach 2.5 to accelerate the aircraft while the T.F.R.J. would produce

enough thrust to overcome drag. This T.F.R.J. was not used at full thrust to reduce the amount of fuel needed to span the transonic region but it was kept operating to allow for a smooth propulsion transition when the solid boosters were jettisoned.

The two boosters are integrated into the aircraft body, one under each wing, see figure Booster1 mounted next to the scramjets. The booster's nose is slanted to lower the drag and also the two-dimensional exit nozzle is located partially behind the aircraft body to reduce the drag. The length of each booster is 15 feet and their combined weight is 15,000 lb. This additional weight puts the aircraft's takeoff weight at approximately 62,000 pounds.

The size and weight of the booster rockets was calculated using a spreadsheet, see figure Booster2 which was based on the constant acceleration that was assigned. An acceleration of 1-G, (32.2 ft/s^2) was chosen to reduce the range traveled and the amount of fuel used. Using the given acceleration the amount of fuel required to maintain the chosen flight profile is calculated and then the required volume is determined. The solid propellant chosen was J.P.N. which has a specific impulse of 240 seconds. This was the upper limit for a solid rocket fuel impulse. The initial weight of the aircraft was 62,000 pounds and the weight of the fuel burned by both the solid rocket boosters and the T.F.R.J. were subtracted from the aircraft weight as it accelerated. The thrust required to accelerate the adjusted mass was calculated and then converted into pounds of propellant. Knowing the density of the propellant the volume required to contain the propellant was determined. With this information a rocket diameter of 2.5 feet was determined to be acceptable in terms of drag and volume for the rocket's tube.

The overall benefits of using the booster pack is a reduction in range of 3 miles due to the large acceleration, a reduction of 500 pounds of fuel needed for the T.F.R.J. in the transonic region, and the additional thrust to offset the thrust lost due to an inefficient T.F.R.J. subsonic inlet.

CENTER OF GRAVITY LOCATION

Gerry Fuerst

The center of gravity for the entire aircraft was found by taking the weighted average of the center of gravity for individual aircraft components. The Analysis was as follows:

COMPONENT	WEIGHT (LBS)	LOCAL C.G. (FT)
Nose *	3365	77.5
Body	5342	40
Fuel Tank	13913	49
TFRJ	6500	20
Scramjets	12000	20
Inlet	400	40
Front Landing Gear	50	50
Rear Landing Gear	150	11
Wing	4675	23.125
Vertical Tail	664.125	11.14

* Note: the nose section contains a portion of the main fuel tank.

When the fuel tank is empty, it not only affects the weight of the fuel tank but also the weight of the nose. Therefore, the empty weight of the fuel tank and nose is 4413 lbs and 1365 lbs respectively. With the above information, the center of gravity was calculated as follows:

$$X_{cg} = \frac{\text{Sum (Weight*Local C.G.)}}{\text{Sum of the Weight}}$$

$X_{cg} \text{ (full tank)} = 35.102 \text{ ft}$

$X_{cg} \text{ (empty tank)} = 29.053 \text{ ft}$

* The C.G. is measured with respect to the rear of the aircraft.

Thomas Greiner

A necessary requirement for any hypersonic vehicle is to minimize the size and weight of the aircraft. The size and weight requirements for this mission were specified by the French based on their launching aircraft requirements. Since the hydrogen fuel used has a large storage volume it is necessary to minimize the amount of fuel required for the flight profile. This mission profile consisting of a five phase flight was initially used to minimize fuel.

Phase One) Acceleration from Mach .8 to Mach 2.5 at 40,000 feet.

Phase Two) Following the Q-Curve of 1850 at Mach 2.5 at 40,000 feet and accelerating to Mach 6 at 75,000 feet while maintaining a climb angle of four degrees.

Phase Three) Leaving the Q-Curve at 75,000 feet and climbing to 100,000 feet while maintaining Mach 6.

Phase Four) Leveling off at 100,000 feet turning on the scramjets, turning off the turbofan-ramjet and, accelerating to Mach 10 and sustaining that speed for two minutes.

Phase Five) Turning off the scramjets and slowing down below Mach 1 and turning the turbofan-ramjet on and heading to Dryden Air Force Base in California under power.

The preceding phases were analyzed using a spreadsheet, see figure Profile1 which uses conditions such as acceleration, time-of-flight, and the climb angle to minimize fuel consumption. Calculations were conducted to follow a constant dynamic pressure line, a Q-curve, which will allow the aircraft to maintain a constant angle of attack from 40,000 to 100,000 feet. Originally, a Q based on Mach 6 at 100,000 feet was attempted but could not be used due to two factors, the magnitude of the aerodynamic forces at the lower altitudes and the lack of thrust of the turbofan-ramjet at higher altitudes to meet the required accelerations.

ORIGINAL PAGE IS
OF POOR QUALITY

in phase 1 the aerodynamic forces were large due to the speed and altituded required to stay on the Q-curve for the entire flight. The Q value is above 2000 which implies there would have to be a substantial increase in structural weight to accept the loads. For a hypersonic aircraft a Q should be about 1800 therefore a new value was chosen based on Mach 6 at 75,000 feet with a Q of 1850. This an acceptable value that will not greatly effect the intial estimate of the structural weight.

The aircraft follows this Q-curve in phase two until it reaches Mach 6 at 75,000 feet. At this time the aircraft enters phase three were it leaves the Q-curve while maintaining a climb angle of four degrees and climbs 100,000 feet while sustaining Mach 6. In this high altitude period of the flight profile the thrust of the turbofan-ramjet falls off, however the thrust required also drops. Since there are no other acceleration requirements to meet other than those caused by the change in the speed of sound due to the atmospheric temperature, at this point the thrust has only to overcome the drag and the force from the weight component, therefore the thrust available is still large enough to meet the thrust required.

In phase four of the flight the aircraft levels off at 100,000 feet, the turbofan-ramjet is turned off and the scramjets are turned on. Based on the data supplied by the spreadsheet it became obvious that the aircraft needed more thrust to reduce time of burn and, in turn, the fuel required to accelerate from Mach 6 to Mach 10. Two additional scramjet modules were added to the aircraft. Adding the engines increased the thrust and allowed for considerable increases in acceleration and reduced the amount of fuel burned during this phase of the flight.

Finally in phase five after the two minute engine test the scramjets are shut off and the plane is decelerated by the force of drag. The aircraft slows down to Mach 1 at 50,000 feet and the turbofan-ramjet is turned on while the aircraft continues to slow down. The hypersonic aircraft maintains Mach .8 and flies to Dryden Air Force Base in California and

lands. The actual flight path along the west coast of the United States is illustrated in figure Profile2.

To further reduce the liquid hydrogen necessary to accomplish the mission an energy state program, was written.

**MINIMUM FUEL FLIGHT PATH
(ENERGY STATE METHOD)**

by
Bob Stonebraker

The accelerated ascent from release to Mach 10 at 100,000 feet was broken into two phases based on the engines used. Phase 1 employs the turbofan-ramjet and two booster rockets to reach Mach 6 at approximately 76,000 feet ($q = 1800$ psi.). Phase 2 then continues the ascent under power of the scramjets to Mach 10 at 100,000 feet to begin the two minute test. The energy state method showed that the altitude vs Mach number flight path which consumed the least fuel was simply one of a constant high dynamic pressure. Temperature limitations determined the highest dynamic pressure to be 1800 psi.

The data provided for the General Electric augmented turbofan-ramjet engine consisted of net thrust (F_n) and specific fuel consumption (sfc) for various Mach numbers and altitudes. To make this data easier to incorporate into a computer program, it was used in a subroutine (SUBROUTINE TFRMJT) to produce values for any Mach number at any altitude. To do this, F_n and sfc were separately plotted vs Mach number for a constant altitude. This was repeated for various altitudes yielding several curves, one for every 10,000 feet from 40,000 to 100,000 (Figure ES-1). A plotting package was then used to obtain best-fit equations of these curves which modeled the given data quite accurately. These polynomials were then used in the subroutine in conjunction with the cubic spline interpolation method for values at altitudes between those of the equations. In this way, the subroutine yields a corresponding net thrust and sfc for any Mach number (.8-6) at any

altitude (40,000' - 100,000'). Where several values of F_n and sfc were given for the same Mach number and altitude in the original data, that for the best fuel economy was chosen for the plots.

The given data for the experimental SCRAMJET was also reduced in a similar manner through a subroutine (SUBROUTINE SCRAMJET) which yields values for a range of Mach numbers (6-10) at any altitude (80,000' - 100,000'), (See Figures ES-2 & ES-3). The data provided, gave thrust (F_n) and specific impulse (I_{sp}) values as a function of dynamic pressure and fuel/air equivalency ratio for various values of altitude and Mach number. Because the data for this engine was given in terms of various dynamic pressures (q) instead of altitude, the best-fit equations in this subroutine have altitude as the independent variable with Mach number held constant. Then the cubic spline interpolation subroutine (SUBROUTINE SPLINE) finds the desired net thrust and I_{sp} for non-integer Mach numbers from 6 to 10. Once the $I_{sp}(\text{sec.})$ is found, the sfc is computed by the following;

$$SFC = \frac{3600}{I_{sp}}$$

Two additional subroutines had to be written for the Energy State program; one for standard atmospheric data as a function of geometric altitude (SUBROUTINE ATMOSFR) and another for the total drag of the aircraft as a function of Mach number and altitude (SUBROUTINE DRAG). The total drag data, computed by another team member, was received in tabulated form and was therefore also reduced through curve-fit polynomials and cubic spline interpolation.

The energy state method can be used to determine the minimum time or minimum fuel required to reach a Mach number and altitude. To compute the minimum fuel accent required five separate programs. The first code (PROGRAM HECONST) determined lines of constant He (ft), which defines the amount of potential and kinetic energy that an aircraft possesses at a certain Mach number and altitude. He is given by;

$$H_e = h_g + \frac{V^2}{2g} = h_g + \frac{M^2(\gamma R T)}{2g}$$

Two additional codes determined contours of constant Fs for phase 1 and phase 2 of the mission (PROGRAM FSCONST & PROGRAM FSCNST2). Fs is the vertical distance traveled per pound of fuel burned and is given by;

$$F_s = \frac{P_s}{T_N \text{ sfc}} = \frac{M a (T_N - D)}{T_N \text{ sfc } W}$$

The minimum fuel trajectory is one in which the lines of constant Fs are tangent to lines of constant He. These plots showed that a greater thrust per pound of fuel is obtained at high Mach numbers and low altitudes. However, aerodynamic heating obviously limits flight in this realm. Therefore, the minimum fuel accent was chosen to be one of a constant $q = 1800$ (Figure ES-4). For comparison, the quantity of fuel required to accelerate from Mach=6 to Mach=10 all at 100,000 feet was determined to be approximately 25,000 lbs. This is obviously unacceptable.

Once the flight path was determined, several values could be

computed along the trajectory. Figure ES-5 shows the thrust available and required curves. The last two codes (PROGRAM PHASE1 and PROGRAM PHASE2) were used for this and to compute the fuel consumed and elapsed time for phase 1 and phase 2 of the mission. The fuel burned is given by;

$$\Delta W_f = \int_{H_{e1}}^{H_{e2}} \frac{1}{F_s} dH_e$$

The elapsed time is given by;

$$\Delta t = \int_{H_{e1}}^{H_{e2}} \frac{1}{P_s} dH_e$$

The range required for these accents was also computed, as shown below, and found to be approximately 130 miles for phase 1 and 970 miles for phase 2.

$$\Delta d = \sqrt{(Ma \Delta t)^2 - (\Delta h_g)^2}$$

Originally, the plan was for Edwards A.F.B. to be the base of operation over all phases of the mission, from carrier aircraft takeoff to test vehicle landing. The plan incorporated a triangular pattern with one leg over the ocean for the accent, acceleration and scramjet test phases. The aircraft was to be carried to the release point approximately 300 miles southwest of base. This would allow a return, either to Edwards or Vandenburg A.F.B. under power of the turbofan-ramjet in the event of scramjet

misfire. However, after a better estimate of required acceleration distances, it was necessary to alter the plan. It was decided to originate the mission from Seattle and release the aircraft over the ocean, then run approximately 100 miles off the coast to land at Edwards. This plan still fulfills the requirement of non-supersonic test vehicle flight over populated areas.

Control of the mission from release to landing is to be fully automated. Based on this, it was determined that the avionics should include a receiver, transmitter, inertial navigation equipment, stability augmentation systems, and a computer. This equipment was estimated to weigh approximately 1000 lbs. The aircraft cooling system was not included in the avionics. The control program will originate from systems based at Edwards and be communicated to the aircraft via satellite. Real time communication between the aircraft and Edwards A.F.B. is also necessary to monitor data from the test scramjets. The on-board computer will maintain a backup control program in addition to its' stability augmentation and engine monitoring functions.

INLET DESIGN

INTRODUCTION

The purpose of an inlet is to supply the right amount of air mass flow rate with an acceptable velocity distribution to the face of the compressor at an appropriate Mach number (Usually $M=0.4$). For supersonic flight, a sophisticated variable geometry inlet having its own automatic control system is required. For supersonic inlets, the efficiency and performance of an inlet is related to the total pressure recovery, quality of air flow going into the compressor, inlet drag, and finally to the weight and cost of the inlet. In the design process, the main purpose was to obtain the highest possible pressure recovery with no or minimal spillage drag while inflicting the least amount of distortion to the airflow reaching the engine.

For the engine to operate efficiently, the Mach number at the face of the compressor has to be about $M=0.4$, therefore, to decelerate the airflow to about $M=0.4$ three types of inlets, characterized by their shockwave system, were examined. First, the pitot (normal) shock type inlet was examined. This inlet type achieves supersonic compression by means of a normal shock; it gives tolerable total pressure recoveries up to Mach 4.6 after which the total pressure recoveries drop drastically according to the normal shock tables and equations. This Mach number limit on the pitot shock inlet rules out its use in the airplane. Then, the external compression type inlet was examined. This type of an inlet accomplishes the flow compression external to the inlet throat with the desired operation (design condition).

having the normal shock at the inlet throat. To accomplish an efficient compression a series of ramps can be used to create a series of oblique shocks which provide higher total pressure recoveries and thus a more efficient compression. Having a series of ramps provides a more efficient compression than using one big ramp. This inlet type provides tolerable total pressure recoveries up to Mach 2.5 after which the pressure recoveries drop. Finally, the mixed compression inlet (internal contraction inlet) was examined, this inlet type combines both external and internal compression of the flow. But for this inlet type, to have a peak performance for a variety of Mach numbers the inlet must have a variable geometry feature. The inlet might include variable angle compression ramps in order to keep the shock on the cowl lip at off design Mach numbers. Another consideration that has to be taken into account when designing any type of inlet is to make sure that enough inlet area is available to supply the required amount of air required by the engine. The mixed compression inlet is mostly used for Mach numbers greater than 2.5, where it can provide sufficiently high total pressure recoveries when compared with the other inlet types discussed here. But the main set backs for a mixed compression inlet are the high cost, high weight, and extremely complex mechanical arrangements that are required to reach the desired total pressure recoveries. But when all the choices were considered, it was decided to use a mixed compression inlet because the hypersonic airplane will be flying over a wide range of Mach numbers.

COMPUTER PROGRAMS

Designing an efficient and reliable inlet is a very tedious and complex problem. Since many variables are involved in the design process, it is a time and effort consuming process. To facilitate and speed the design process three computer programs were written.

Program INLETAREA finds the capture area corrected for boundary layer bleed of the turbofanramjet. The required inputs are Mach #, mass flow, and the boundary layer bleed correction factor from figure 16.11 in Nicolai. These factors are entered in according to the flight path altitude. The inlet capture area is calculated using the mass flow relationship. Program INLETAREA is in Appendix C.

Program INLETANGLE16 was design to find the most efficient ramp configuration for a Mach 6 inlet having 6 ramps. It does this by first inputting the theta's to be tested. It then calculates beta from an iterative routine. Next the normal and oblique shock relations are used to find the inlet efficiency, TPTR. Many theta's were tested in many combinations. Listing of the program INLETANGLE16 and sample listing of theta's tested is given in Appendix C. The maximum efficient inlet combination is highlighted in blue.

Program INLETANGLE is very similar to program INLETANGLE16 except that INLETANGLE uses the theta angles for the various Mach numbers given from program INLETLENGTH. The efficiency term is TPOTR. The terms under the dashed lines are the totals resulting from the oblique shocks. The terms under the asterisks are the total results including the throat normal shock. Program INLETANGLE is in Appendix C.

Program INLETLENGTH main purpose is to ensure that all the shockwaves off of the different ramps hit the same point on the cowl tip. This is done in order to insure that minimal or no spillage drag is being incurred. The program INLETANGLE provided us with the most efficient ramp angles for the flow at Mach 6 (design point), after which the corresponding lengths of these ramps were found using simple geometric relations; therefore, the total length of our ramps was found. In the program INLETLENGTH the vertical length from the first ramp to the cowl lip was fixed, in addition, the first ramp deflection angle was fixed. By fixing these two parameters and for a given initial Mach number, the program INLETLENGTH would provide us with the ramp angles and shock angles for the rest of the ramps. After the program INLETLENGTH was run several times for the lower Mach numbers, it was obvious that at the lower Mach numbers fewer ramps would be needed to achieve an efficient compression. Therefore, the program INLETLENGTH was then modified to find the theta's and beta's for five, three, and two external ramps. A listing of the program INLETLENGTH three versions can be found in appendix C.

INLET CONFIGURATION

The first consideration involving the inlet was how big to make it. This was determined by first looking at the flight path, Table A1, and running the program INLETAREA. These results are in Table A2. From these results it was judged to optimize the inlet for Mach 6 at 30,000 ft.

ORIGINAL PAGE IS
OF POOR QUALITY

Program INLETANGLEM6 was run to optimize the 8 ramp theta's for the highest efficiency. This efficiency was found to be 69.6 %. Next the 8 ramp lengths for Mach 6 were calculated by hand using trigonometry. Using these length values and adjusting them by adding additional hinges to the ramp surfaces making 9 total hinges for each side of the inlet, the best ramp lengths were found by running Program INLETLENGTH and checking the theta values for high efficiency by running Program INLETANGLE. These lengths are listed in Table: IN3. The theta's selected for each Mach # from INLETANGLE are listed in Tables: IN4-IN9. The inlet is an XB-70 type and is shown installed on the aircraft in Figure: IN1. The open and closed positions of the inlet are shown in Figure: IN2. The inlet will be in the closed position during flight above Mach 6 and half of the inlet will be closed from Mach 2.5 to Mach 6 at 85000 ft this will be done to reduce by-pass drag due to the small capture area required at these Mach #s and altitudes. The inlet ramp configurations at Mach 1.4 - 6 is shown in Figures IN3 and IN4. Tables IN4- IN9 list the theta's and beta's. This inlet configuration's total pressure recovery efficiencies are higher at every Mach # in the flight path than the Mill-Speed ones, Figure: IN5.

ORIGINAL PAGE IS
OF POOR QUALITY

AERODYNAMICS

The lift and drag of an airplane are the key factors in determining the type of engines and the performance of the airplane. For the first phase of the design process, an initial configuration was approved, an estimate of the CD_0 of our airplane was calculated using the build up method. The initial calculations indicated that using one full scale GE turbofan-ramjet would be sufficient to overcome the drag of the airplane at the various phases of flight where GE's turbofan-ramjet would be used. After the first phase of the design process was completed, the drag of the airplane was more accurately calculated using Nicolai's (chapters 2 & 11), and the Datcom reference. After several iterations on the drag numbers because of slight modifications to the airplane design, final drag numbers were calculated to the final airplane configuration. This data was then given to the flight path group which was responsible for determining the flight path and the fuel requirements of the mission. After the fuel requirement and time of flight for the mission profile were calculated using the thrust provided by the two scram-jet engines it was obvious that an additional two scram-jets, one on each side of the airplane, would be required to cut the fuel requirement and time of flight. These additions effects on the drag were included as a 10% increase to the CD_0 of the airplane because these modifications were done the day before the final presentation for Winter quarter. Therefore, the effects of these additions had to be calculated more accurately in Spring quarter.

The last minute modifications, that were introduced at the end of Winter quarter, were studied more closely at the beginig of Spring quarter and it was obvious that some modifications to the shape of the airplane had to be done. After the final shape of the airplane was modified and approved, the final drag numbers were calculated. The drag numbers for the old configuration could not be modified to account for the changes in the airplane configuration mainly because the fundemental parameters used in calculating the old drag numbers were drastically changed by the new design; these parameters include the airplane fineness ratio (l_B/d), the nose fineness ratio (l_N/d), the after-body fineness ratio (l_A/d), the aspect ratio of the wing, the surface area of the wing, the taper ratio, and finally the length of the airplane. Therefore, the drag numbers for the new configuration had to be calculated from scratch. The three coefficients that had to be calculated to provide us with sufficiently accurate drag numbers were CD_0 , K (factor of drag due to lift), and CL . These three coefficients need to be calculated seperately for the four flight regimes in our flight path.

SUBSONIC

For the wing, the zero lift drag is composed of two parts, skin friction drag and pressure drag. As for skin friction drag, it is caused by shearing stresses within a thin layer of retarded air on the surface of the wing called

the boundary layer. The amount of viscous resistance depends on whether the flow is laminar or turbulent; for our airplane turbulent flow was assumed for all flight regimes. As for the pressure drag, it is usually small compared to skin friction and it is primarily caused by the displacement thickness of the boundary layer. Methods for predicting subsonic CD_0 for wings are essentially empirical and are based on streamwise airfoil thickness ratio (t/c).

For the body, at subsonic speeds the drag of smooth slender bodies is primarily skin friction. The Reynold's number is based on body length, boundary layer condition, and surface roughness. The pressure drag is also generally small for fineness ratios above 4 (The airplane's fineness ratio is 7.083) but becomes significant for blunt bodies. At the subsonic region, A CD_0 of 0.0129885 was calculated at $M=0.8$. Also at $M=0.8$ and at 40,000 ft, the drag is 7508.25 lbs with a L/D of 6.433.

TRANSONIC

For the wing, the transonic range varies greatly with airfoil shape and thickness, but for simplicity it can be considered to begin at approximately $M=0.9$ and end at $M=1.2$. Because of the mixed flows, drag in the transonic region does not lend itself to theoretical or experimental analysis. The wing drag at the transonic region is mainly composed of skin friction and wave drag. As for skin friction, a little increase in drag is experienced due

to viscosity. Therefore, the skin friction drag will be assumed constant and equal to the subsonic skin drag throughout the transonic range. As for the wave drag, the variables involved in a wing design that effect the manner in which shock waves develop on the surface are many; they include sweep, aspect ratio, taper ratio, thickness ratio variations between root and tip thickness, position of the maximum thickness, incidence and leading edge thickness. As a result its very hard to predict the wave drag in the transonic reigon. Estimates for the wave drag can be obtained by finding the drag divergence Mach number and then using figure 11.10 in Nicolai's to find CD_0 .

For the body, the general approach consists of predicting the skin friction, the drag divergence Mach number, the variation of base drag with Mach number, and the variation of pressure drag for Mach numbers above 1. Therefore, the drag of the body at transonic speeds consists of skin friction, base pressure, subsonic pressure drag, and supersonic wave drag. At the transonic reigon, as predicted, a CD_0 of 0.039493 at $M=1.2$ was the largest. Also at $M=1.2$ at 40,000 ft, the drag was 146983.92 lbs with a L/D of 3.273.

SUPERSONIC

For the wing, at supersonic speeds an increase in the Mach number results in a decrease in the skin friction coefficient at constant Reynolds numbers. This variation is primarily due to the variation in the temperature

and density at the surface. The full reduction in skin friction at supersonic Mach numbers is justified only when stabilized conditions and zero heat transfer are attained. For transient flight the skin friction will be assumed equal to the incompressible value although in reality it varies between this value and the zero heat transfer. Another important factor for estimating drag at the supersonic speeds is the Reynolds number, this can be accounted for by taking into account the ratio of compressible to incompressible skin friction coefficients. As for the wave drag, the well known linearized supersonic theory is used in predicting wing wave drag. For the airplane the wave coefficients were obtained using equation in Nicolai's which are based on the supersonic linear theory.

For the body, the characteristics of compressible skin friction drag for bodies are similar to those of wings; the skin friction coefficients decrease as the Mach number increases. As for the wave drag, two methods for estimating the fore-body and after-body wave drag are presented in the Datcom reference. The second method, which was used, is based on similarity parameters. The wave drag is separated into the fore-body drag, the isolated after body drag, and the interference drag of the fore-body and center section of the after-body. In the supersonic region, a CD_0 of 0.0242 was calculated at $M=3.0$. Also at $M=3.0$ and at 65,500 ft, the drag was 40666.36 lbs with a L/D of 1.1592.

HYPersonic

For the wing, due to the non-linearity of hypersonic flow, approximate methods for estimating force characteristics are very desirable. Among the methods used, Newtonian and modified non-Newtonian flow theory have proved very useful. Newtonian theory is based on the assumption that the shock coincides with the wing surface and no friction exists between the wing and the boundary layer. The fluid particles ahead of the wing are not disturbed until they encounter the wing.

For the body at hypersonic speeds the drag of the body is caused primarily by the pressure and skin friction drag of the nose. Both the after-body and the base drag become insignificant at higher Mach numbers. The drag coefficient was calculated at $M=6.0$ and at $M=10.0$ using Newtonian flow theory and it was also calculated using the supersonic linear theory; the discrepancy between the two methods was less than 10% (the Newtonian flow provided the lower drag values). It was decided to stick with the CD_0 's found using the supersonic linear equations since the discrepancy between the two methods was relatively small. At $M=6.0$ a CD_0 of 0.018758 was calculated and at $M=10.0$ a CD_0 of 0.015517 was calculated. At $M=6.0$ and at 76,000 ft the drag was 32294 lbs with a L/D of 1.4002, and at $M=10.0$ at 100,000 ft the drag was 26036 ilbs with a L/D of 1.449.

After the CD_0 was calculated for the various flight regimes a 10% increase was added to CD_0 to include the interference effects. In addition, the coefficient of drag due to lift (K) had to be calculated in order to account for the effect of lift on the drag of the airplane. For the subsonic region the equations in Nicolai's (Chapter 11) were used. For the supersonic and hypersonic regions the K values were calculated using the supersonic linear theory. Finally the values of K for the transonic region had to be approximated. After obtaining the CD_0 's and the K values for the various Mach numbers, the drag at the various altitudes and Mach numbers was calculated. Three separate programs were written to calculate the drag and angles of attack at the various Mach numbers and altitudes. A listing of the equations and procedures used in calculating the drag are listed in Appendix A and the listing of the programs used in calculating the drag can be found in Appendix B. The tables AD1-AD6 and the figures AD1-AD8 include the results of this chapter.

BASIC STABILITY ANALYSIS

Gerry Fuenst

Due to the large amount of fuel on board the test plane, there will be a considerable shift in the C.G. during flight. The C.G. will shift down and towards the rear of the aircraft as the fuel is burned. The distance towards the rear of the plane that the C.G. will travel was computed as follows:

$$\text{C.G. Travel} = 35.102 - 29.053 = 6.05 \text{ ft}$$

For stability, it is necessary to have a positive static margin. The SM is directly related to the distance between the center of gravity and the aerodynamic center. Although the C.G. travels back 6.05 feet, it always remains ahead of the aerodynamic center. This means that the static margin always remains negative. The calculation of the static margin was as follows:

$$\text{Static Margin: } SM = (X_{ac} - X_{cg})/MAC$$

$$\text{Full Tank: } SM = 13/27.037 = 0.4808$$

$$\text{Empty Tank: } SM = 6.875/.037 = 0.2543$$

For an aircraft to be statically stable, its value of $C_m(\alpha)$ must be negative. When this is the case, the aircraft is trimmed at a positive angle of attack. When the angle of attack is suddenly increased, the aircraft will generate a negative moment to push the nose back down to the original trimmed angle of attack. The $C_m(\alpha)$ for the test plane was found to be negative for both the full and empty tank cases. It was computed as follows:

$$C_m(\alpha) = -C_L(\alpha) \cdot (X_{ac} - X_{cg})/MAC = -C_L(\alpha) \cdot SM$$

Case 1: Mach .8

Full Tank: $C_m(\alpha) = -.7965/\text{rad}$

Empty Tank: $C_m(\alpha) = -.4213/\text{rad}$

Case 2: Mach 10

Full Tank: $C_m(\alpha) = -.1957/\text{rad}$

Empty Tank: $C_m(\alpha) = -.1035/\text{rad}$

The C_m cg of the test plane was calculated for three different cases: subsonic ($M=.8$); supersonic ($M=2$); and hypersonic ($M=10$). Refer to tables S1 thru S3 for C_m cg versus angle of attack, CL , and CD . C_m cg is plotted versus angle of attack in figures S1 thru S3.

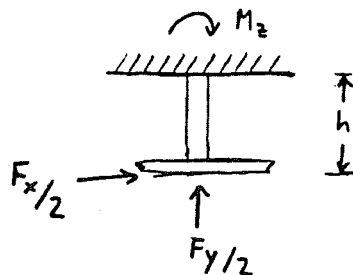
LANDING GEAR

Gerry Fuerst

The landing gear of the test plane will consist of two rear skids and one forward wheel. This configuration was chosen primarily for its reliability and simplicity. The rear skids are better suited in handling the high temperatures that will be experienced during flight. A forward wheel will be used because it will allow for the steering of the aircraft after it has landed. This wheel will be kept cool in flight by surrounding its compartment with the liquid hydrogen fuel tank. The rear skids are located 11 feet from the rear of the aircraft, while the front wheel is 50 feet from the rear.

In designing the landing gear, it is necessary to determine the maximum loads that will be experienced during landing. These maximum loads will occur as a short impulse when the landing gear touches down. It is assumed that the test plane will land at a velocity of 211 ft/s, and it will be descending with a glide angle of 5 degrees. The glide angle is the angle that the plane's descent makes with the ground. The 5 degree glide angle will be the maximum that the plane experiences and was chosen to determine the largest possible loads on the landing gear. Finally, the last assumption that was made is that the time of impulse will be 0.5 seconds.

A simple free-body diagram of the landing gear is as follows:



Constants:

Landing Weight of Plane, $W = 47000$ lbs

Height of the Landing Gear, $h = 4.0$ ft

Kinetic Friction Coefficient, $U_k = 0.6$

Landing Velocity, $V = 211.0$ ft/s

Glide Angle, $\theta = 5$ deg

Time of Impulse, $\Delta T = 0.5$ sec

Gravitational Acceleration, $g = 32.2$ ft/s²

The maximum force, on both skids, in the vertical direction (F_y) can be calculated from the following formula:

$$F_y = \frac{(W/g) * V_y}{\Delta T} \quad \text{where } V_y = V \sin(\theta)$$
$$V_y = 211.0 \sin(5)$$
$$= 18.39 \text{ ft/s}$$

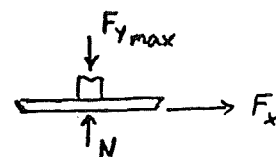
$$F_y = \frac{(47000/32.2) * 18.39}{0.5}$$

$$F_y = 53685.093 \text{ lbs}$$

This is the maximum vertical load that will be experienced by both skids together. Each skid will, therefore, experience half of F_y or 26842.547 lbs.

The maximum force experienced by both skids in the horizontal direction (F_x) can be calculated from the following formula:

$$F_x = U_k * N$$



where N is the maximum normal force

The maximum normal force on both skids is equal to the maximum vertical force on the skids (53685.093 lbs).

Therefore:

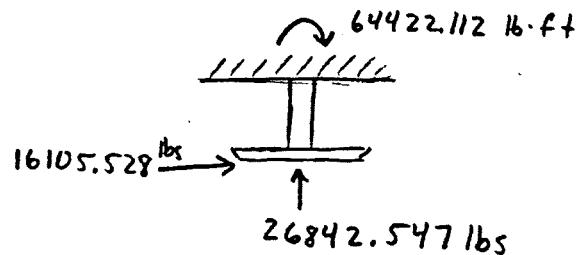
$$\begin{aligned} F_x &= 0.6 * 179279.503 \text{ lbs} \\ &= 32211.056 \text{ lbs} \end{aligned}$$

The maximum horizontal force on each skid separately will be half of F_x or 16105.528 lbs.

The maximum moment produced by each skid (M_z) can be computed from the following formula:

$$\begin{aligned} M_z &= (F_x/2) * h \\ &= (16105.528) * 4.0 \text{ ft} \\ &= 64422.112 \text{ ft lb} \end{aligned}$$

The following is a free-body diagram of a skid with the maximum loads in place:



Materials and Cooling Systems

by
Todd Wray

Throughout history, the advancement of higher speed aircraft has been plagued with the problems of what materials, size and strength, and cooling systems to use, that are most beneficial to the mission. High thermal loadings and body forces acting along the entire aircraft require new technologies to be developed. This section of the report deals with ideas and concepts that can be used in the development of this aircraft.

The first step in developing the materials and cooling systems is to calculate a temperature distribution along the aircraft. The temperature distribution is shown through color coding in Figure MS1. The program and data tables are shown in appendix D. This program is based on empirical data and the geometric structure of the aircraft. It should be noted that the program created is for the worst case scenario. This program does not include spanwise heating. This is the heating along or parallel to the leading edge. The values in the program were found in many books and converted to have the same units. The emissivity of the material will be considered to be .89, the reason will be discussed later. Note that in the Figure MS1 it can be seen that the boundary layer changes from laminar to turbulent at approximate 5.5 feet (noted in the higher temperature). This program does not however consider the transition from laminar to turbulent. The hottest temperatures can be seen to be at the leading

ORIGINAL PAGE IS
OF POOR QUALITY

edges, the nose, the inlets, and the vertical tail.

With the aid of the temperature distribution, a material design for these temperatures can be obtained. Noting the high temperatures, the first material to look at would be a ceramic because of its high resistance to temperature and heat. The problem is that ceramics are not fully developed. A ceramic material can withstand the high temperatures, but the dynamic forces on the body as great as they are, will damage the ceramic, maybe causing failure due to cracking or chipping. Thus, for safety reasons ceramics can not be used. Materials for the skin of the aircraft have to have certain characteristics. The material for this aircraft should have high thermal resistivity, low creep, and low oxidation coefficients. The material chosen is an alloy of aluminum and titanium. This material is very strong, but light, and has good traits on the aforementioned characteristics(Ref.2). The emissivity of this material is .5 but with a special black coating, like on the SR-71, the emissivity rises to .89.

The material on the skin will average in thickness from .1 in. to .2 in. The titanium alluminide can withstand temperatures of up to 1500 F, which is very beneficial(Ref.1), because as Figure MS3 shows, this substantially reduces the amount of wing area that needs to be actively cooled.

Knowing what types of materials to use and where to actively cool,

the next objective is to pick a cooling system to use. Narrowing down the choices there seems to be three useful choices (Figures MS3,MS4,MS5).

Figure MS6 shows a panel configuration for the inlet. This is the only area along with the under belly of the plane needed to be cooled by a panel configuration. The idea is that liquid hydrogen is pushed through the panel, the hydrogen then acts as a heat sink, extracting heat from the skin, then the hydrogen is run through a heat exchanger where it is then let out into the free stream or put into the engine as fuel. This will only be used for the inlets and under belly of the plane, it is not efficient enough for the entire aircraft. The major advantage of this system is the low weight. Its major disadvantage being that it requires a large fuel heat sink.

The nose is very complex when it comes to heating. The diameter of the nose and the curvature of the cone all add to the complexity of the system. Therefore, the use of a nose cap is the proper choice. This nose cap is composed of a JTA carbon composite. This cap is very strong and durable, plus the reusability of this cap is a major advantage, cost wise.

The leading edges require the most work, and are the major problem. The wings and vertical tail require heating with a large system. The leading edges can be cooled by two methods. Figure MS4 shows a spray cooling system. The objective of this system is that a liquid is to be sprayed through a spray head onto a section of the leading edge, thus cooling the edge and then it is transported through tubes to a heat

ORIGINAL PAGE IS
OF POOR QUALITY

exchanger, the system then starts over again in a continuous cycle. The major advantage of this type of system is that the leading edge radii can be very small, but the major disadvantage is that it is unforgiving to local failure.

The second type of leading edge system is a tube system, Figure MS3. The concept behind this system is that the leading edge would be composed of a carbon-carbon composite which is meshed or embedded with tubes that run throughout the leading edges. The tubes filled with a liquid run through the leading edge acting as heat sink, then the liquid is transported to a heat exchanger where the cycle starts all over again. The advantage to this system is that the cooling system can act past the leading edge, even to six feet past the leading edge, onto the wings where it is needed.

These two types of cooling have good points, but the deciding factor is that in the carbon-carbon composite tube cooling the idea of cooling past the leading edge outways any aspect that the spray cooling has. The carbon-carbon tube cooling will act for the first fifteen feet of the wing, after that, areas that needed cooling can be cooled without carbon-carbon, just tube cooling will be used after(Ref. 3).

The vertical tail is quite similar to the leading edges of the wing, except that the maximum temperatures expected will be on the order of 2000 F. The tail will be cooled with just a simple tube cooling system, with carbon-carbon just at the first foot of the vertical tail.

The fuel tanks are very difficult to keep at the proper temperature. On one side of the fuel tank the temperature is approximately -419 F, while on the otherside the temperature is approximately 1800 F. There are two types of purge systems that can be used.

The first purge system is a N_2 purge system (Figure MS6). The major advantage of this type of system is that you can use available insulations and it is reasonably inexpensive. Its major disadvantages is that it has temperature limitations and it is difficult to inspect.

The second purge system is the CO_2 purge system (Figure MS7). The major advantage of this type of system is that it limits liquid hydrogen boil off and there is no liquid phase. Its major disadvantages is that there are complex ground handling requirements and it to is difficult to inspect.

The decision is to use the CO_2 system basically because the carbon dioxide is better suited for the heating and cooling, and also because it limits liquid hydrogen boil off. Liquid hydrogen boil off is of major importance in deciding what to use, because you could ultimately lose 30 percent of your fuel to hydrogen boiloff. The addition of a vapor shield on the tank wall will further decrease the boiloff inside the tank(Ref. 3).

The choice of which coolant to use for the cooling systems for the leading edges was simple to choose. The only liquid with a high specific heat so as to absorb more energy is lithium. The other liquids in

comparson are not even close. It will be easy to use and is the most efficient.

Fuel Tank Insulation Thickness For a

Mach 10 Hypersonic Aircraft

By John Don Tong & Gerry Fuerst

In hypersonic flight, it is necessarily to have to have sufficient insulation around the tank to maintain the hydrogen in a liquid form. A slight increase in temperature of liquid-hydrogen fuel may results in tremendous increase in pressure. For example, hydrogen at its liquid state at -423°F has a density of 70.1 g/liter but at its vapor state, it has 1.3 g/liter. If insulation is not used adequately, the tank will explode. It is our goal to design an insulation system that will insulate the fuel used for a cruising time of approximately 20 minutes.

The derivation of the equation used to calculate the thickness of insulation was taken from NASA Technical Memorandum Paper TM X-2025 by Mark D. Ardema. The author used standard analytical techniques to develop procedures for calculating the insulation's thickness. The assumptions that were used are :

1. Only heat transfer by conduction is considered since radiation and convection effects are negligible compared with conduction.
2. Thickness of insulation used is much smaller than the diameter of the fuselage.
3. Conductivity of insulation is much smaller than the conductivity of all structural elements.

4. Thermal constants are independent of time, temperature, and position.
5. Insulation is continuous and homogeneous.
6. The temperature at the wall of the inner fuselage is the same as the temperature of the liquid-hydrogen fuel.
7. Exterior surface of fuselage is exposed to square temperature pulse.

With the above assumptions, the following equation is obtained:

$$h_{fg} \rho_i / \rho_H - K t_f (T_S - T_H) / L^2 - 2K(T_S - T_0) / k * (1/12 + \sum (-1)^n (1/n^2 \pi^2 + 2k t_f / L^2) e^{(-n^2 \pi^2 k t_f / L^2)}) = 0$$

where the definition of the symbols used are as follows:

- h_{fg} - hydrogen heat of transformation, (Btu/ft³)
- k - diffusivity, (ft²/hr)
- K - insulation conductivity, (Btu/hr-ft-°F)
- L_B - tank thickness, (ft)
- t_f - cruise time, (hr)
- T_H - liquid hydrogen fuel temperature, (°F)
- T_0 - initial exterior surface temperature, (°F)
- T_S - cruise exterior surface temperature, (°F)
- ρ_i - insulation density, (lb/ft³)
- ρ_B - tank density, (lb/ft³)

ρ_H - hydrogen fuel density, (lb/ft³);

It can be seen from the equation that for fixed materials and temperatures, the optimum insulation thickness is proportional to the square root of the cruise time. The above equation can be simplified further if we consider the steady-state condition. The steady-state equation can be obtained by setting the initial exterior temperature equal to the cruise exterior temperature. The equation is as follows:

$$h_{tg} \rho / \rho_H - K t_r (T_S - T_H) / L_{ss}^2 = 0$$

For our design, the insulation must keep the hydrogen fuel at - 435°F to ensure that it will remain in its liquid state. Furthermore, the cruise exterior temperature is approximated to be 1200°F. The material that was chosen for the insulation is Silica Fibers. In the calculation of the insulation thickness, the thickness of insulation was found to be 0.34 ft. The weight of this insulation is approximately 450 lbs.

The thickness of insulation can be reduced further if a better insulation is used. One such insulation is Quartz Fiber which has a lower density (.66 at 700°F), and a greater maximum temperature limit (2500°F). The reason we have not included such fiber in the design was that we were unable to obtain its thermal constants.

We strongly believe that there are better insulation materials other than those mentioned above. If further information on insulation materials can be obtained, the thickness of insulation will be reduced substantially.

Cost Analysis

Thomas Greiner

The cost analysis method used in determining the total cost of the hypersonic aircraft design was found in a book by Nicolai, Fundamentals of Aircraft Design (see references) and referred all dollar amounts to the cost in the year 1970. The final cost estimate was multiplied by the inflation factor of 2.35 to adjust for the current year 1990. The analysis based the cost on three main parameters,

1) AMPR Weight which is the weight of the dry aircraft minus the weight of the engines, the starter, all cooling fluids, wheels, brakes, instruments, auxiliary power and batteries. The value used was an average of the gold design team and the WAATS program weight estimate, AMPR=18526 lbs.

2) S which is the maximum speed at the "best" altitude in knots. This description is vague therefore the velocity for Mach 6 at 80,000 feet was used due to the large available thrust, $S=5178.22$ knots

3) Q which is the combined number of test aircraft and the number to be built during production. Since there is to be only one test aircraft to be built $Q=1$.

Using the equation supplied in the book the cost of engineering hours was the largest cost at 1.7 billion dollars, see figure cost1 while the smallest expense is the manufacturing and material cost at 11 million dollars. The materials estimate appears to be too low due to the unique alloys needed to cool and maintain structural integrity in the intense heat of hypersonic flight.

The total price of the aircraft is 3.3 billion dollars which is most likely a gross underestimate. The initial development costs of the B-2

Stealth bomber was approximately 40 billion dollars. Although the hypersonic aircraft would not need the technology of the B-2 bomber it stands as a good indication of the expense of applying new technologies to aircraft design. This aircraft would use the state of the art technologies in structural composites, ceramics in cooling, and propulsion to achieve its mission requirements. This total cost would be spread over a period of approximately five years.

WIND TUNNEL MODEL
by
Bob Stonebraker

A 1/65 scale model of the preliminary design was built for tunnel testing and to aid presentations. This scale was selected to match that of other designs for relative comparison and to avoid overloading the tunnel measuring device with too large of a wing area. The model was constructed of wood and finished with black pigmented lacquer. Pine was chosen over balsa or fiber-glassed styrofoam for reasons of better durability and lower cost. Lacquer was chosen as the finish to allow polishing and provide a smooth, low drag surface. Construction took place only after approval of the preliminary three-view drawing.

The model will be used to study the longitudinal stability and landing characteristics of the design. Tunnel testing will yield lift, drag and pitching moment for various angles of attack. Reynolds numbers up to 1.8 million can be obtained in the available tunnel with reference to the longitudinal dimension of the vehicle. Since this is a preliminary design, it is subject to change. Data from this model will be used in an additional design iteration and another model will be built and tested to incorporate changes.

Conclusion

This report has described and presented many concepts on how and why a hypersonic aircraft should be designed similar to the gold design for the given mission requirements.

This paper attempted to find answers to questions concerning the areas of aerodynamics, thermodynamics, structural design, and aircraft configuration in a hypersonic environment. It can be concluded that these major design concerns have been addressed but the aircraft still remains in the early stage of development.

Some problems as inlet design, fuel reduction, and dynamic stability still need to be resolved for the hypersonic aircraft. These problems currently exist within the aerospace industry and will have to be solved before hypersonic flight to be commonplace

References

Anderson, John D. Introduction to Flight. McGraw-Hill Book Company, New York, 1985.

Ardema, Mark D. NASA Technival Memorandum Paper TM X-2025.

Carriero, L. E., Preliminary Design and Weights Analysis Program for Aerospace Vehicles, 1Lt., Wright Research and Development Center Air Force Systems Command, Wright-Patterson AFB, OH., WRDC-TR-90-2005.

DATCOM, United States Air Force, Wright-Patterson Air Force Base,
*Revised 1975.

Ellison, D. E., "U.S.A.F. Stability and Control Handbook (DATCOM)," Air Force Flight Dynamics Laboratory, AFFDL/FDCC, Wright-Patterson AFB, Ohio, August 1968.

Glatt, C R. Weights Analysis Of Advanced Transportation Systems. Aerophysics Research Corporation, Hampton, Va., N.A.S.A. CR-2420.

Hill & Peterson. Mechanics of Thermodynamics of Propulsion. Addison-Wesley Publishing Co., Reading, Massachusetts, 1965.

Nicolai, L. M., Fundamentals of Aircraft Design. University of Dayton, Dayton, Ohio, 1984.

Roskam, J. Airplane Flight Dynamics and Automatic Flight Controls. Roskom Aviation and Engineerong Corp., 1979.

Stein, B. & Walter IIIq & John Buckley., Structural Materials for Hypersonic Aircraft, Langley Research Center, NASA Report 74N73077, 1974.

Stone, J. E. & L. C. Koch, Hypersonic Airframe Structure Technology Needs
and Flight Test Requirements. NASA Center, NASA Report 3130, July 1970.

TABLE: IN 1 FLIGHT PATH

Q Based On M=6 at 75,000 ft.

a= 967.9421

v= 5807.6528078

Q= 1858.795

CLIMB ANGLE=4 DEGREES

U_{int} 1404.843

M=.8=774.353FT/S

Altitude (ft.)	Temp. (R)	Density (slug/ft ³)	Q (SLUG/S ²)	U (FT/S)	M
40000	389.99	0.000587		774.3537	0.8
40000	389.99	0.000587		967.9421	1
40000	389.99	0.000587		1161.530	1.2
40000	389.99	0.000587		1451.913	1.5
40000	389.99	0.000587		1935.884	2
40000	389.99	0.000587		2419.855	2.5
40000	389.99	0.000587	1858.75	2515.976	2.599304
45000	389.99	0.000462	1858.75	2835.813	2.929734
50000	389.99	0.000364	1858.75	3196.159	3.302015
55000	389.99	0.000287	1858.75	3602.035	3.721333
60000	389.99	0.000226	1858.75	4059.254	4.193695
65000	389.99	0.000178	1858.75	4574.234	4.725731
70000	389.99	0.000140	1858.75	5154.304	5.325013
75000	389.99	0.000110		5807.651	5.999999
80000	389.99	0.000087		5807.651	5.999999
85000	394.32	0.000068		5839.803	5.999999
90000	402.48	0.000053		5899.918	5.999999
95000	410.64	0.000041		5959.426	5.999999
100000	418.79	0.000032		6018.274	5.999999
100000	418.79	0.000032		6519.798	6.5
100000	418.79	0.000032		7021.321	7
100000	418.79	0.000032		7522.844	7.5
100000	418.79	0.000032		8024.367	8
100000	418.79	0.000032		8525.890	8.5
100000	418.79	0.000032		9027.413	9
100000	418.79	0.000032		9528.936	9.5
100000	418.79	0.000032		10030.45	10
100000	418.79	0.000032		10030.45	10

TABLE: IN2 INLET AREA VERSUS MACH # AND ALTITUDE

Mach #	Altitude (ft)	Mass flow (lb/sec)	Area (ft**2)	Corrected Area (ft**2)	Y (ft**2)
.80	40000.0	495.0	33.804	33.804	4.829
1.00	40000.0	495.0	27.043	27.449	3.921
1.20	40000.0	495.0	22.536	23.077	3.297
1.50	40000.0	478.0	17.410	18.002	2.572
2.00	40000.0	380.0	10.380	10.899	1.557
2.50	40000.0	304.0	6.643	7.108	1.015
2.60	40000.0	290.0	6.094	6.563	.938
2.93	45000.0	250.0	5.922	6.467	.924
3.30	50000.0	210.0	5.611	6.200	.886
3.72	55000.0	175.0	5.268	5.889	.841
4.19	60000.0	148.0	5.023	5.681	.812
4.72	65000.0	126.0	4.821	5.532	.790
5.32	70000.0	110.0	4.741	5.529	.790
6.00	75000.0	94.0	4.560	5.416	.774
6.00	80000.0	94.0	5.789	6.874	.982
6.00	85000.0	94.0	7.379	8.763	1.252
6.00	90000.0	94.0	9.419	11.185	1.598
6.00	95000.0	94.0	11.956	14.198	2.028
6.00	100000.0	94.0	15.106	17.939	2.563

ORIGINAL PAGE IS
OF POOR QUALITY

Table IN3 : RAMP LENGTHS VS. MACH NUMBER.

M=6 , NR=8	M=5, NR=8	M=4, NR=8
7.2746	5.6746	3.6746
3.9430	3.4430	2.0000
2.0864	2.1000	1.6000
1.0900	1.1000	1.8430
M=3 , NR=5	M=2, NR=3	M=1.4, NR=1
3.6746	1.6746	-
2.0000	-	-

THETA, BETA, EFFICIENCY FOR: TABLE: IN 4 Mach # = 1.40

THETA	BETA	M(I)	M(I+1)	POR	PR	TR	XT
5.25	53.23	1.400	1.205	.99815	1.3005	1.0785	2.80

TPOR	TPR	TTR	TPOTR	TPTR	TTTR	MNT	
.99815	1.3005	1.0785	.99043	1.9881	1.2203	.8388	

THETA, BETA, EFFICIENCY FOR: TABLE: IN 5 Mach # = 2.00

THETA	BETA	M(I)	M(I+1)	POR	PR	TR	XT
5.25	34.53	2.000	1.812	.99758	1.3331	1.0864	5.45
5.16	38.32	1.812	1.634	.99806	1.3063	1.0799	4.75
10.41	50.28	1.634	1.261	.98607	1.6773	1.1639	3.12

TPOR	TPR	TTR	TPOTR	TPTR	TTTR	MNT	
.98178	2.9209	1.3655	.96753	4.9344	1.5928	.8064	

THETA, BETA, EFFICIENCY FOR: TABLE: IN 6 Mach # = 3.00

THETA	BETA	M(I)	M(I+1)	POR	PR	TR	XT
5.25	23.33	3.000	2.738	.99388	1.4803	1.1206	8.35
10.13	29.60	2.738	2.282	.96924	1.9669	1.2241	6.34
4.27	29.36	2.282	2.116	.99826	1.2938	1.0769	6.40
5.90	33.16	2.116	1.899	.99621	1.3966	1.1013	5.51
13.75	46.23	1.899	1.401	.96506	2.0271	1.2362	3.45

TPOR	TPR	TTR	TPOTR	TPTR	TTTR	MNT	
.92452	10.6647	2.0111	.88575	22.6281	2.5240	.7395	

THETA, BETA, EFFICIENCY FOR:

TABLE: IN 7

Mach # = 4.00

THETA	BETA	M(I)	M(I+1)	POR	PR	TR	XT
5.25	18.22	4.000	3.621	.98701	1.6573	1.1596	10.64
4.41	19.15	3.621	3.342	.99393	1.4787	1.1202	10.08
3.43	19.82	3.342	3.145	.99763	1.3306	1.0858	9.71
5.42	22.50	3.145	2.859	.99244	1.5236	1.1303	8.45
11.04	29.42	2.859	2.340	.95710	2.1343	1.2575	6.21
3.55	28.04	2.340	2.199	.99893	1.2452	1.0650	6.57
12.25	38.15	2.199	1.735	.96790	1.9866	1.2281	4.46
13.75	51.72	1.735	1.229	.96715	1.9974	1.2302	2.76

TPOR	TPR	TTR	TPOTR	TPTR	TTTR	MNT	
.86929	52.3936	3.2256	.86032	83.6254	3.6975	.8245	

THETA, BETA, EFFICIENCY FOR:

TABLE: IN 8

Mach # = 5.00

THETA	BETA	M(I)	M(I+1)	POR	PR	TR	XT
5.25	15.27	5.000	4.469	.97634	1.8565	1.2015	12.82
6.08	17.32	4.469	3.954	.97370	1.8989	1.2103	11.22
7.16	19.94	3.954	3.448	.97013	1.9538	1.2214	9.65
9.01	23.77	3.448	2.921	.96073	2.0865	1.2481	7.95
8.13	26.30	2.921	2.529	.98034	1.7879	1.1873	7.08
9.63	31.18	2.529	2.127	.97768	1.8341	1.1969	5.78
12.25	39.39	2.127	1.671	.96985	1.9579	1.2223	4.26
13.75	54.75	1.671	1.151	.96663	2.0049	1.2318	2.47

TPOR	TPR	TTR	TPOTR	TPTR	TTTR	MNT	
.79615	184.9801	4.7428	.79345	255.1881	5.2045	.8742	

THETA, BETA, EFFICIENCY FOR:

TABLE: IN 9

Mach # = 6.00

THETA	BETA	M(I)	M(I+1)	POR	PR	TR	XT
5.25	13.36	6.000	5.282	.96146	2.0766	1.2461	14.73
6.25	15.47	5.282	4.594	.95595	2.1491	1.2604	12.65
7.25	17.94	4.594	3.956	.95443	2.1666	1.2643	10.81
8.50	21.07	3.956	3.357	.95252	2.1926	1.2690	9.08
9.75	24.91	3.357	2.806	.95462	2.1661	1.2638	7.54
11.00	29.82	2.806	2.299	.95932	2.1052	1.2518	6.11
12.25	36.63	2.299	1.822	.96497	2.0283	1.2365	4.71
13.75	48.54	1.822	1.323	.96644	2.0076	1.2323	3.09

TPOR	TPR	TTR	TPOTR	TPTR	TTTR	MNT	
.71362	394.0211	6.0736	.69591	738.9285	7.3213	.7745	

TABLES

TABLE AD1 Components of the drag coefficient for the wing at different Mach numbers.

M	C_{Df}	C_{Do}	C_{Dle}	C_{Dw}
0.8	0.005156	-	-	-
0.9	0.005156	0.001643	-	-
1.0	0.005156	0.013970	-	-
1.1	0.005026	0.014010	-	-
1.2	0.004872	0.014092	-	-
1.5	0.004382	-	0.000612	0.01263
2.0	0.004021	-	0.001225	0.00545
2.5	0.003531	-	0.001904	0.00510
3.0	0.003196	-	0.002522	0.00508
3.5	0.002835	-	0.003021	0.00520
4.0	0.002578	-	0.003398	0.00529
4.5	0.002320	-	0.003675	0.00534
5.0	0.002114	-	0.003877	0.00537
5.5	0.001907	-	0.004066	0.00542
6.0	0.001730	-	0.004135	0.00537
6.5	0.001624	-	0.004218	0.00536
7.0	0.001443	-	0.004280	0.00534
7.5	0.001392	-	0.004329	0.00531
8.0	0.001289	-	0.004366	0.00529
8.5	0.001160	-	0.004400	0.00527
9.0	0.001108	-	0.004420	0.00524
9.5	0.001057	-	0.004440	0.00521
10.0	0.000830	-	0.004540	0.00519

TABLE AD2 Components of the drag coefficient for the body at different Mach numbers.

M	C_{Df}	C_{Db}	C_{Dp}	C_{Dp}	C_{DN2}	C_{DA}	$C_{DA(NC)}$
0.8	0.08808	0.000587	-	-	-	-	-
0.9	0.08007	0.006136	0.00795	-	-	-	-
1.0	0.08007	0.016874	0.00795	0.083	-	-	-
1.1	0.07807	0.012272	0.00375	0.145	-	-	-
1.2	0.07567	0.009972	0.00100	0.154	-	-	-
1.5	0.06806	0.001022	-	-	0.10869	0.03168	0.0222
2.0	0.06245	0.002315	-	-	0.10640	0.02620	0.0222
2.5	0.05485	0.005676	-	-	0.09496	0.02200	0.0222
3.0	0.04964	0.007670	-	-	0.08695	0.02020	0.0222
3.5	0.04404	0.007593	-	-	0.08009	0.01843	0.02222
4.0	0.04004	0.007287	-	-	0.07780	0.01613	0.0222
4.5	0.03603	0.006443	-	-	0.07440	0.01469	0.0222
5.0	0.03283	0.005753	-	-	0.07322	0.01354	0.0222
5.5	0.02963	0.004909	-	-	0.07151	0.01267	0.0222
6.0	0.02722	0.04295	-	-	0.06980	0.01152	0.0222
6.5	0.02522	0.00399	-	-	0.06868	0.01037	0.02221
7.0	0.02242	0.03990	-	-	0.06750	0.01008	0.0222
7.5	0.02162	0.03990	-	-	0.06693	0.00922	0.0222
8.0	0.02002	0.03990	-	-	0.06636	0.00864	0.0222
8.5	0.01842	0.03990	-	-	0.06579	0.00806	0.0222
9.0	0.01722	0.03990	-	-	0.06521	0.00777	0.0222
9.5	0.01644	0.03990	-	-	0.06464	0.07488	0.0222
10.0	0.01353	0.03990	-	-	0.06407	0.006912	0.0222

TABLE AD3 C_{D0} for the different Mach numbers.

M	$(C_{D0})_{total}$
0.0	0.012051
0.5	0.012988
0.8	0.012988
0.9	0.014719
1.0	0.034345
1.1	0.039220
1.2	0.039493
1.5	0.037375
2.0	0.028804
2.5	0.025900
3.0	0.024200
3.5	0.022705
4.0	0.021767
4.5	0.020770
5.0	0.020104
5.5	0.019427
6.0	0.018758
6.5	0.018237
7.0	0.017658
7.5	0.017373
8.0	0.017012
8.5	0.016643
9.0	0.016390
9.5	0.016125
10.0	0.015517

TABLE AD4 Shows C_L for the different Mach numbers.

M					
1.5	-	0.4292	-	5.7	2.188
2.0	-	0.6650	-	5.45	2.092
2.5	-	0.8794	-	5.0	1.9193
3.0	0.921	-	4.70	-	1.662
3.5	0.777	-	4.60	-	1.371
4.0	0.673	-	4.40	-	1.136
4.5	0.594	-	4.30	-	0.980
5.0	0.532	-	4.22	-	0.861
5.5	0.482	-	4.18	-	0.773
6.0	0.440	-	4.16	-	0.703
6.5	0.406	-	4.14	-	0.645
7.0	0.376	-	4.14	-	0.598
7.5	0.350	-	4.13	-	0.556
8.0	0.328	-	4.13	-	0.520
8.5	0.309	-	4.12	-	0.488
9.0	0.291	-	4.10	-	0.458
9.5	0.276	-	4.07	-	0.431
10.0	0.262	-	4.05	-	0.407

TABLE AD5 C_L /rad, C_L /degree, and K for different Mach numbers.

M	C_L /rad	K
0.1	1.633	0.31032
0.2	1.640	0.31032
0.3	1.645	0.31032
0.4	1.651	0.31032
0.5	1.656	0.31032
0.6	1.662	0.31032
0.7	1.670	0.31032
0.8	1.689	0.31032
1.5	2.188	0.35000
2.0	2.092	0.43000
2.5	1.919	0.57100
3.0	1.662	0.60200
3.5	1.371	0.72940
4.0	1.136	0.88020
4.5	0.980	1.02000
5.0	0.861	1.16100
5.5	0.773	1.29400
6.0	0.703	1.42200
6.5	0.645	1.55000
7.0	0.598	1.67200
7.5	0.556	1.79900
8.0	0.520	1.92200
8.5	0.488	2.04900
9.0	0.458	2.18300
9.5	0.431	2.32000
10.0	0.407	2.45700

TABLE AD6 C_L , C_D , and C_L/C_D for our mission profile.

M	C_L	C_D	C_L/C_D
0.8	0.37966	0.05902	6.43292
1	0.24244	0.05541	4.37519
1.2	0.16807	0.05135	3.27296
1.5	0.10727	0.05075	2.11384
2.0	0.06003	0.03755	1.59855
3.0	0.03597	0.03103	1.15919
4.0	0.03542	0.027319	1.2964
5.0	0.03524	0.02657	1.32637
6.0	0.03531	0.02522	1.40017
7.0	0.03371	0.02397	1.40635
8.0	0.3308	0.02337	1.41544
9.0	0.03108	0.0226	1.35729
10.0	0.02883	0.02144	1.34487
10.0	0.02947	0.02153	1.36874
10.0	0.03010	0.02162	1.39206
10.0	0.03074	0.02172	1.4154
10.0	0.03139	0.02182	1.4388

MACH .8			
Cm cg	Angle of Attack	CL	CD
.0009005	0.0	0.0	.0129885
-.046966	3.459	0.1	.016090
-.094403	6.917	0.2	.025400
-.141408	10.376	0.3	.040920
-.187984	13.835	0.4	.062640
-.234129	17.293	0.5	.090569
-.279844	20.752	0.6	.124705
-.325128	24.211	0.7	.165047
-.369982	27.669	0.8	.211596
-.414405	31.128	0.9	.264351
-.458398	34.586	1.0	.323312

Table S1: $C_{m_{cg}}$ vs. α, C_L, C_D ($M=.8$)

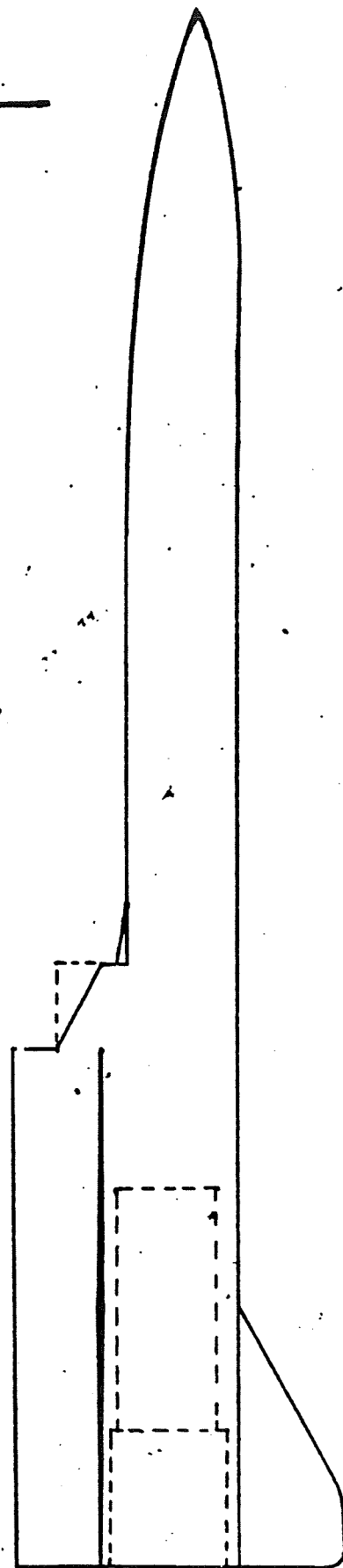
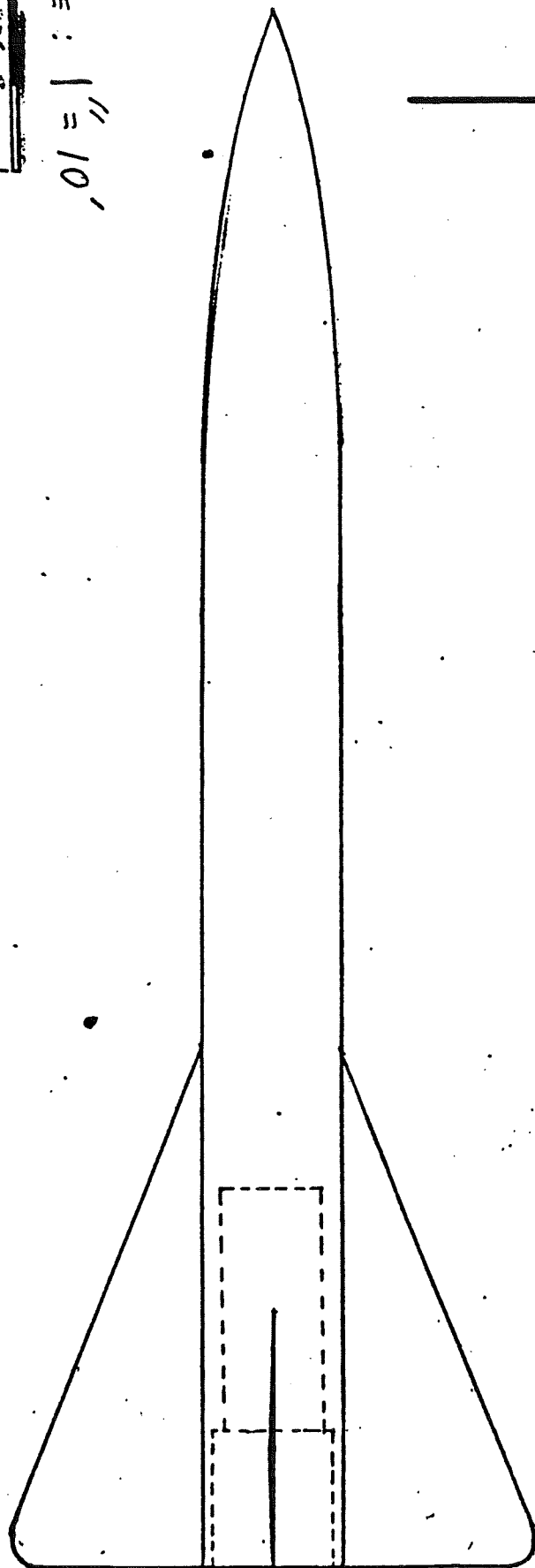
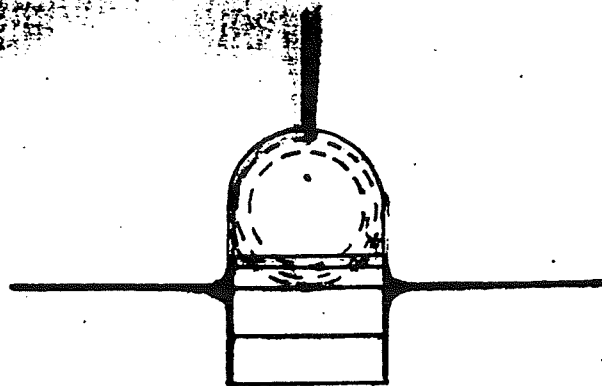
MACH 2			
Cm cg	Angle of Attack	CL	CD
.0019975	0.0	0.0	.028804
-.0457467	2.563	0.1	.033674
-.0928155	5.126	0.2	.048284
-.1392088	7.689	0.3	.072634
-.1849266	10.252	0.4	.106724
-.2299690	12.815	0.5	.150554
-.2743360	15.378	0.6	.204124
-.3180274	17.941	0.7	.267434
-.3610434	20.504	0.8	.340484
-.4033839	23.067	0.9	.423274
-.4450489	25.630	1.0	.515804

Table S2: $C_{m_{cg}}$ vs. α, C_L, C_D ($M=2$)

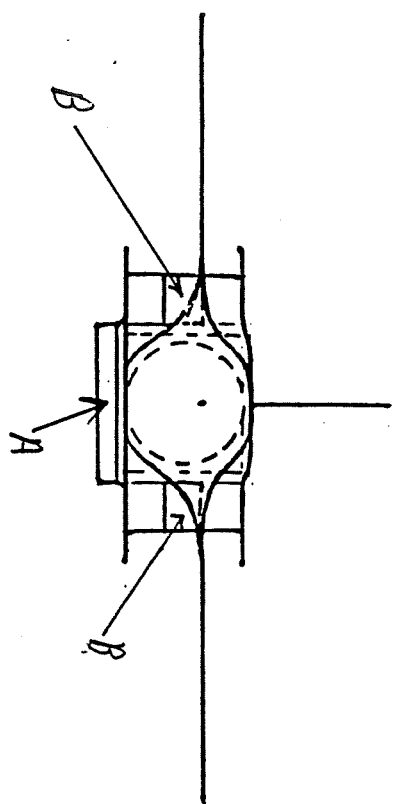
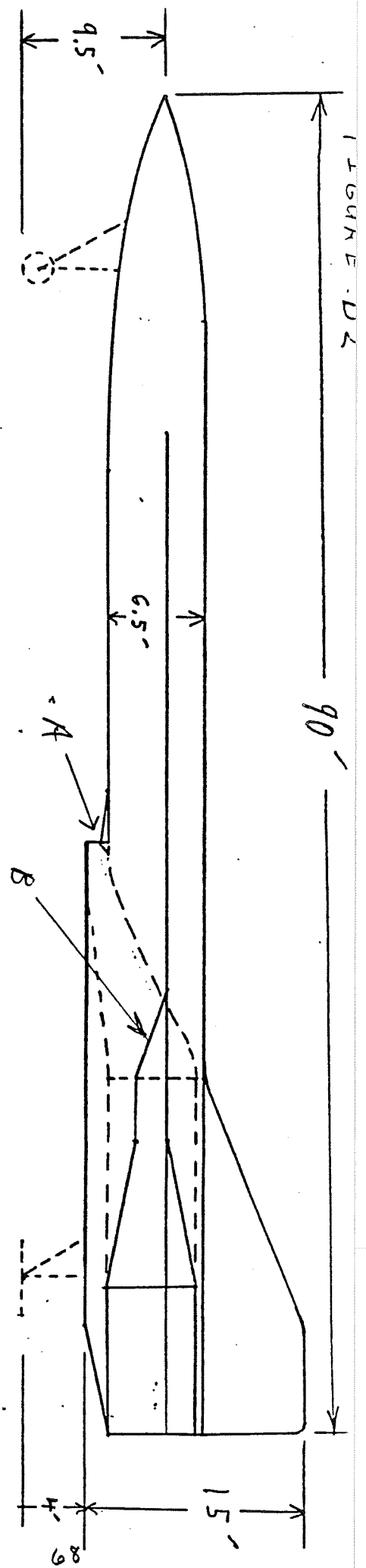
MACH 10			
Cm cg	Angle of Attack	CL	CD
.0010761	0.0	0.0	.015517
-.003715	1.408	0.01	.01576
-.008472	2.816	0.02	.01650
-.013195	4.223	0.03	.01773
-.017884	5.631	0.04	.01945
-.022539	7.039	0.05	.02166
-.027160	8.447	0.06	.02436
-.031746	9.854	0.07	.02756
-.036299	11.262	0.08	.03124
-.040817	12.670	0.09	.03542
-.045302	14.078	0.10	.04009
-.088272	28.155	0.20	.11380
-.127834	42.233	0.30	.23665
-.163989	56.310	0.40	.40864
-.196735	70.388	0.50	.62977
-.226074	84.466	0.60	.90004

Table S3: $C_{m_{cg}}$ vs. α, C_L, C_D ($M=10$)

SCALE : 1" = 10'



ORIGINAL PAGE IS
OF POOR QUALITY



1" = 10'

ORIGINAL PAGE IS
OF POOR QUALITY

A - TURBOFAN JET INLET
B - SCRAMJET INLET

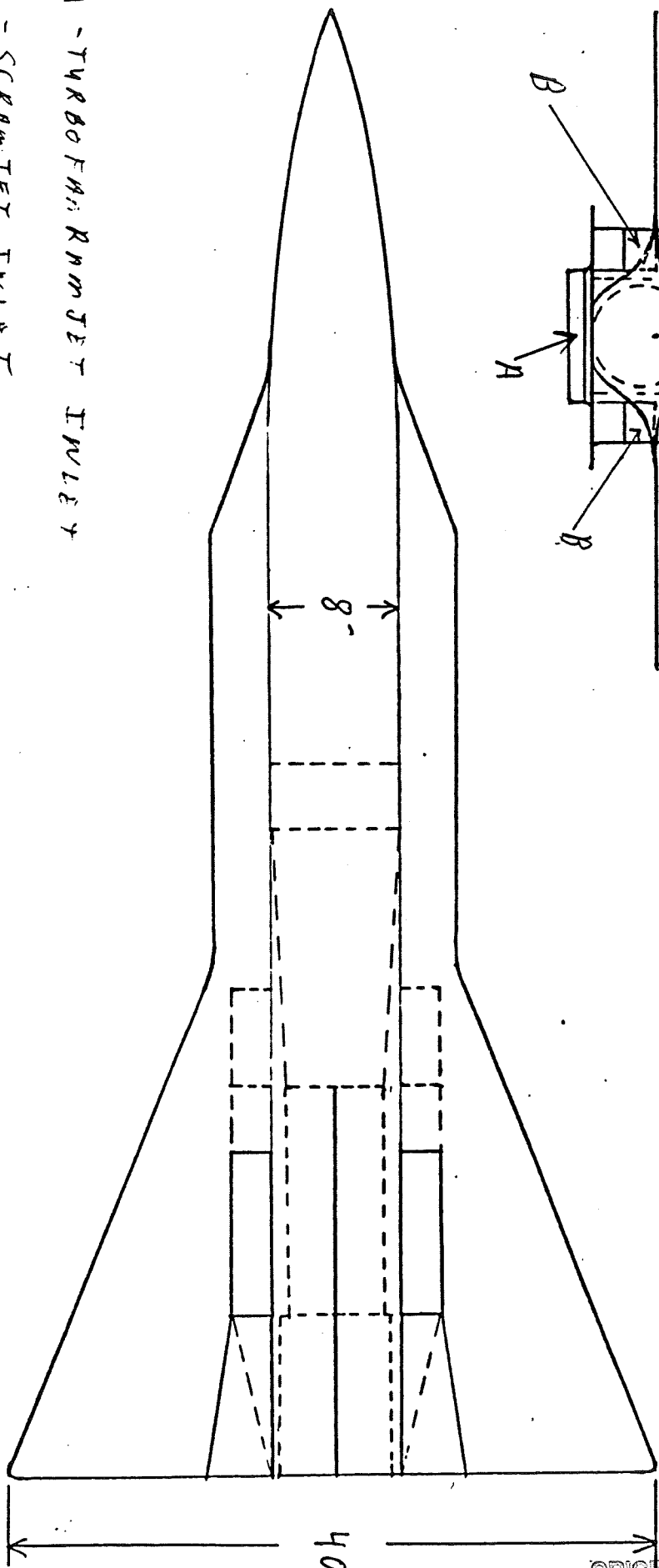
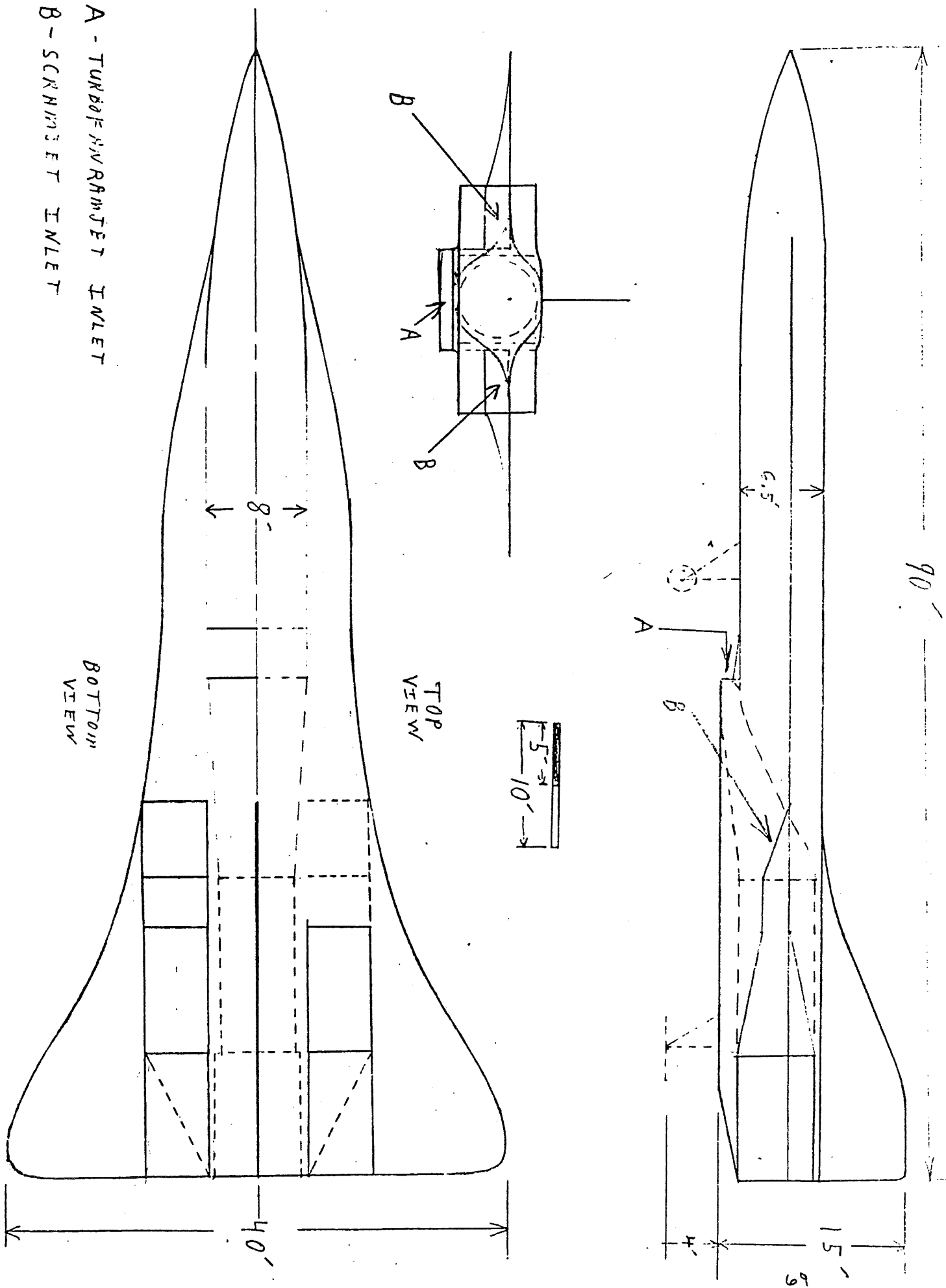
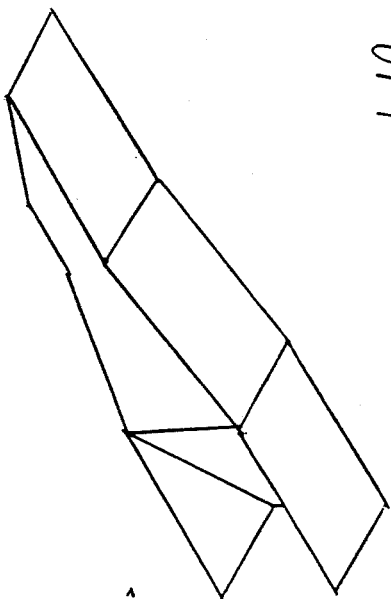


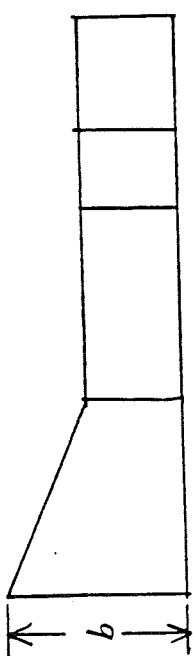
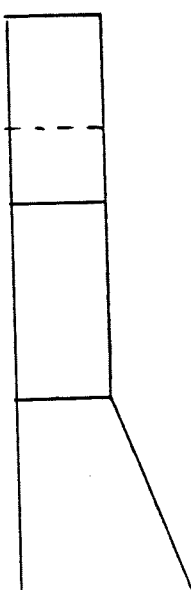
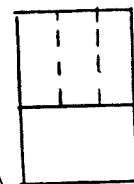
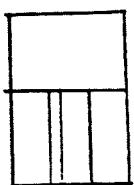
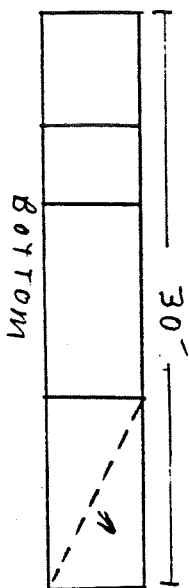
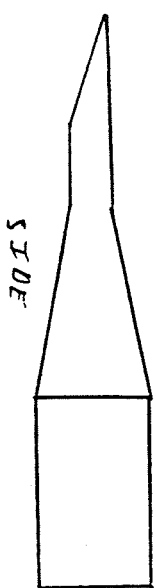
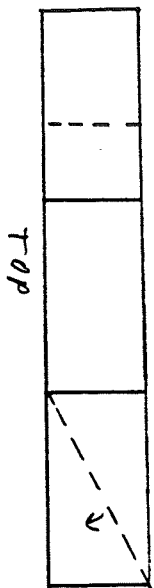
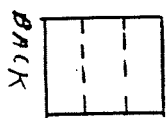
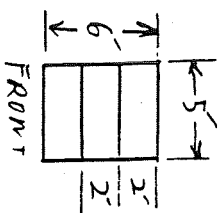
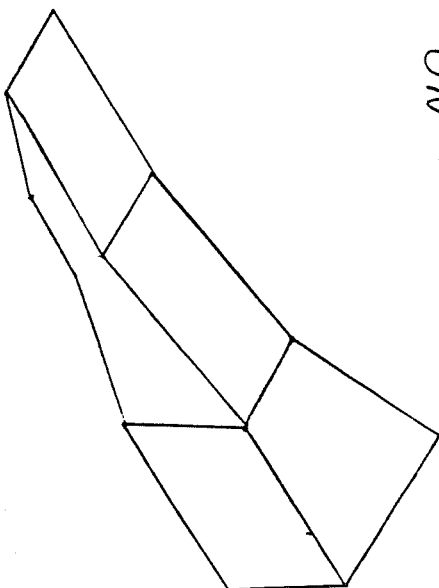
FIGURE D3



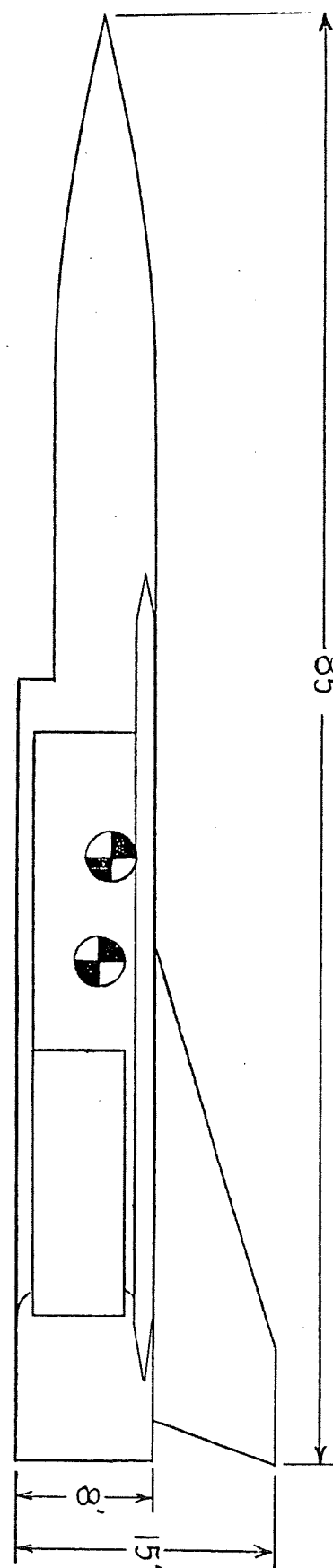
OFF



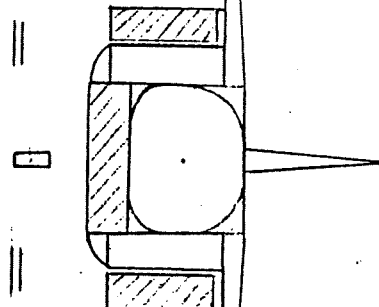
ON



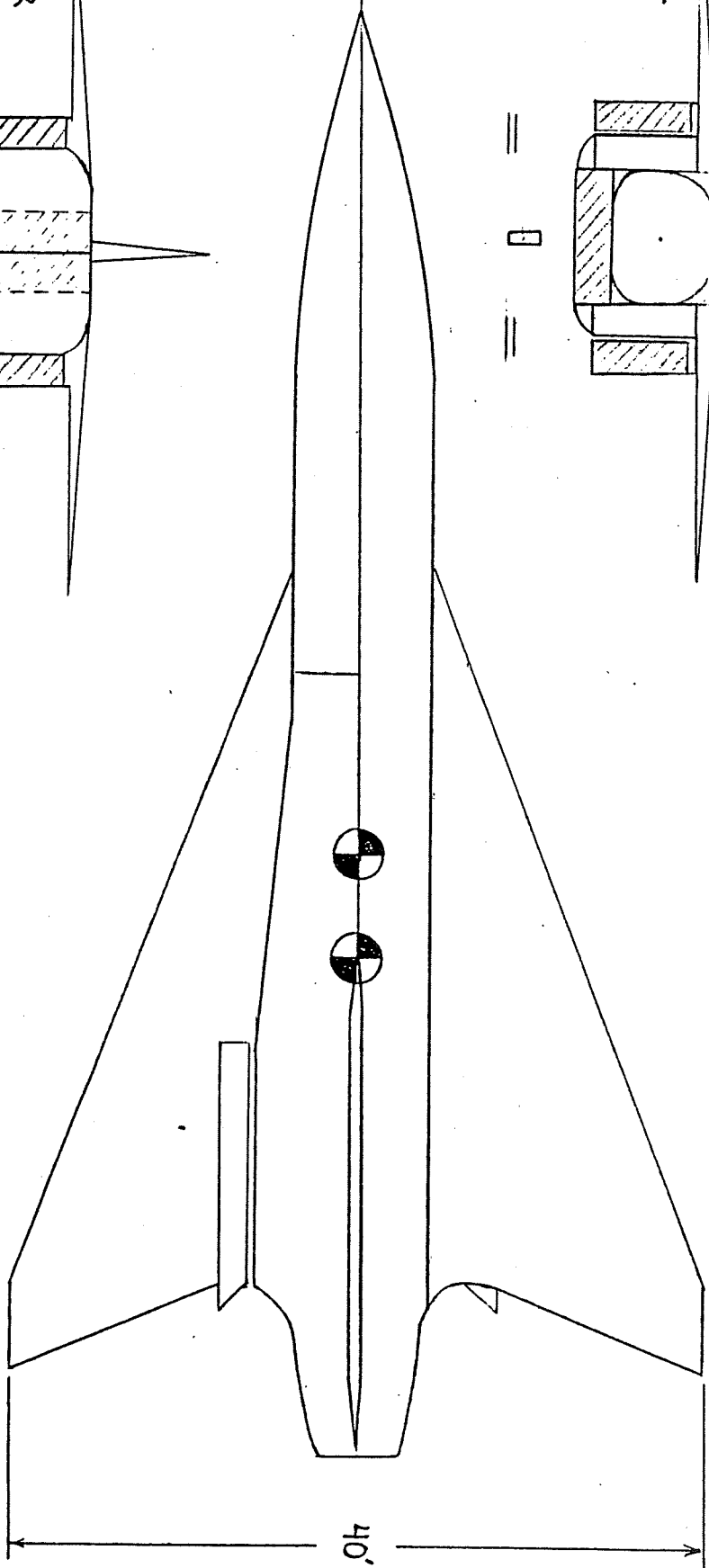
85'



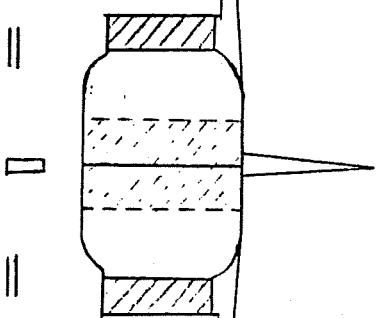
FRONT



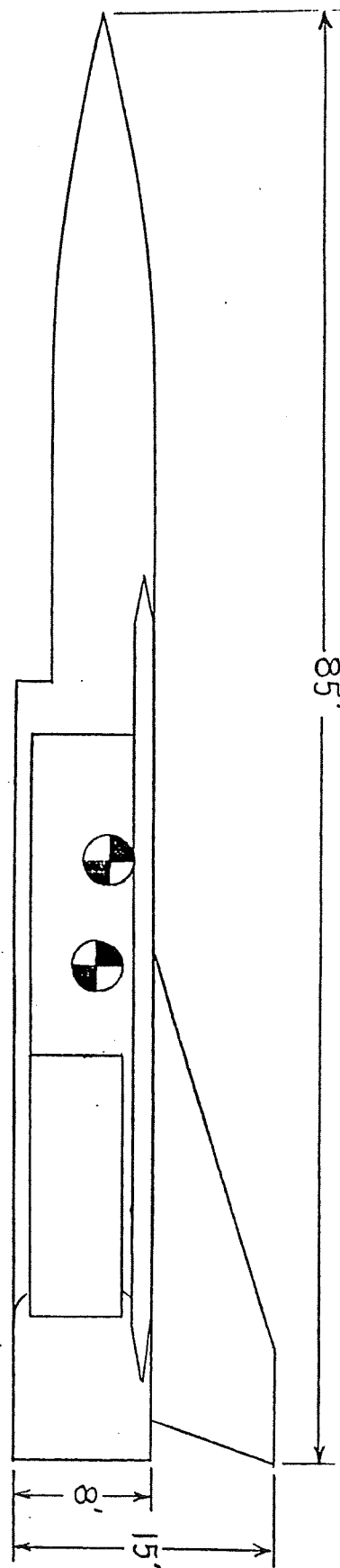
TOP
BOTTOM



REAR

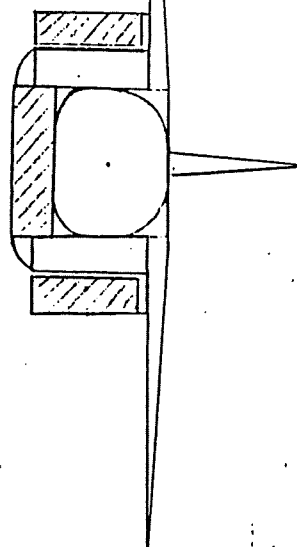


85'



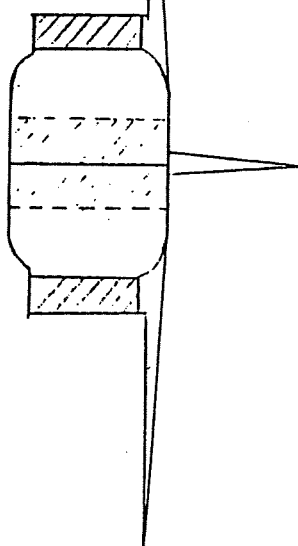
27

FRONT



TOP
BOTTOM

REAR



CLOSED
POSITION

OPENED
POSITION

40'

Vehicle Summary

Vehicle Name: tscram

Vehicle Description: UMANNED SCRAMJET TESTBED

File = B:GOLD.DAT
Date = 01-01-1980
Time = 00:01:27

Output File = B:GOLD.OUT
Date = 01-01-1980
Time = 00:03:13

h = 73	Height = 8	Span = 32	TRoot = 5.1
y = 1,570	SWing = 508	SVert = 51	SHorz = 0
Number of: RamJets = 5	Rockets = 0	TurbRamJets = 0	
Weight of: = 100,000	= 0	= 0	
= 10,000	Fuel Density = 4.389	LOX = 0	
Weights: GTOW = 44,133	Payload = 0	Dry = 33,903	
Landing = 34,013	Entry = 34,093		
Weights: GTOW/S = 86.94	AR = 1.980	T/GTOW = 11.33	T/S = 985.00

Weight Statement

=====			
Group 1:	Aero surfaces	910	
	Wing	549	
	Vertical	361	
	Horizontal	0	
	Fairing	0	
Group 2:	Body structure		12,821
	Basic body	6,182	
	Secondary	1,539	
	Thrust	3,194	
	Integral fuel tanks	1,906	
	Integral Ox tanks	0	
Group 3:	Thermal Protection System		2,352
	Vehicle insulation	2,352	
	Cover panels	0	
Group 4:	Launch and Recovery Gear		1,638
	Launch gear	110	
	Landing gear	1,527	
Group 5:	Propulsion		10,959
	Rocket engines	0	
	Ramjets	7,000	
	Turboramjet	0	
	Nonstructural fuel tank	0	
	Nonstructural Ox tank	0	
	Fuel tank insulation	704	
	Ox tank insulation	706	
	Fuel system	650	
	Oxidizer system	299	
	Pressurization system	1,025	
	Inlets	175	

FIGURE WEIGHT 1

Group 6:	Orientation Control System		894
	Engine gimbal system	0	
	Attitude control system	183	
	Aerodynamic controls	579	
	Seperation system	132	
	ACS tankage	0	
Group 8:	Power supply		754
	Electrical System	716	
	Hydraulic/Pneumatic Sys	38	
Group 10:	Avionics		3,153
Group 14:	Crew Provisions		422

	Vehicle Dry Weight		33,903
Group 17:	Crew		35
Group 18:	Payload		0
Group 21:	Residual Propellant		75
	Trapped fuel	75	
	Trapped Oxidizer	0	

	Landing Weight		34,013
Group 22:	Reserve Propellants		80
	Fuel	80	
	Oxidizer	0	
	ACS fuel	0	
	ACS oxidizer	0	

	Entry Weight		34,093
Group 23:	Inflight Losses		40
	Fuel	40	
	Oxidizer	0	
Group 25:	Main Propellants		10,000
	Fuel	10,000	
	Oxidizer	0	

	Gross Weight		44,133

FIGURE WEIGHT 1
CONTINUED

Gold Weight Estimate

Thomas Greiner

Structure-

Skin 7955 lb.

Internal 2386 lb.

Total 10,341 lb.

Engines

Scramjets 1500 lb. x 4 12,000 lb.

T.F.R.J. 6500 lb. 6500 lb.

Total 18,500 lb.

Electrical

Computers 75 lb.

Batteries 300 lb.

Avionics 100 lb.

Transmitter 35 lb.

Total 510 lb.

Cooling Systems

Coolant 315 lb.

Distribution 435 lb.

Heat Exchanger 485 lb.

Pumps 75 lb.

Total 1310 lb.

Fuel Tank 4013 lb.

Insulation 400 lb.

Landing Gear 200 lb. Empty Weight 36,274 lb.

Fuel 11,500 lb. Gross Weight 47,774 lb.

Figure: Weight2

**ORIGINAL PAGE IS
OF POOR QUALITY**

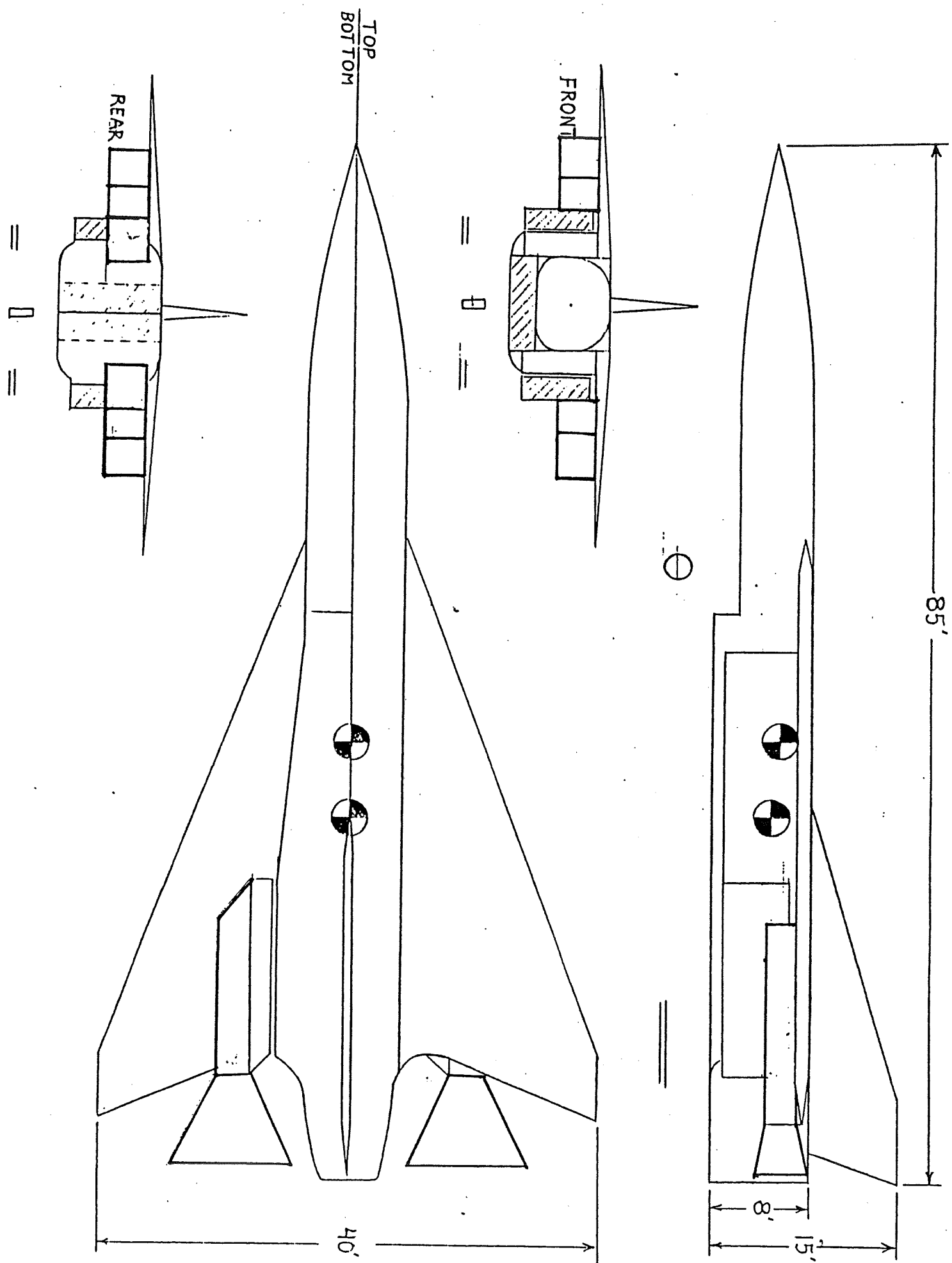


FIG 8 BOOSTER 1

Rocket Booster Fuel Estimate for Hypersonic Vehicle -----

Aircraft weight 47000 lb

Estimated booster weight 15000 lb

Estimated total weight 62000 lb.

Specific Impulse 240 s

1g acceleration

Mach #	Vel (ft/s)	Thrust (lb)	t (s)	Total t (s)	W-dot (lb/s)	Rocket Fuel (lb)	SFC Seconds
0.8	774.35	0	0	0	0	0	0.000099
1	967.94	62000	6.012111	6.012111	258.3333	1553.128	0.0002
1.2	1161.53	60436.18	6.012111	12.02422	251.8174	1513.954	0.000196
1.5	1451.913	58888.26	9.018105	21.04232	245.3677	2212.752	0.000194
2	1935.834	56610.25	15.03015	36.07248	235.8760	3545.254	0.00021
2.5	2419.85	52887.42	15.03	51.10248	220.3642	3312.075	0.000219
							12137.16

Figure: Booster2

Drag	TFRJ Fuel (lb/s)	TFRJ Fuel (lbs.)	A/C Weight (lb.)	rocket Volume (ft^3)	Section length ft	
7177	0.710523	0	62000	0	0	0
8886.99	1.777398	10.68591	60436.18	15.30176	3.117252	74.55018
14413.38	2.825022	33.96870	58888.26	14.91580	3.038626	71.21642
15984	3.100896	65.25007	56610.25	21.80051	4.441168	103.0257
23442	4.92282	177.5783	52887.42	34.92861	7.115604	178.6808
31258	6.845502	349.8221	49225.52	32.63128	6.647595	174.0826
		637.3051			24.36024	601.5558

Figure: Booster2 continued.

Q based on M=6 at 70,000

a= 967.9421

v= 5807.6528078

Q= 2359.837

CLIMB ANGLE=4 DEGREES

Vint 1404.843

M=.8=774.353FT/S

Altitude (ft.)	Temp. (R)	Density (slug/ft ³)	Q (SLUG/S ²)	V (FT/S)	M
40000	389.99	0.000587		774.3537	0.8
40000	389.99	0.000587		967.9421	1
40000	389.99	0.000587		1161.530	1.2
40000	389.99	0.000587		1451.913	1.5
40000	389.99	0.000587		1935.884	2
40000	389.99	0.000587		2419.855	2.5
40000	389.99	0.000587	2359.837	2834.895	2.928786
45000	389.99	0.000482	2359.837	3195.274	3.301100
50000	389.99	0.000364	2359.837	3601.297	3.720571
55000	389.99	0.000287	2359.837	4058.621	4.193041
60000	389.99	0.000226	2359.837	4573.796	4.725278
65000	389.99	0.000178	2359.837	5154.053	5.324754
70000	389.99	0.000140	2359.837	5807.651	5.999999
75000	389.99	0.000110		5807.651	5.999999
80000	389.99	0.000087		5807.651	5.999999
85000	394.32	0.000068		5839.803	5.999999
90000	402.48	0.000053		5899.918	5.999999
95000	410.64	0.000041		5959.426	5.999999
100000	418.79	0.000032		6018.274	5.999999
100000	418.79	0.000032		6519.798	6.5
100000	418.79	0.000032		7021.321	7
100000	418.79	0.000032		7522.844	7.5
100000	418.79	0.000032		8024.367	8
100000	418.79	0.000032		8525.890	8.5
100000	418.79	0.000032		9027.413	9
100000	418.79	0.000032		9528.936	9.5
100000	418.79	0.000032		10030.45	10
100000	418.79	0.000032		10030.45	10

Figure: Profile1

dist (angle 4)	t (seconds)	Total t (seconds)	x (ft)	Total Dist (ft)	Total Dist (miles)	acc ft/s ²	G
	5	5	3871.768	3871.768	0.733289	0	0
	20	25	17422.95	21294.72	4.033092	9.679421	0.300603
	20	45	21294.72	42589.45	8.066184	9.679421	0.300603
	20	65	26134.43	68723.89	13.01588	14.51913	0.450904
	20	85	33877.97	102601.8	19.43217	24.19855	0.751507
	20	105	43557.39	146159.2	27.68167	24.19855	0.751507
71677.99	27.28121	132.2812	71505.44	217664.7	41.22437	15.21341	0.472466
71677.99	23.77312	156.0543	71505.44	239170.1	54.76707	15.15907	0.470778
71677.99	21.09239	177.1467	71505.44	360675.6	68.30977	19.24974	0.597818
71677.99	18.71507	195.8618	71505.44	432181.0	81.85247	24.43610	0.758885
71677.99	16.60670	212.4685	71505.44	503686.4	95.39516	31.02211	0.963419
71677.99	14.73665	227.2051	71505.44	575191.9	108.9378	39.37510	1.222829
71677.99	13.07789	240.2830	71505.44	646697.3	122.4805	49.97733	1.552091
71677.99	12.34199	252.6250	71505.44	718202.8	136.0232	0	0
71677.99	12.34199	264.9670	71505.44	789708.2	149.5659	0	0
71677.99	12.30792	277.2749	71505.44	861213.7	163.1086	2.612280	0.081126
71677.99	12.21119	289.4861	71505.44	932719.1	176.6513	4.922911	0.152885
71677.99	12.03801	301.5741	71505.44	1004224.	190.1940	4.922911	0.152885
71677.99	11.96857	313.5427	71505.44	1075730	203.7367	4.916878	0.152698
	43	356.5427	269568.5	1345298.	254.7914	11.66334	0.362215
	43	399.5427	291134.0	1636432.	309.9304	11.66332	0.362215
	70	469.5427	509045.7	2145478.	406.3406	7.164613	0.222503
	70	539.5427	544152.4	2689630.	509.3997	7.164613	0.222503
	70	609.5427	579259.0	3268889.	619.1079	7.164613	0.222503
	70	679.5427	614365.6	3883255.	735.4650	7.164613	0.222503
	70	749.5427	649472.2	4532727.	858.4711	7.164613	0.222503
	70	819.5427	684578.8	5217306.	988.1262	7.164613	0.222503
	120	939.5427	1203655	6420961.	1216.091	0	0

M=.8 to 6

time	minutes	x-dist	miles
939.5427	15.65904	5217306.	988.1262

M=6 to 10

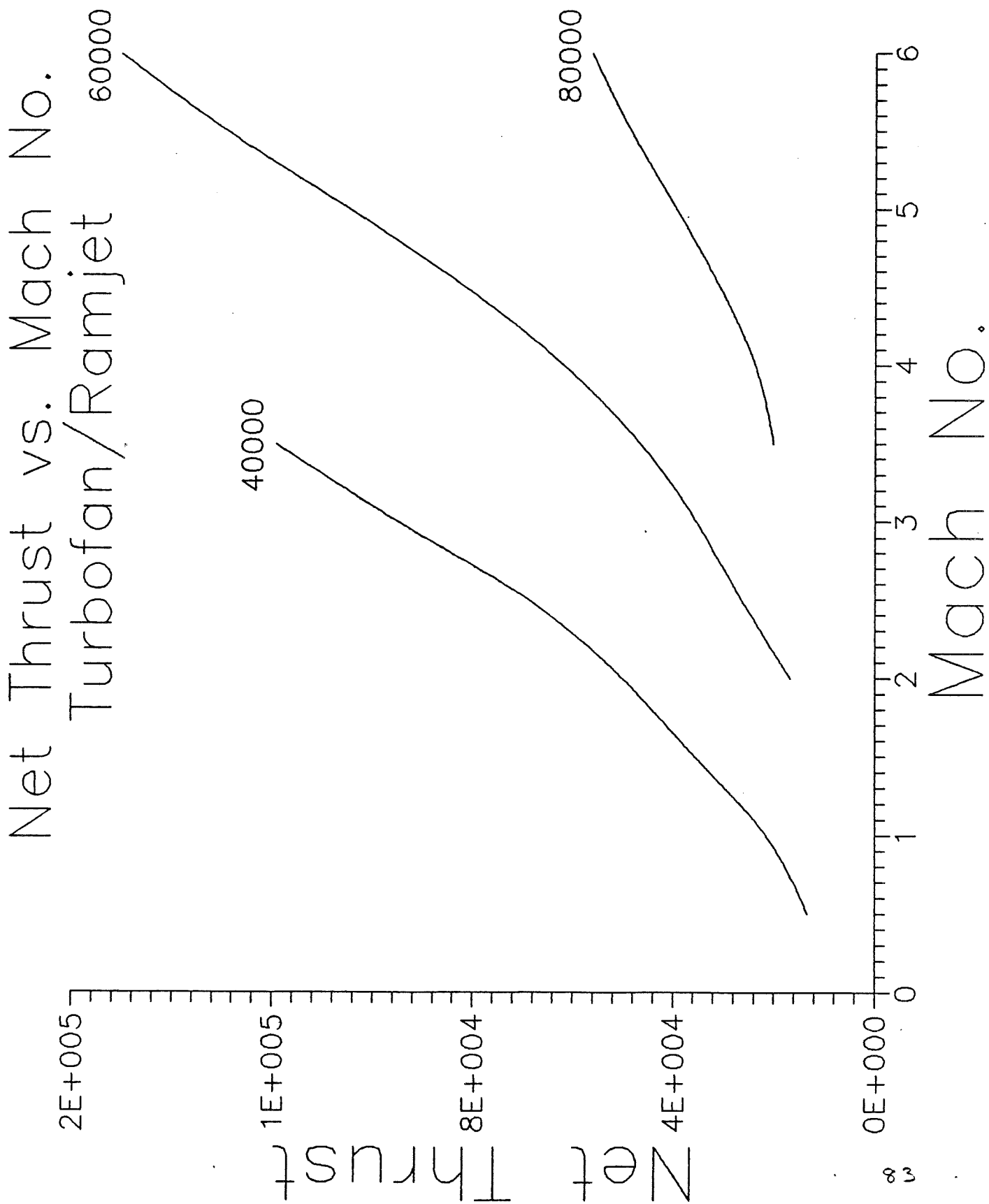
time	minutes	x-dist	miles
626	10.43333	5345231.	1012.354

Figure: Profile1

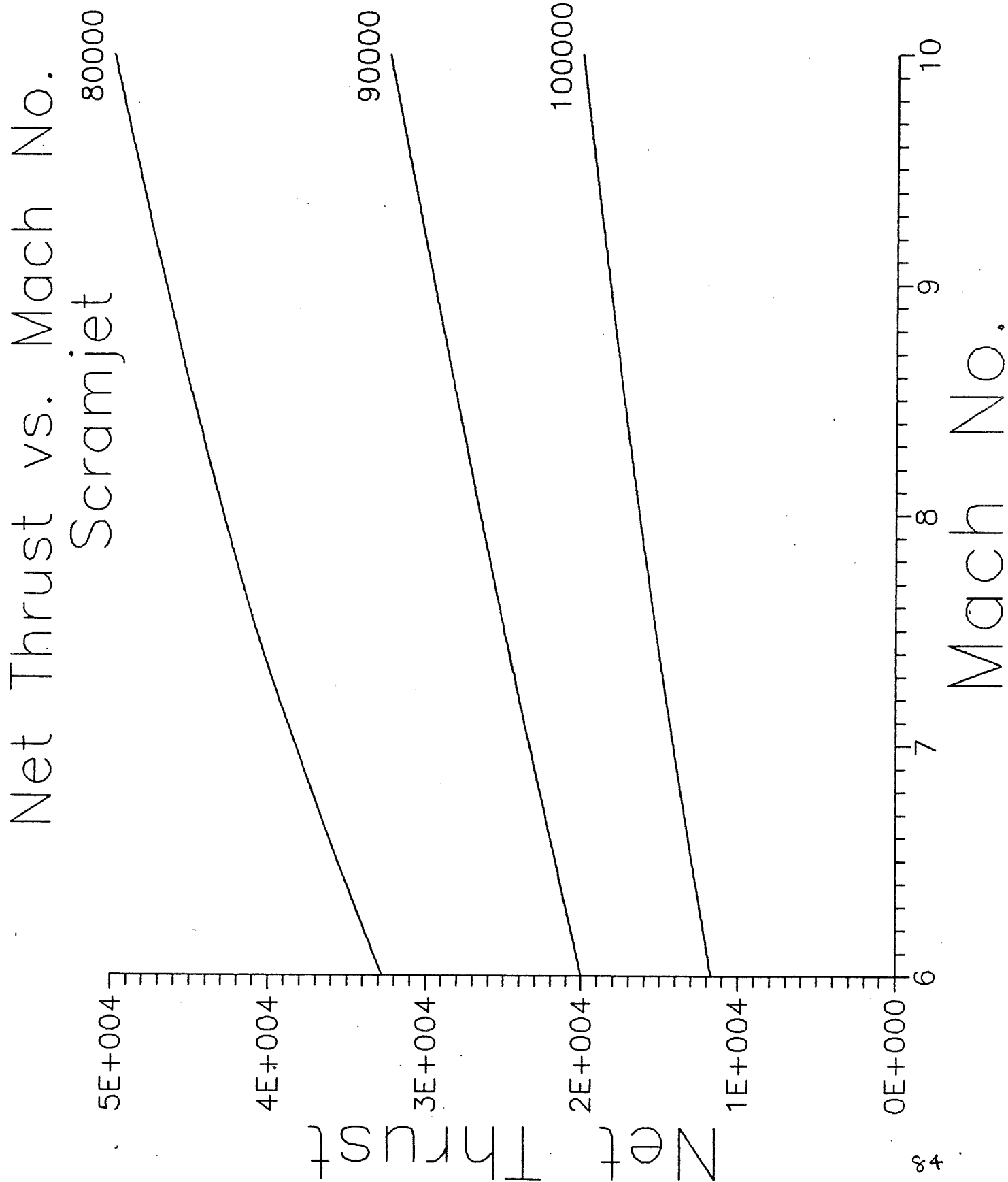
Thrust acc	Drag	Thrust req	SFC hour	SFC seconds	Final lb/s	Final Weight burned	A/C Weight
0	5977	5977	0.357	0.000099	0.592719	2.963595	45000
13526.25	7252	20778.25	0.721	0.000200	4.161421	83.22843	44997.03
13501.23	11630	25131.23	0.709	0.000196	4.949456	98.98913	44913.80
20207.21	12849	33056.21	0.7	0.000194	6.427597	128.5519	44814.81
33582.08	18795	52377.08	0.8	0.000222	11.63935	232.7870	44686.26
33407.13	25046	58453.13	0.78	0.000216	12.66484	253.2969	44453.47
20883.09	12849.4	36871.53	0.63	0.000175	6.452518	176.0325	44200.18
20725.63	11500.0	35296.59	0.7	0.000194	6.863227	163.1603	44024.15
26220.89	11000.0	40280.48	0.73	0.000202	8.167986	172.2824	43860.99
33154.72	10153.7	46355.98	0.75	0.000208	9.657497	180.7408	43688.70
41916.43	9000.0	53951.39	0.845	0.000234	12.66359	210.3005	43507.96
52945.65	10000.0	65965.94	1	0.000277	18.32387	270.0326	43297.66
66782.81	10158.0	79942.26	1.063	0.000295	23.60517	308.7058	43027.63
0	11300.0	14279.91	1	0.000277	3.966644	48.95629	42718.92
0	11300.0	14276.50	1.02	0.000283	4.045009	49.92347	42669.97
3457.624	10990.0	17420.64	1.03	0.000286	4.984240	61.34564	42620.04
6506.606	10750.0	20225.34	1.045	0.000290	5.870969	71.69152	42558.70
6495.645	10670.0	20129.38	1.045	0.000290	5.843113	70.63167	42487.01
6476.899	10652.0	20087.71	1.12	0.000311	6.249511	74.79773	42416.37
15336.78	10652	25988.78	2	0.000555	14.43821	1241.686	42341.58
14878.42	11233	26111.42	2	0.000555	14.50634	1247.545	41099.89
8856.467	11790	20646.46	2	0.000555	11.47025	1605.836	39852.34
8499.162	12292	20791.16	2	0.000555	11.55064	1617.090	38246.51
8139.354	12832	20971.35	2	0.000555	11.65075	1631.105	36629.42
7776.427	13406	21182.42	2	0.000555	11.76801	1647.522	34998.31
7409.848	14007	21416.84	2	0.000555	11.89824	1665.754	33350.79
7038.647	14708	21746.64	2	0.000555	12.08147	1691.405	31685.03
0	14708	14708	2	0.000555	8.171111	1961.066	29993.63
		fuel	Volume				
		15006.36	3387.441				

Figure: Profile1
Continued

(Fig. ES-1)



(Fig. ES-2)



(Fig ES-3)

SFC vs. Mach No.
Scramjet

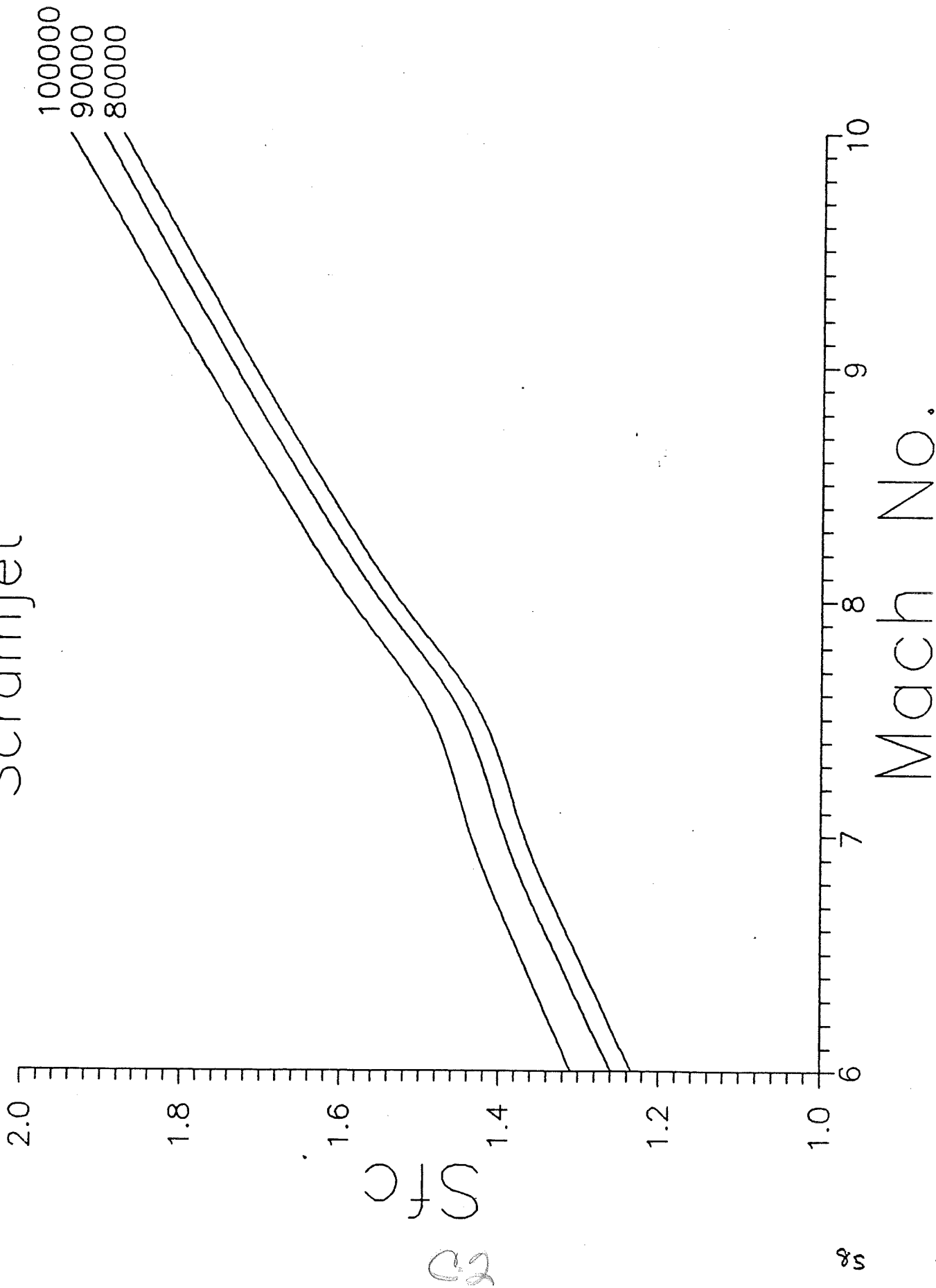


(Fig. E.S-4)

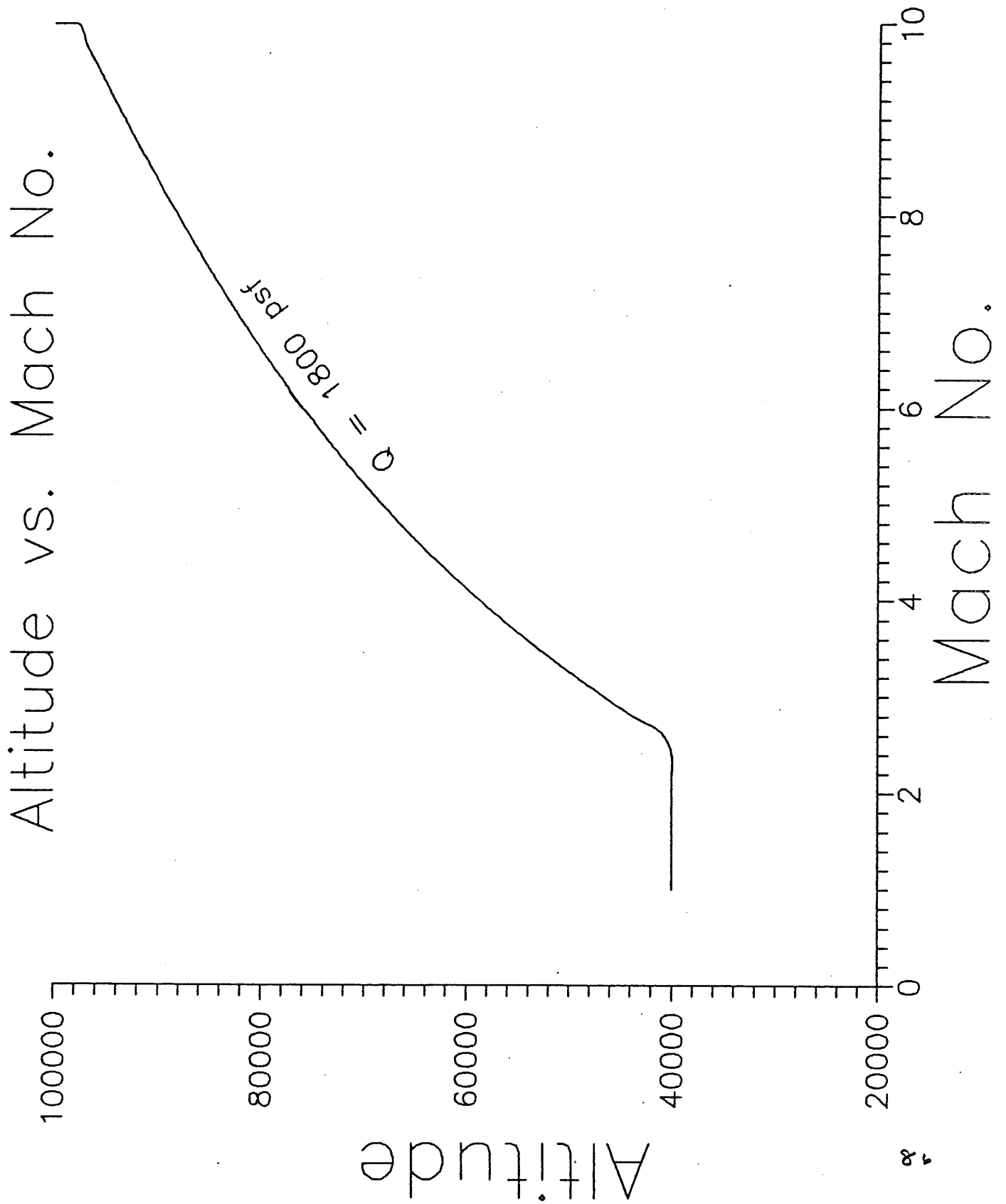


(Fig. ES-5)

Thrust/Drag vs. Mach No.

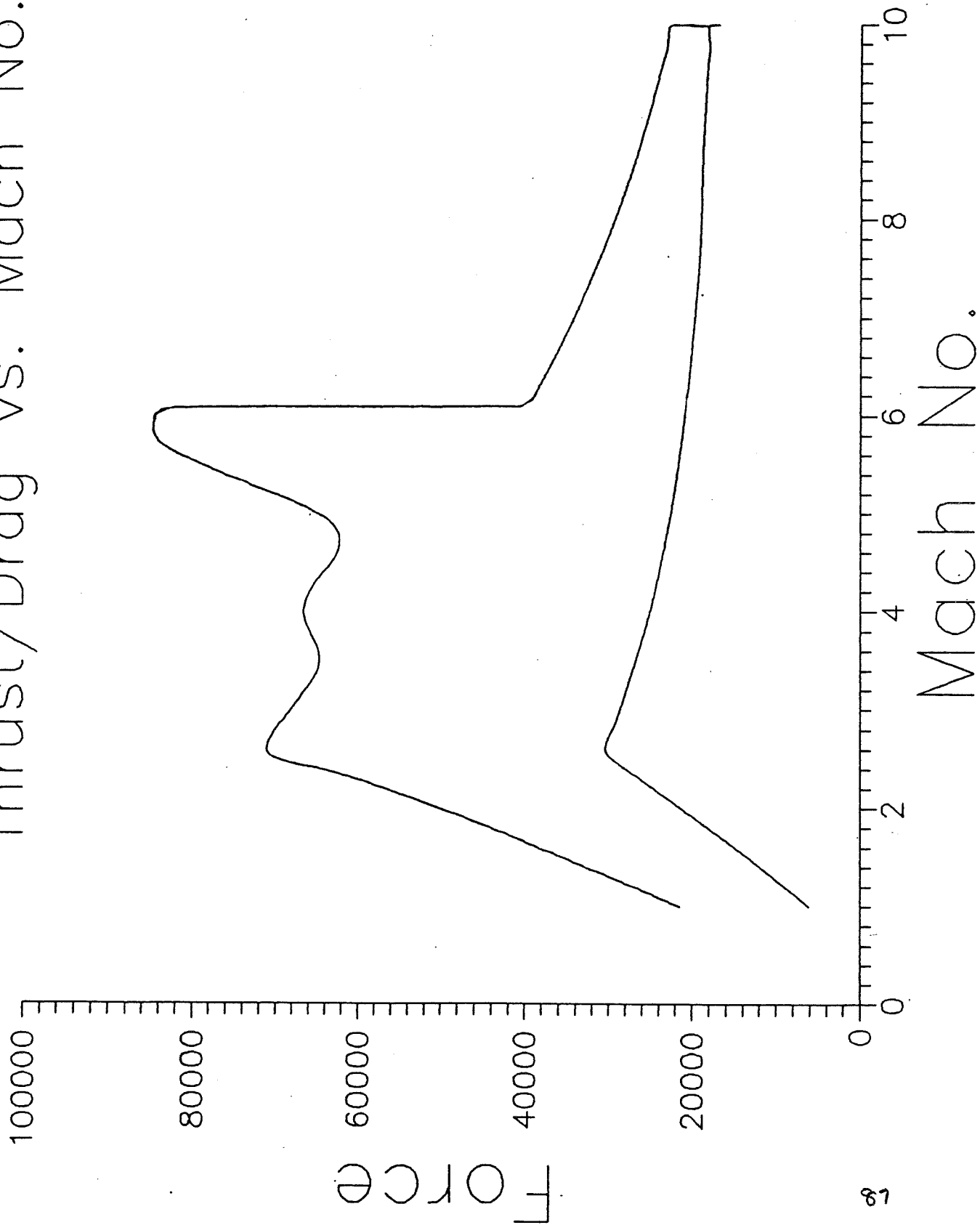


FIGURE: FN 1

INLET INSTALLED ON PLANE

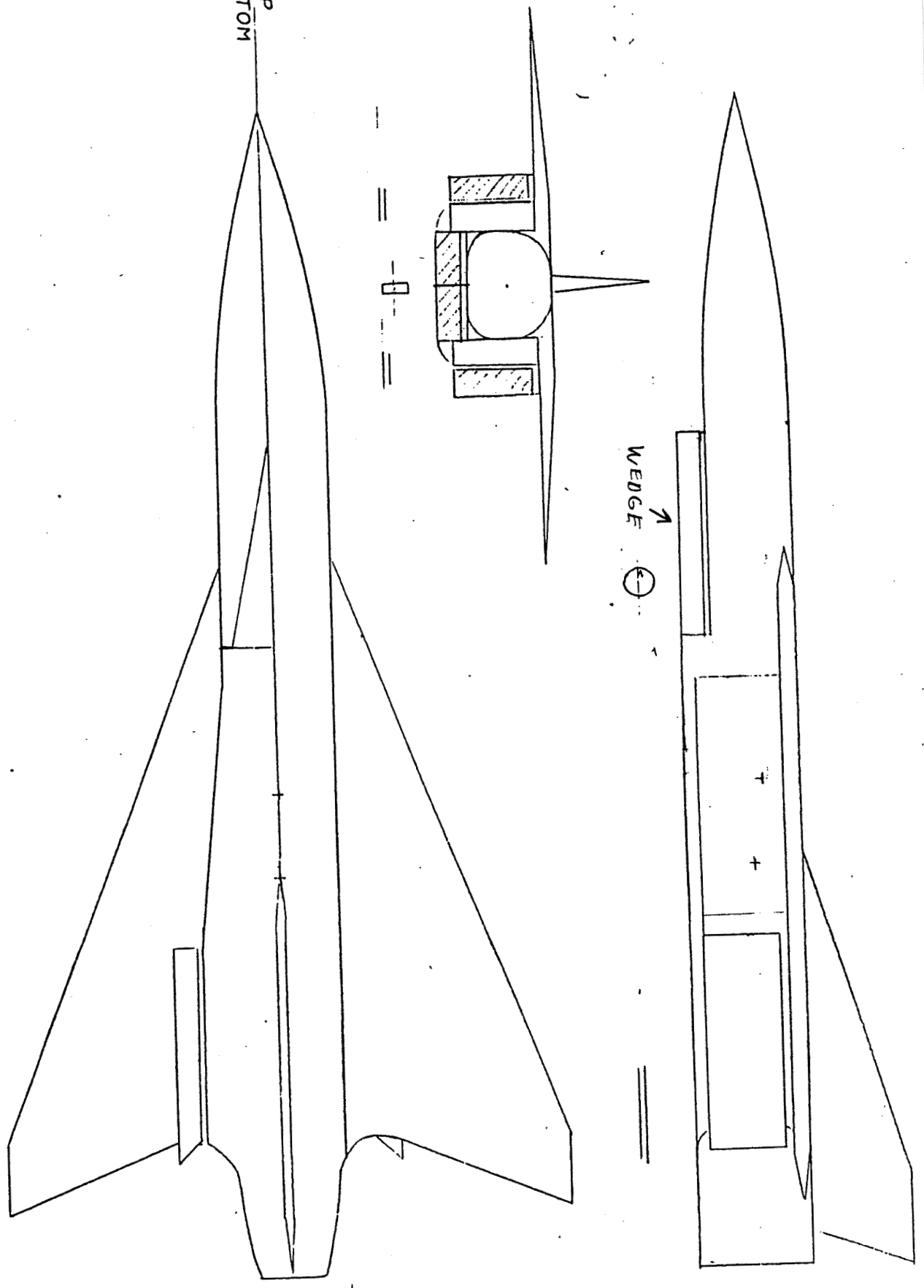


FIGURE IN 2 INLET OPEN AND CLOSED POSITIONS

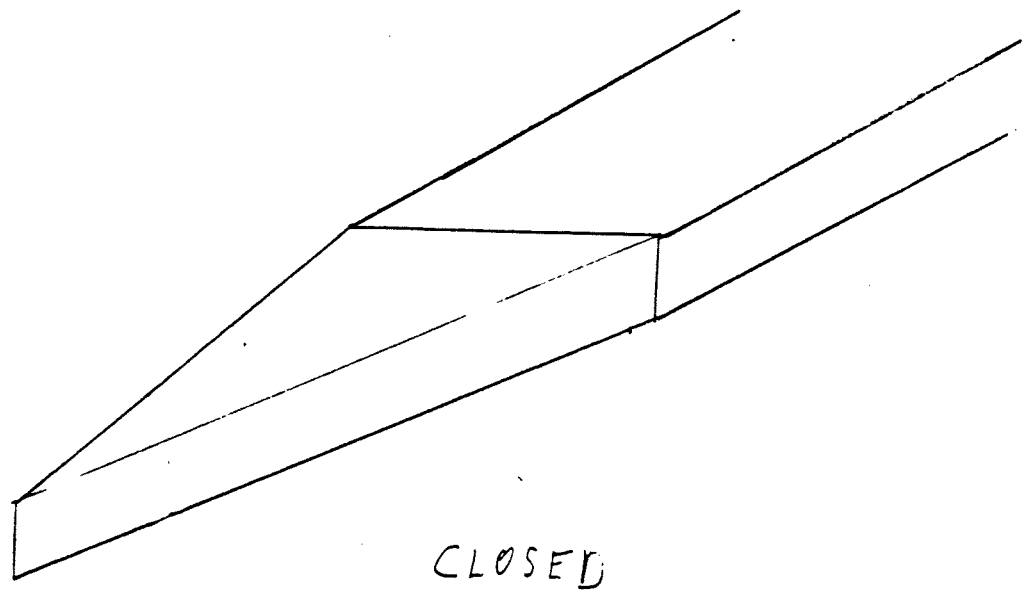
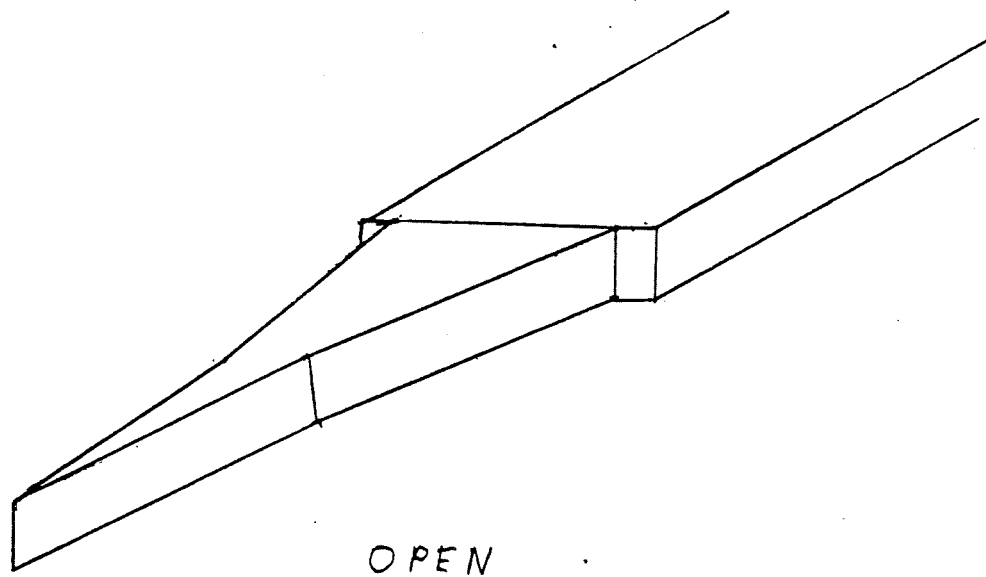


FIGURE IN3. WEDGE PROFILES AT $M_\infty = 3, 2, 1.4$

SCALE
1" \rightarrow 1'

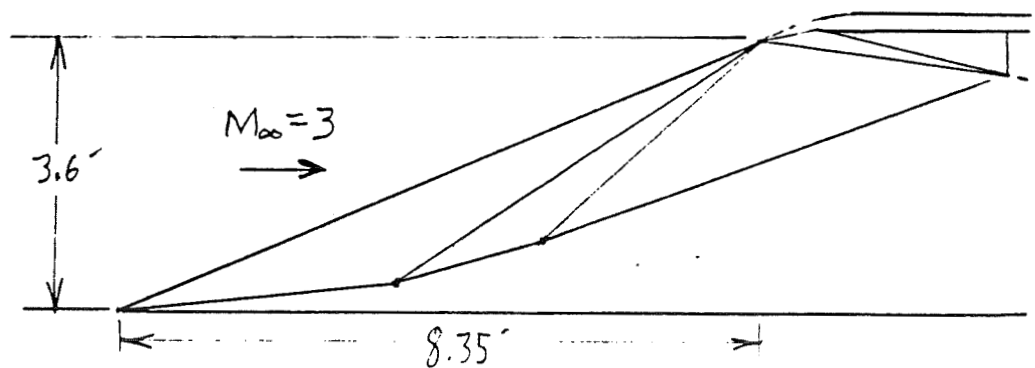
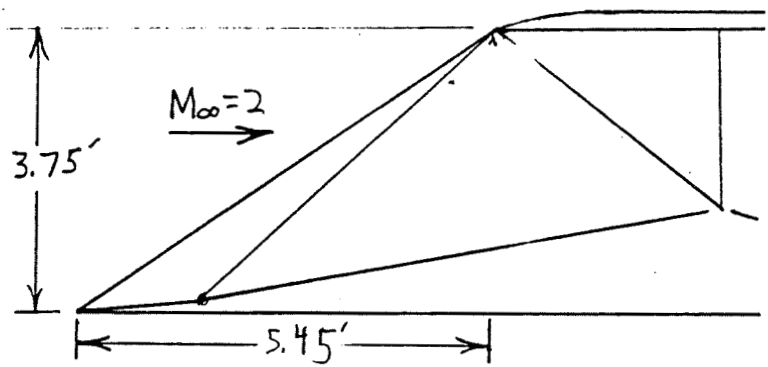
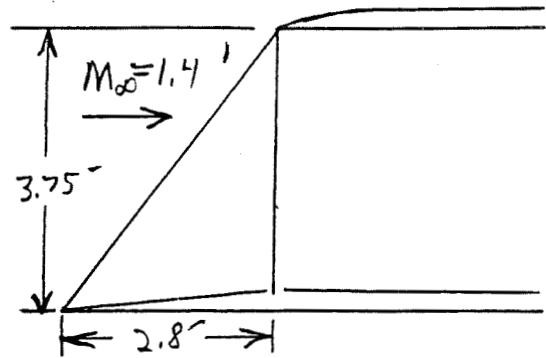


FIGURE IN 4 WEDGE PROFILES AT $M_\infty = 4, 5, \text{ AND } 6$

SCALE
 $\leftarrow 1'' \rightarrow$
 $\leftarrow 2'' \rightarrow$

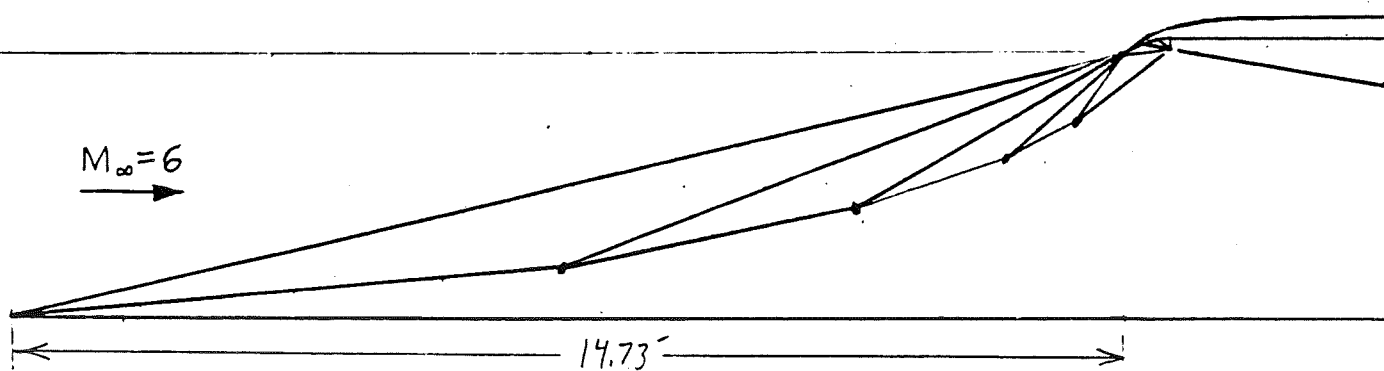
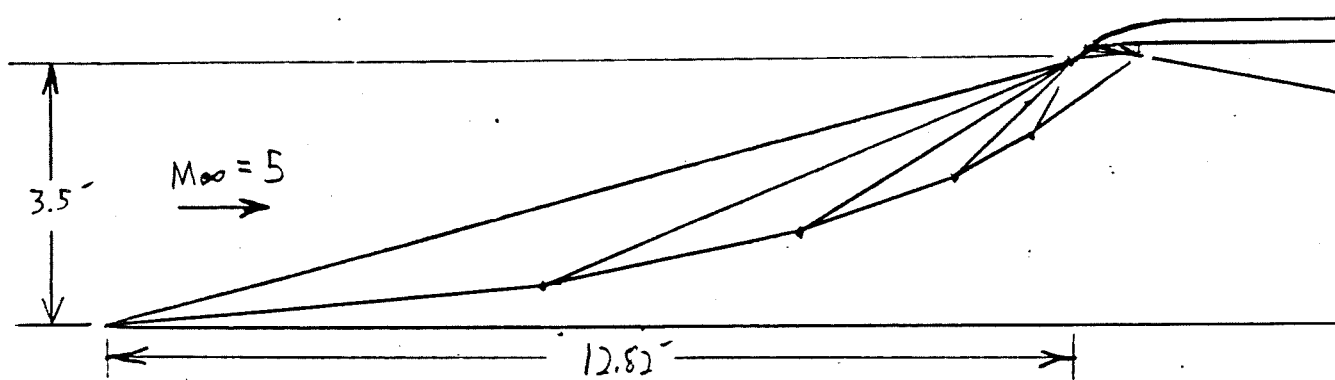
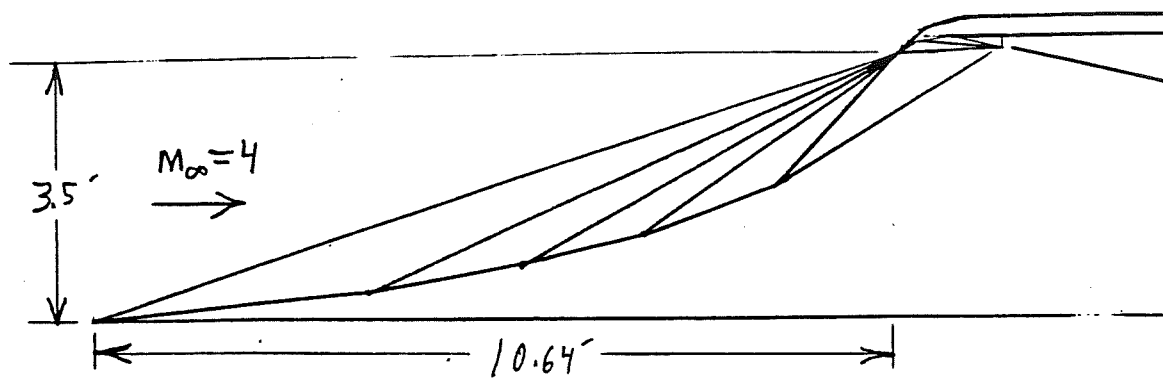
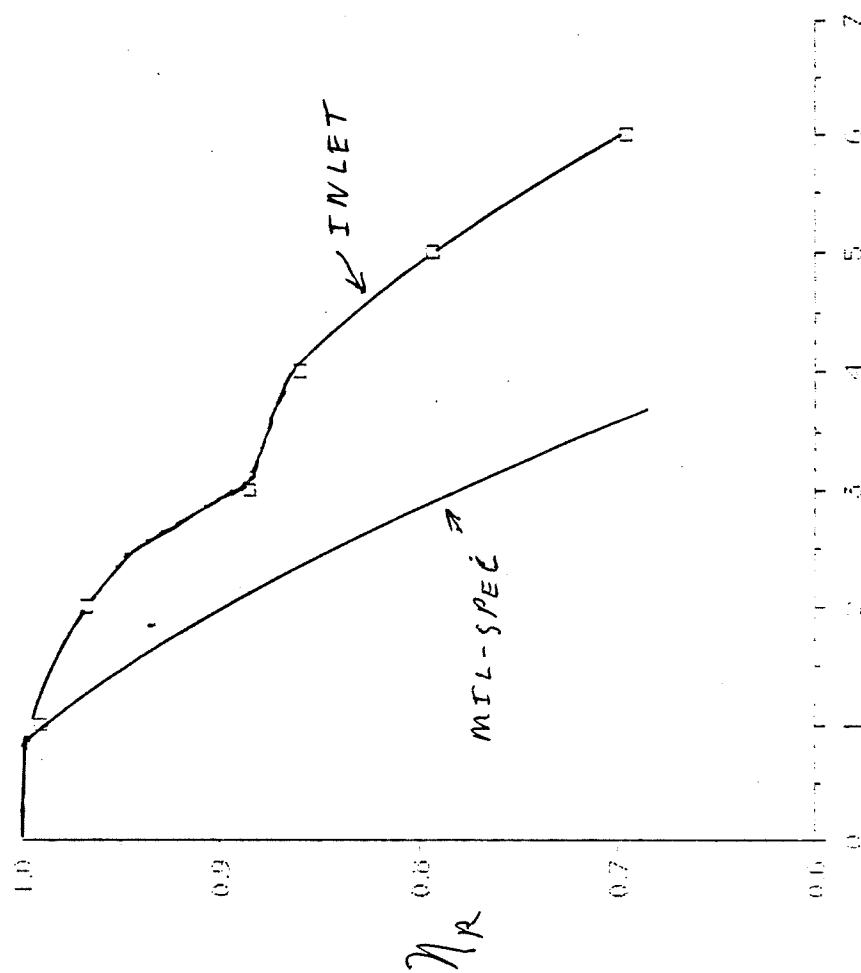


FIGURE 1 IN5 TOTAL PRESSURE RECOVERY VS MACH NUMBER



ORIGINAL PAGE IS
OF POOR QUALITY

FIG AD1

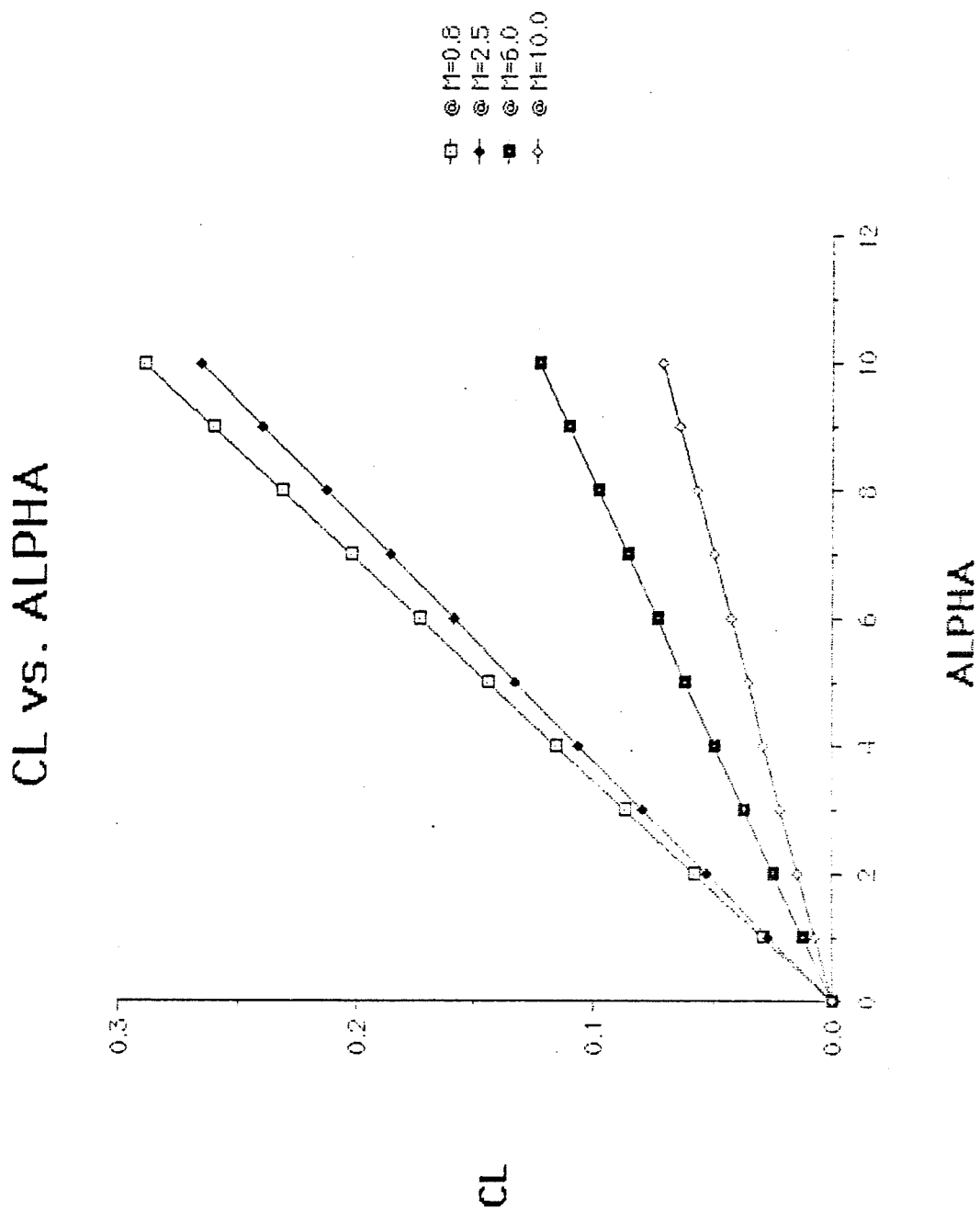
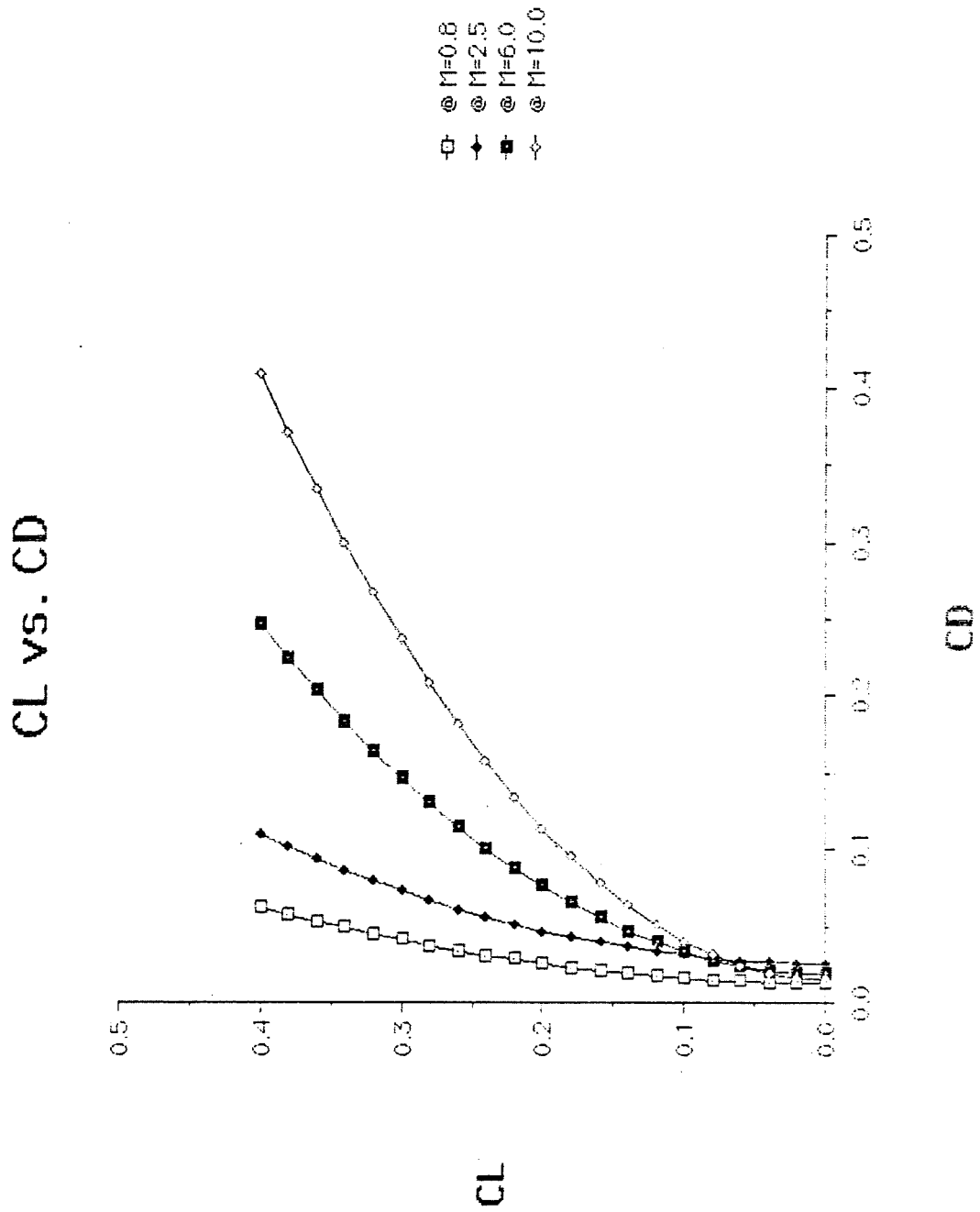
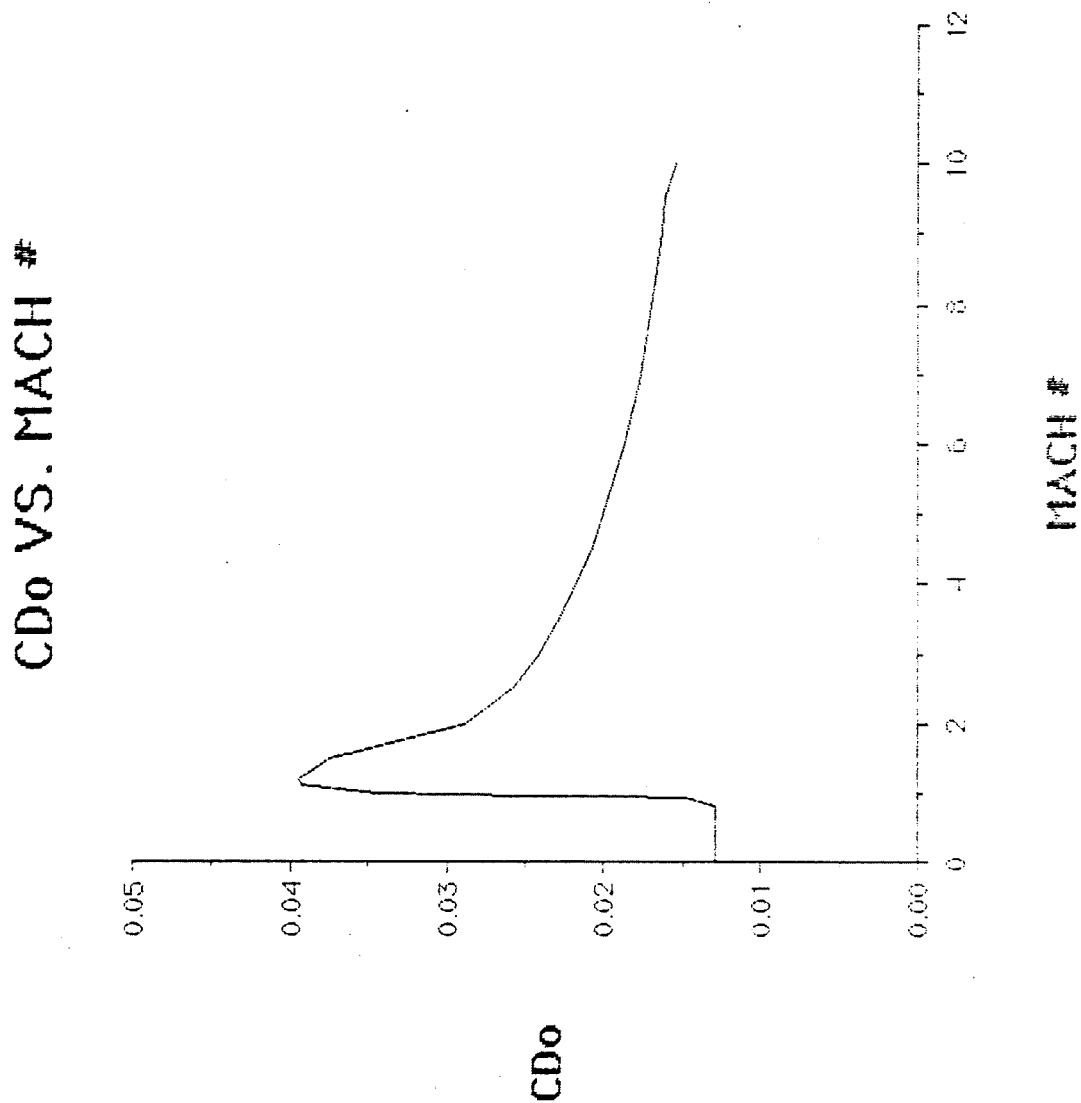


FIG AD2



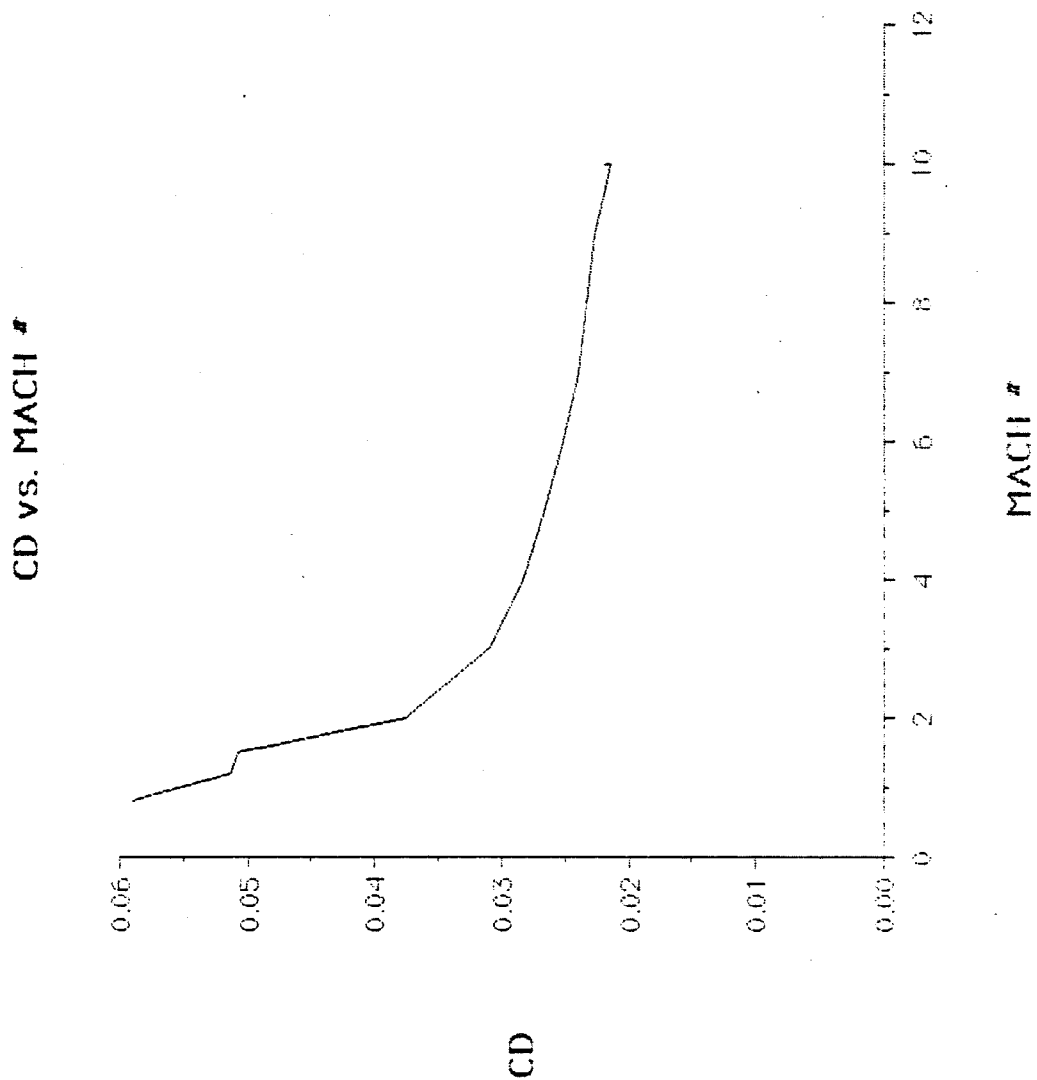
ORIGINAL PAGE IS
OF POOR QUALITY

FIG AD3



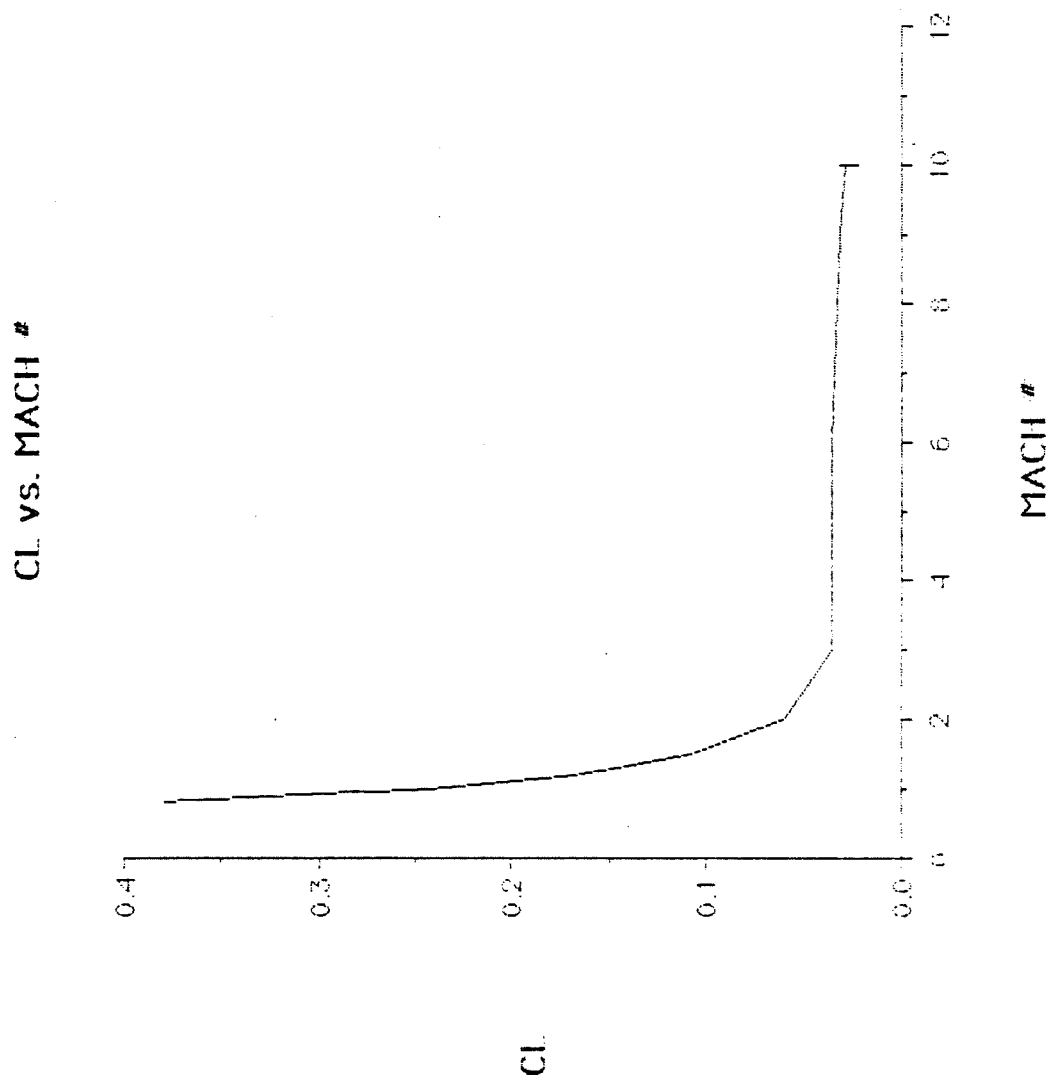
ORIGINAL PAGE IS
OF POOR QUALITY

FIG AD4



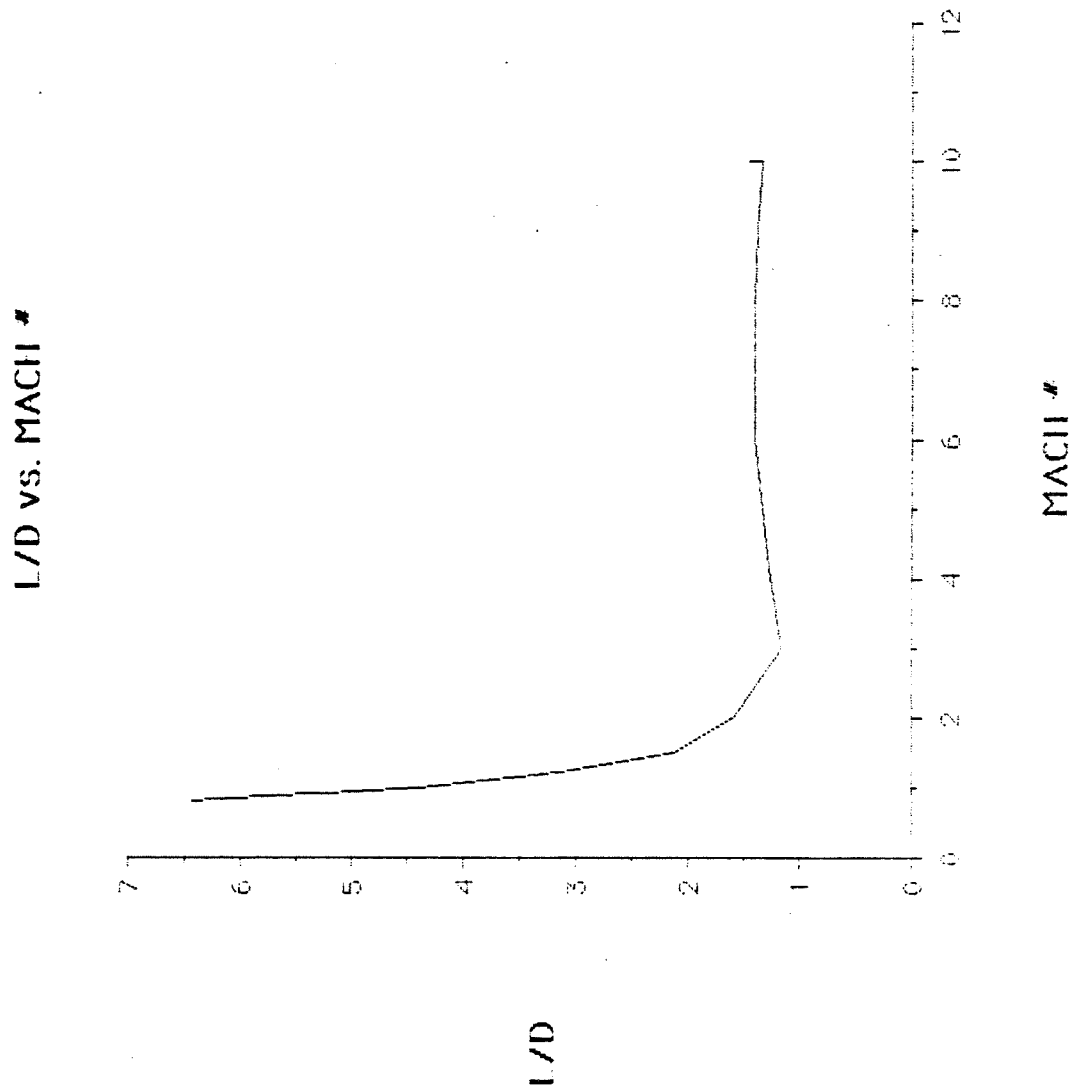
ORIGINAL PAGE IS
OF POOR QUALITY

FIG AD5



ORIGINAL PAGE IS
OF POOR QUALITY

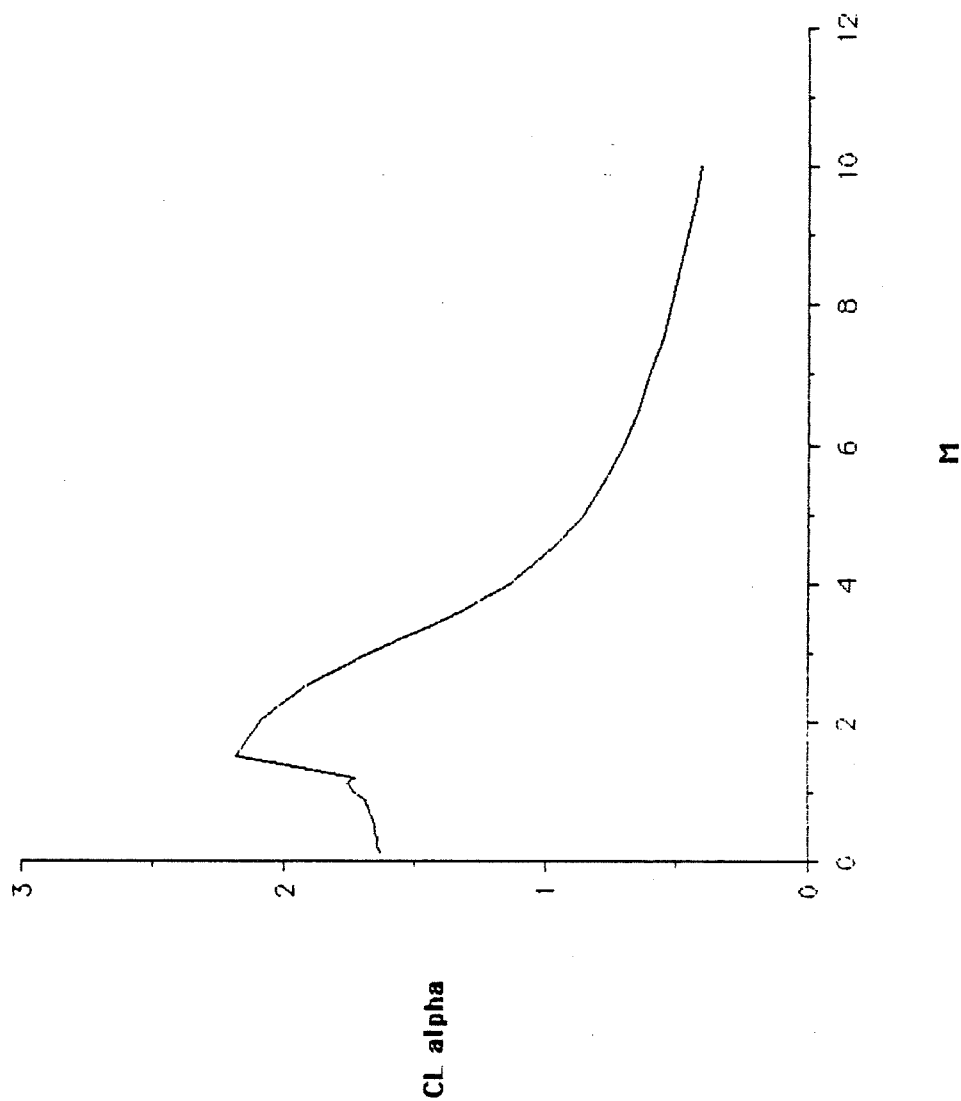
FIG AD6



ORIGINAL PAGE IS
OF POOR QUALITY

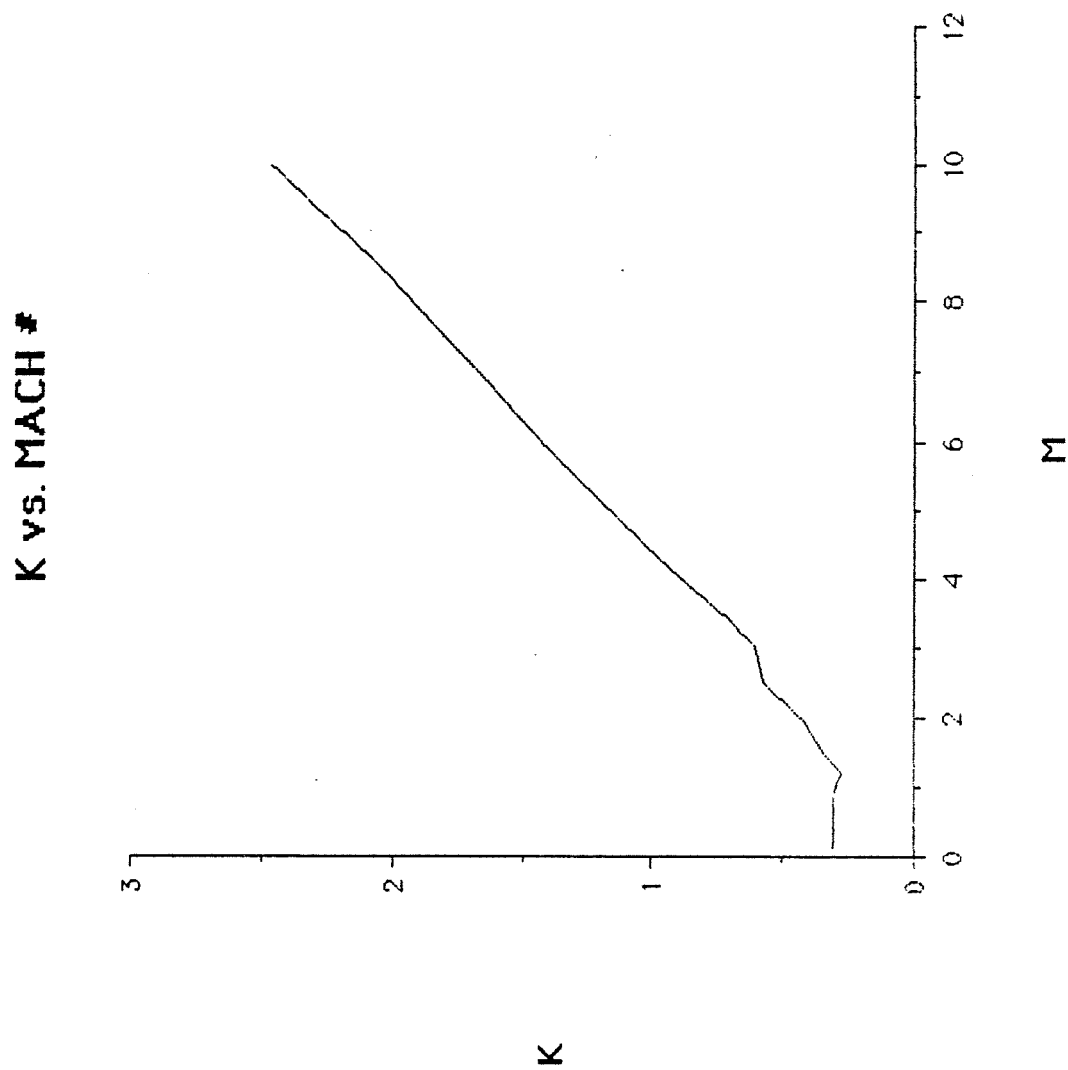
FIG AD7

CL alpha vs. MACH #

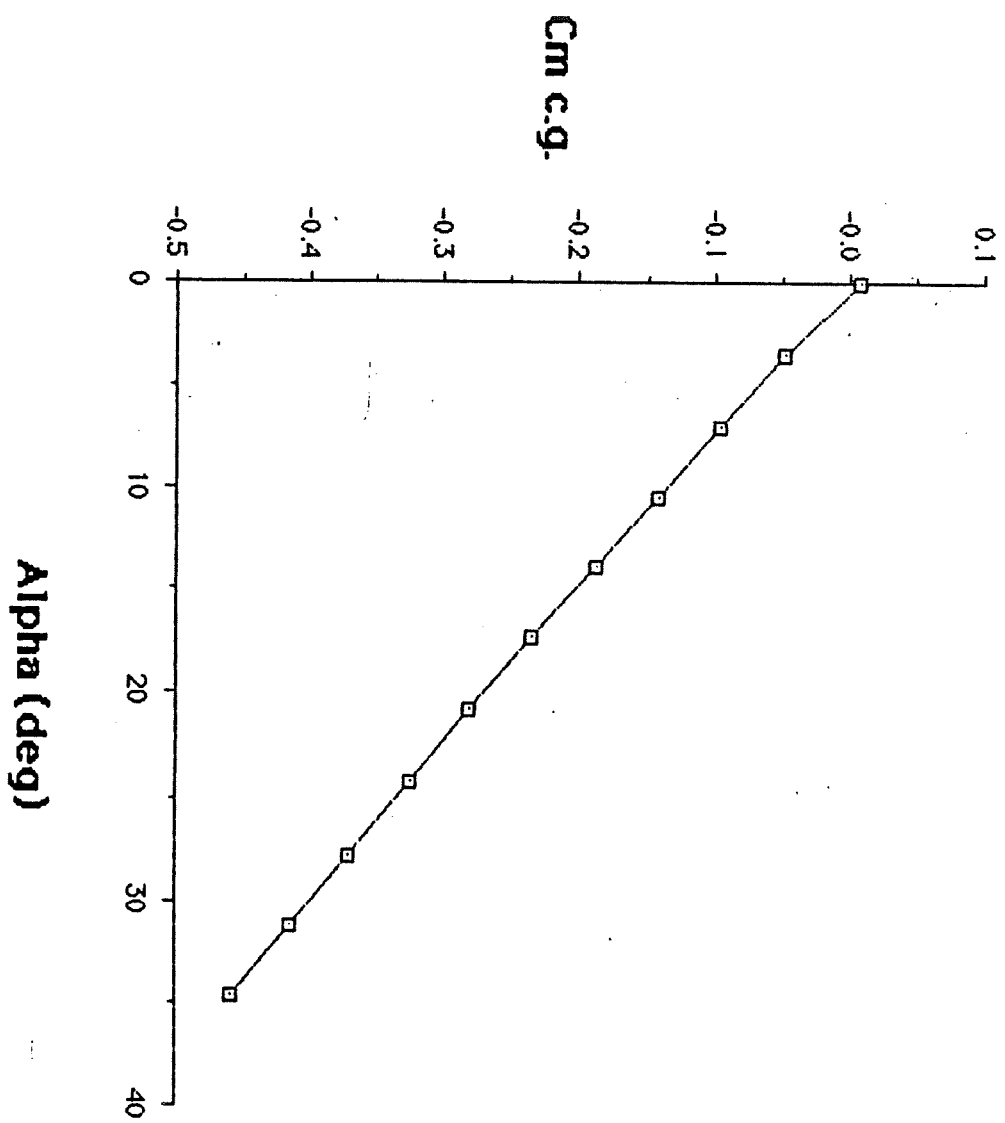


ORIGINAL PAGE IS
OF POOR QUALITY

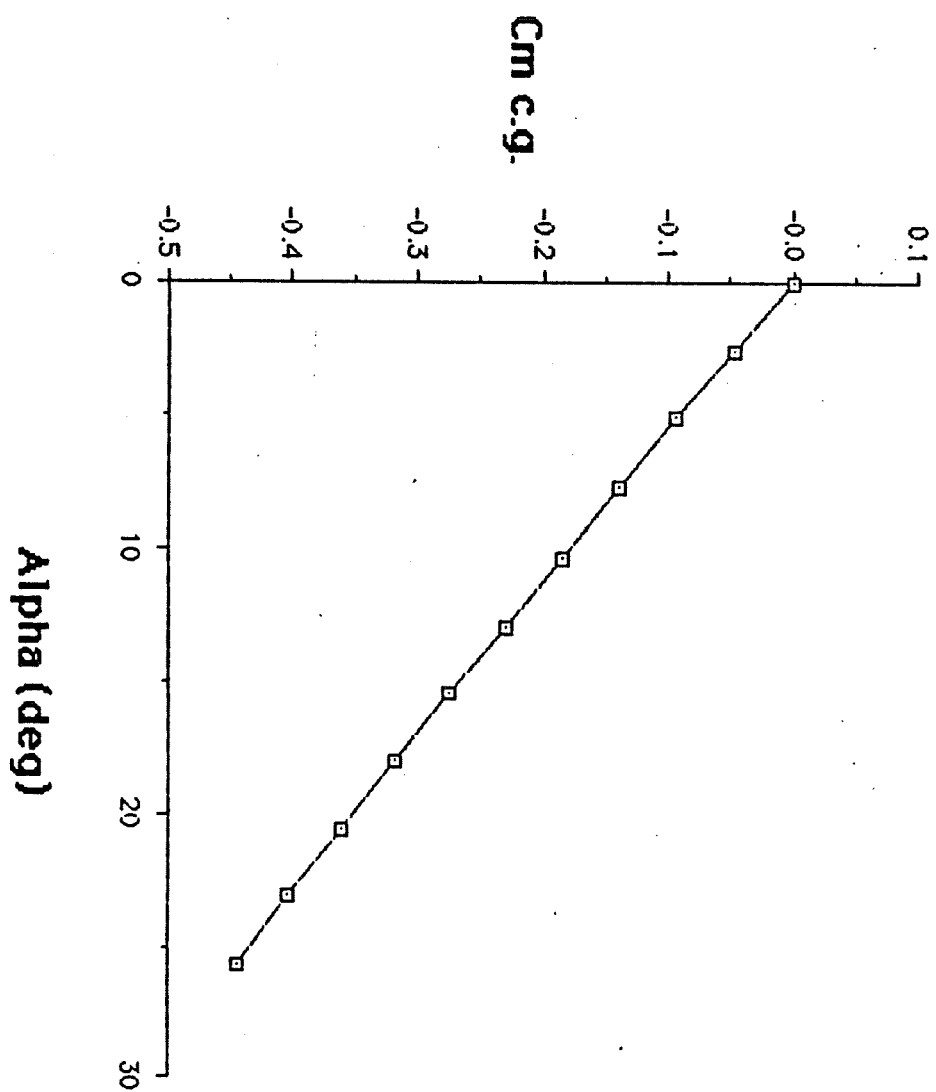
FIG AD8



Cm c.g. vs. Alpha (Mach .8)



Cm c.g. vs. Alpha (Mach 2)



Cm c.g. vs. Alpha (Mach 10)

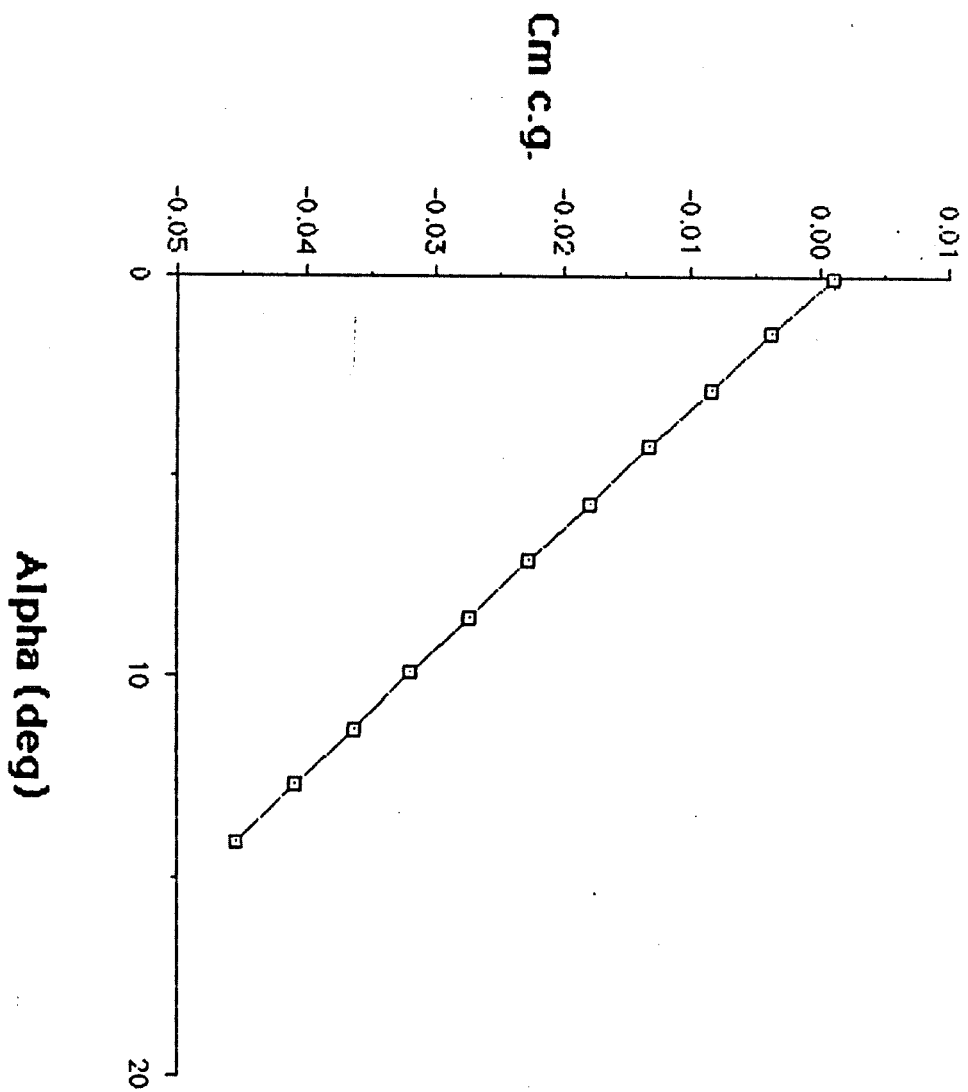


Figure: MS1
Temp. Dist.

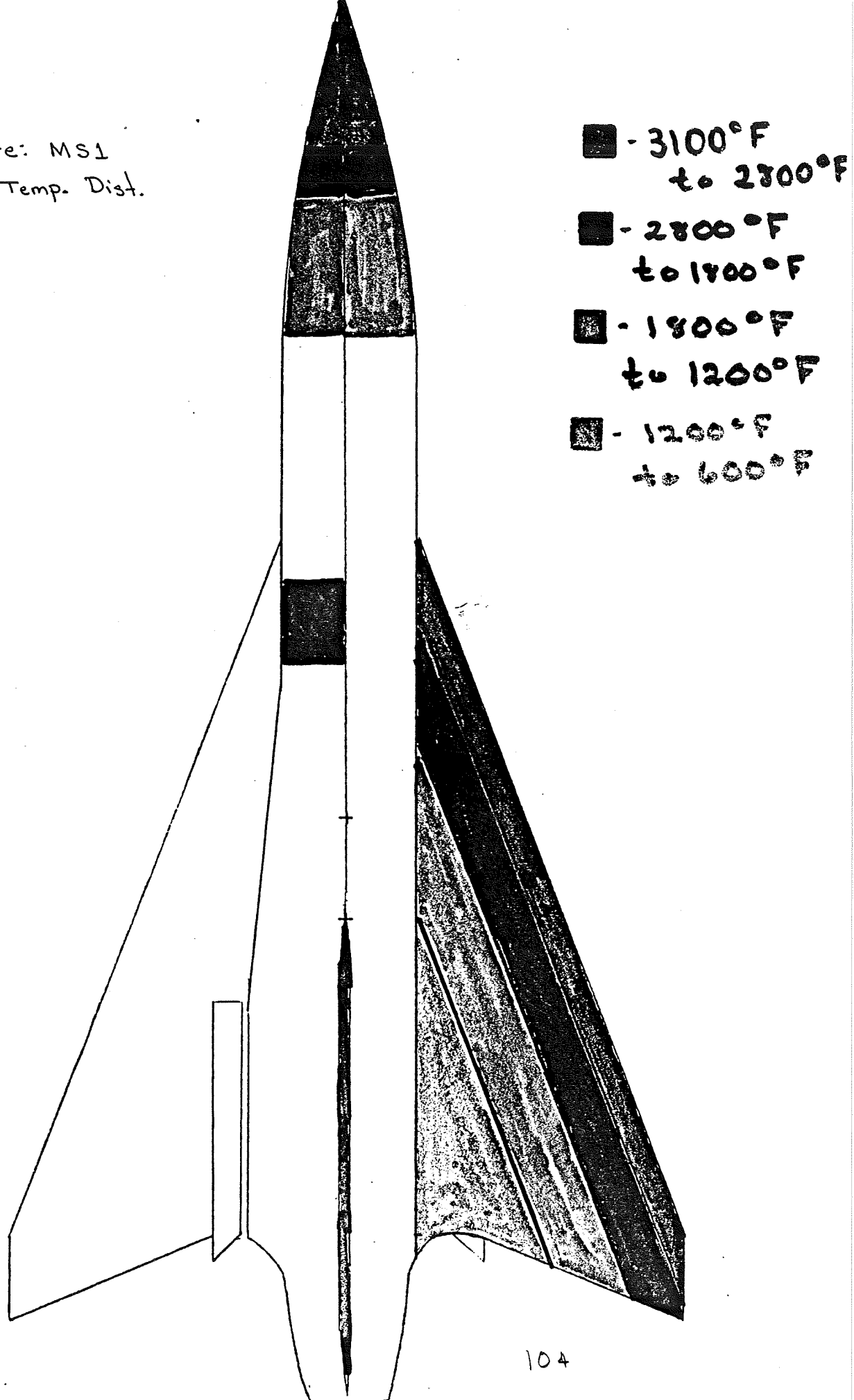
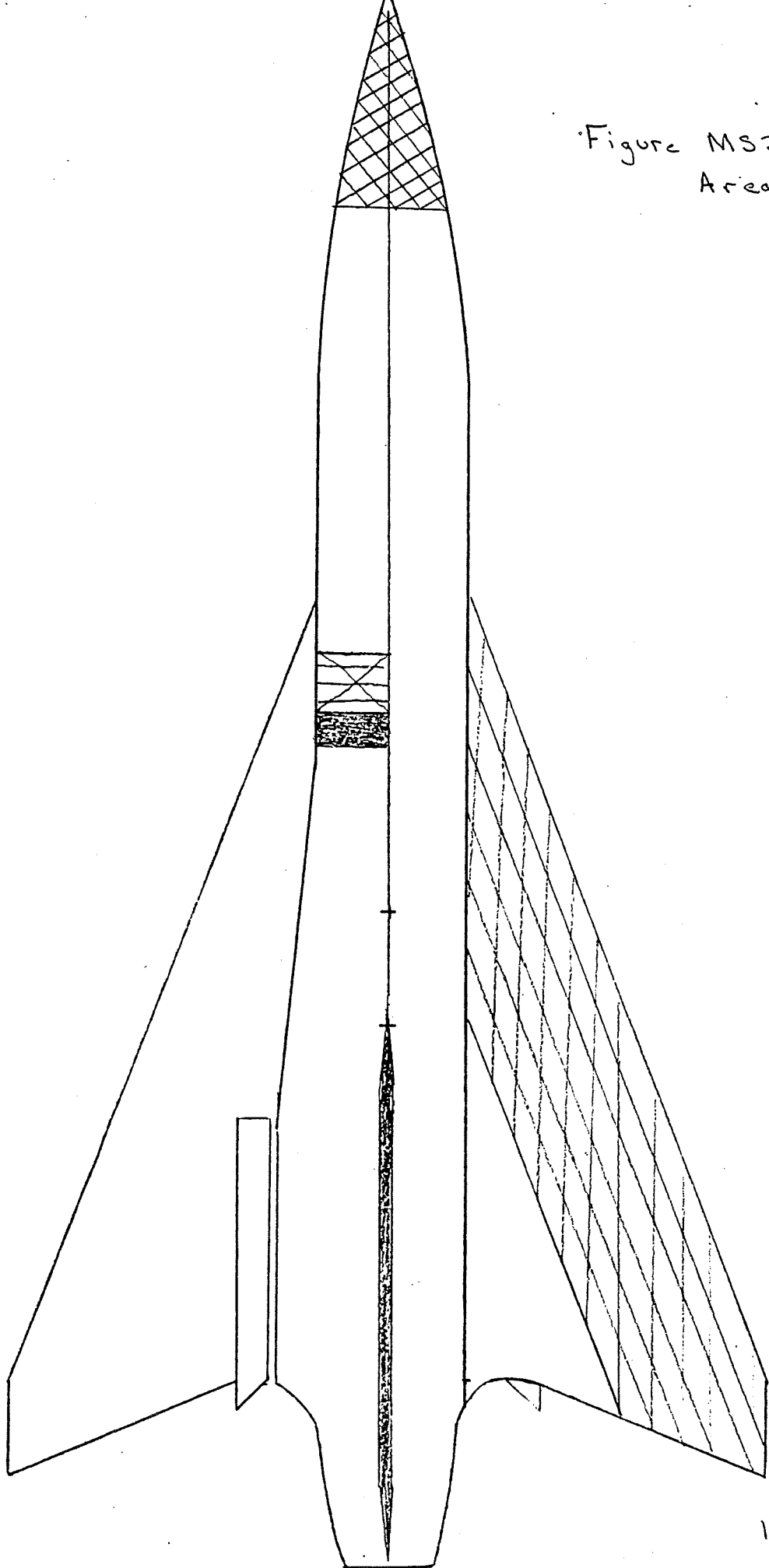
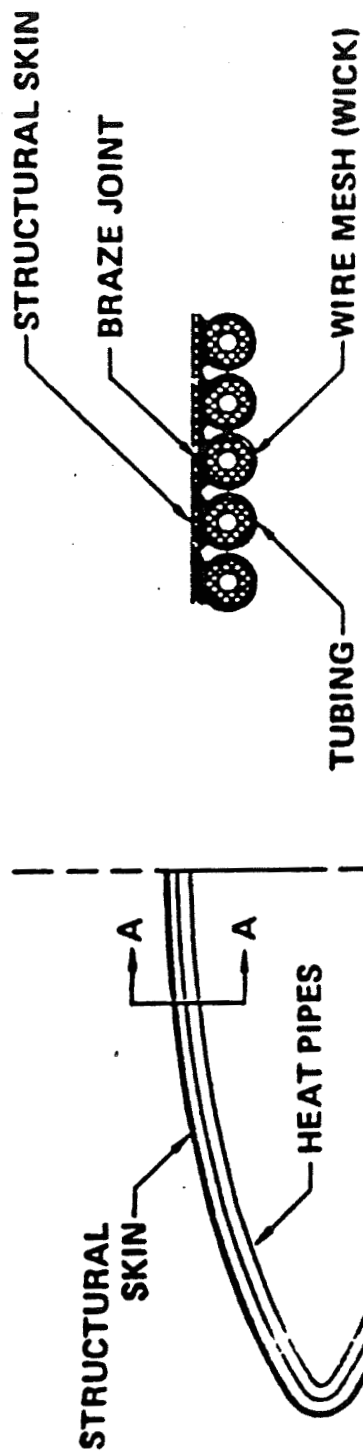


Figure MS2:
Areas to
cool





POTENTIAL DISADVANTAGES/LIMITATIONS

- WEIGHT
- RELIABILITY
- LEADING EDGE
RADIUS REQUIREMENT

POTENTIAL ADVANTAGES

- USE OF LOW TEMPERATURE METALS
- REASONABLE COST

Figure MS3:

Tube Cooling

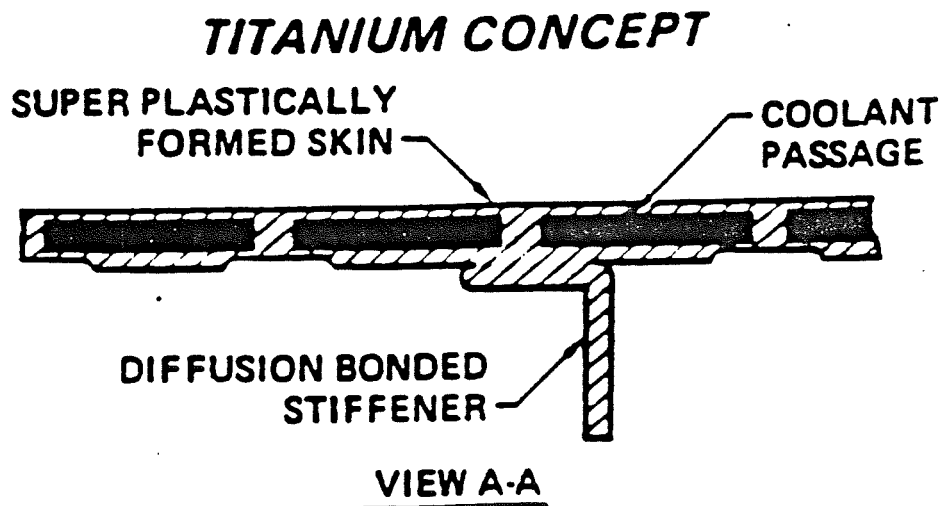
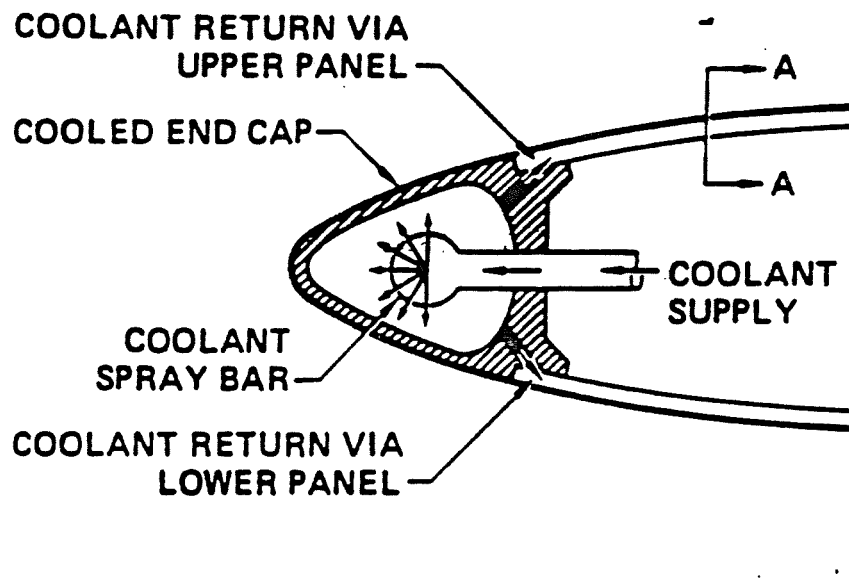
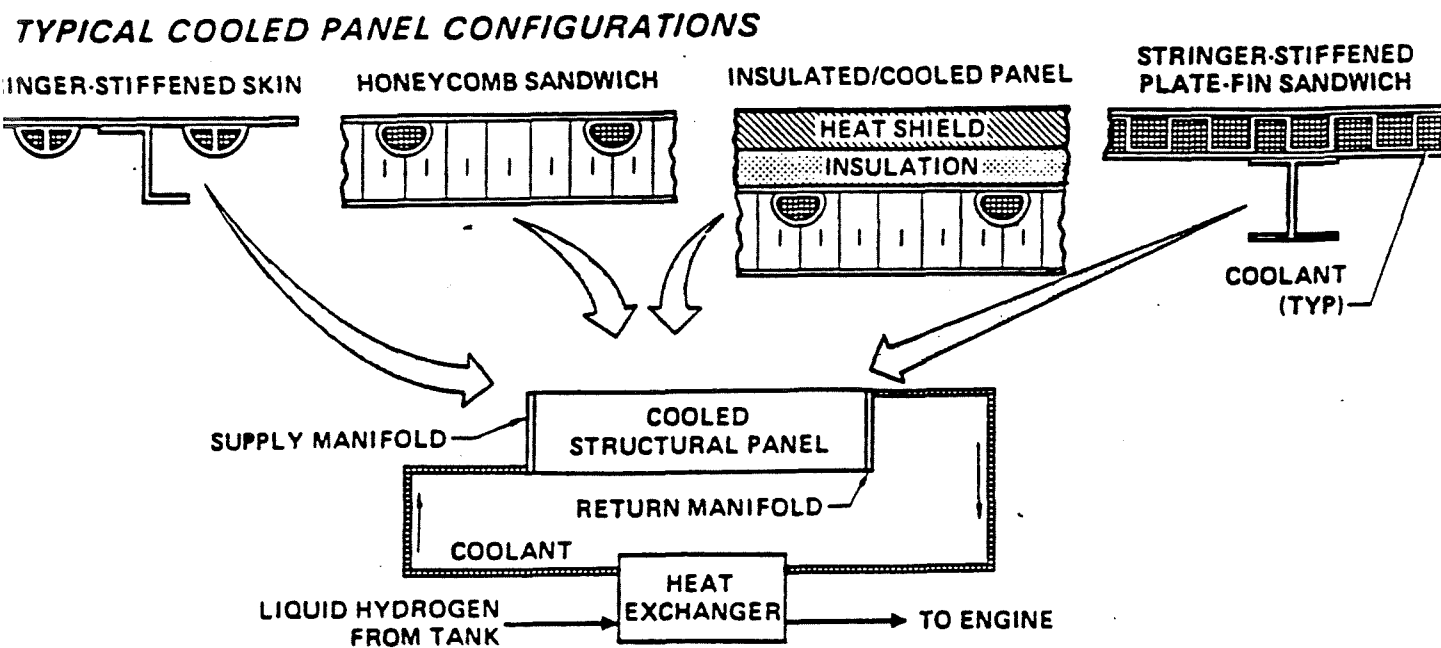


Figure MS4:

Spray Bar Cooling



POTENTIAL ADVANTAGES

- USE OF ALUMINUM MATERIALS
- LOW WEIGHT
- VOLUMETRIC EFFICIENCY

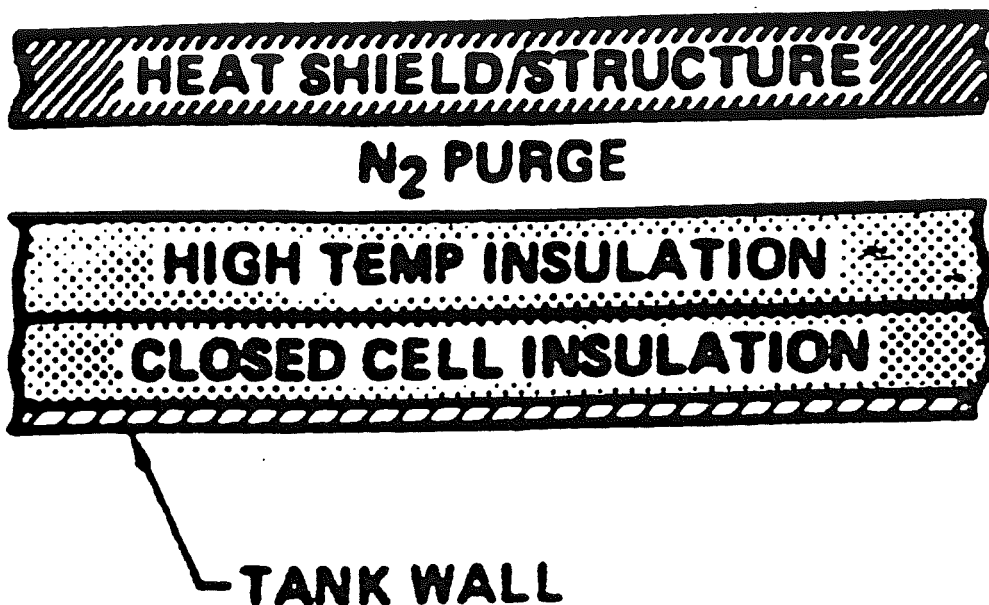
POTENTIAL DISADVANTAGES/LIMITATIONS

- REQUIRES LARGE FUEL HEAT SINK
- COMPLEX SYSTEM ARRANGEMENT
- MAY REQUIRE ADDITIONAL THERMAL PROTECTION DEVELOPMENT

Figure M35:

Panel Configuration

Figure M56: N₂ purge System



CO₂ FROST SYSTEM

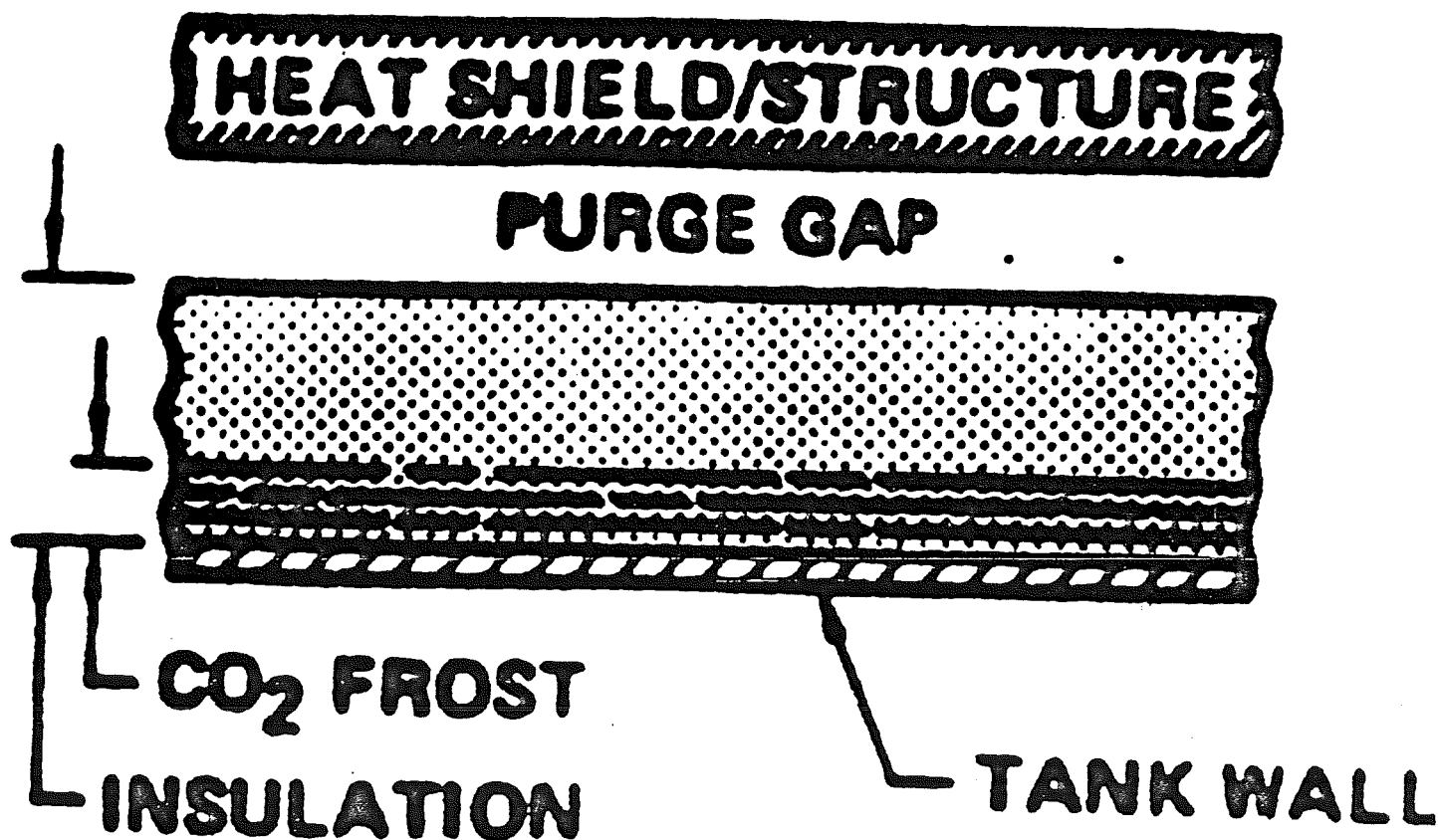


Figure M57: CO₂ purge System

Total Development and Evaluation

Airframe Engineering	1,697,859,405.60
Development Support	1,384,147,764.00
Flight Test Aircraft	501,706,296.40
Engines & Avionic	20,414,855.50
Manufacturing Labor	106,997,571.50
Material & Equipment	10,931,449.70
Tooling	350,190,800.20
Quality Control	13,171,619.50
Flight Test Operations	32,259,410.80
Test Facilities	<u>0.00</u>
Total	\$3,615,972,876.80

Figure: Cost I

Appendix

A

APPENDIX A

WING:

SUBSONIC:

$$C_{D0} = C_{Df} = C_f [1 + 2*t/c + 100*(t/c)^4] S_{wet}/S_{ref}$$

C_{Df} : Skin friction drag coefficient which is constant in the subsonic region.

C_f : Turbulent flat plate skin friction coefficient,
(Nicolai, Figure E2).

TRANSONIC:

$$C_{D0} = C_{Df} + C_{D0} = C_f [1 + t/c] S_{wet}/S_{ref} + \Delta C_{D0}$$

ΔC_{D0} : Wave drag coefficient (Nicolai, Figure 11.10).

SUPERSONIC:

For wings with round-nosed airfoil sections and supersonic leading edge use :

$$C_{D0} = C_{Df} + C_{Dle} + [16/3/\beta] * (t/c)^2 * S_{wet}/S_{ref}$$

$$C_{Df} = C_f * S_{wet}/S_{ref}$$

$$C_f = [C_{fc}/C_{fi}] * C_{fi}$$

$$C_{Dle} = (2.56/b) * [r_{le} * AR * \cos^2 \Lambda_{le}] / [1 + \frac{1}{M_{\infty}^2 \cos^2 \Lambda_{le}}]$$

C_{fc}/C_{fi} : Account for compressibility effects above Mach # 1

(Datcom, Figure 4.1.5.1-15).

C_{Dle} : Leading edge bluntness term.

The C_{D0} for the wing is listed in Table AD1.

BODY:

SUBSONIC:

$$C_{D0} = C_{Df} + C_{Db}$$

$$C_{Df} = 1.02 * C_f * (1 + 1.5 / (\ell/d)^2 + 7 / (\ell/d)^4) S_{ref} / S_B$$

$$C_{Db} = 0.029 * (d_b/d)^3 / (C_{Df})^{0.5}$$

where C_{Db} : Base pressure drag coefficient.

TRANSONIC:

$$C_{D0} = C_{Df} + C_{Db} + C_{Dp} + C_{Dp}$$

$$C_{Df} = 1.02 * C_f * [C_{fc} / C_f] * S_{ref} / S_B$$

$$C_{Dp}' = 1.02 * C_f [1.5 / (\ell/d)^2 + 7 / (\ell/d)^4] * S_{ref} / S_B$$

$$C_{Db} = -C_{pb} * (d_b/d)^2$$

C_{pb} : Base pressure coefficient (Datcom, Figure 4.2.3.1-17).

C_{Dp}' : Subsonic Pressure Drag.

C_{Dp} : Supersonic Wave Drag (Datcom, Figure 4.2.3.1-18).

SUPERSONIC:

$$C_{D0} = C_f * S_{ref} / S_B + C_{DN2} + C_{DA} + C_{DA(NC)} + C_{Db}$$

C_{DN2} : Nose wave drag (Datcom, Figure 4.2.3.1-50).

C_{DA} : Body after body wave drag (Datcom, Figure 4.2.3.1-[36-38]).

$C_{DA(NC)}$: Interference drag coefficient acting on after body due to center body and nose (Datcom, Figure 4.2.3.1-54).

C_{Db} : Base pressure drag coefficient (Datcom, Figure 4.2.3.1-44)

The C_{D0} for the body is listed in Table AD2.

The final C_{D0} value can be obtained from the following equation:

$$C_{D0} = [C_{D0}]_{wing} + [C_{D0}]_{body} * S_{ref} / S_B$$

The $(C_{D0})_{Total}$ is listed in Table AD3

WING-BODY COMBINATION:

SUBSONIC:

$$C_D = C_{D0} + K' * C_L^2 + K'' * [C_L - C_{Lmin}]^2$$

$$K' = 1 / [\pi * AR * e]$$

$$e = e' * [1 - (d/b)^2]$$

K' : Inviscid drag due to lift (Induced drag).

K'' : Viscous drag due to lift due to flow separation and increased skin friction (Nicolai, Figure 11.6).

e : Wing efficiency factor.

e' : Wing planform efficiency factor (Nicolai, Figure 11.5).

TRANSONIC:

The values for C_L and K have been estimated using Figure AD7 and

Figure AD8. In these graphs the values of C_L and K were estimated

by simply connecting the subsonic and supersonic values and then just reading the corresponding C_L and K for the transonic region.

SUPERSONIC:

$$C_D = C_{D0} + K * [C_L - C_{Lmin}]^2$$

$$K = 1/C_{L\alpha} - \Delta N \text{ for subsonic leading edge.}$$

$$K = 1/C_{L\alpha}$$

$$\Delta N = (\Delta N / \Delta N_{M=1.0}) * \Delta N_{M=1.0}$$

$$\Delta N_{M=1.0} = 1/C_{L\alpha_{M=1.0}} - (K' + K'')$$

K: Drag due to lift factor.

ΔN : Leading edge suction parameter.

C_L : supersonic lift curve slope (Nicolai, Figure 11.2).

$(\Delta N / \Delta N_{M=1.0})$: Nicolai, Figure 11.7.

Tables AD4, AD5, and AD6 list values for $C_{L\alpha}$ /degree, ΔN , and

K, respectively, for the different Mach numbers.

Appendix

B

CALCULATIONS FOR THE SUBSONIC REGION}

program AAES15H;

const

s = 722.5;
pi = 3.141593;
cdo = 0.0129885;
xk = 0.3103235;

var

xm, cl, cd, d, v, h, t, r, xx, ala, cla, W : real;
outfile : text;
tt : boolean;
aaa : integer;

begin

showtext;
rewrite(outfile, 'hani:out4');
tt := false;
while not tt do

begin

writeln('input W,h,t,r');
readln(W);
readln(h);
readln(t);
readln(r);
writeln('w = ', w : 1 : 2, ' lbs');
writeln(outfile, 'w = ', w : 1 : 2, ' lbs');

xm := 0.1;
cla := 1.6566 * pi / 180.0;

while (xm <= 0.9) do

begin

v := xm * sqrt(1.4 * 1716 * t);
cl := 2 * (w) / r / s / (v * v);
cd := cdo * 1.1 + (xk * cl * cl);
d := cd * s * (v * v) * r * 0.5;
xx := cl / cd;
ala := cl / cla;
write(outfile, h : 1 : 1, ' ', xm : 1 : 1, ' ', v : 1 : 2, ' ', cl : 1 : 5, ' ');
writeln(outfile, cd : 1 : 5, ' ', xx : 1 : 5, ' ', d : 1 : 2, ' ', ala : 1 : 3);
write(h : 1 : 1, ' ', xm : 1 : 1, ' ', v : 1 : 2, ' ', cl : 1 : 5, ' ');
writeln(cd : 1 : 5, ' ', xx : 1 : 5, ' ', d : 1 : 2, ' ', ala : 1 : 3);
xm := xm + 0.1;

```
    xm := xm + 0.1;  
end;  
writeln(' hit 1 to exit');  
readln(aaa);  
if (aaa = 1) then  
    tt := true;  
end;  
end.
```

CALCULATIONS FOR THE TRANSONIC REGIONS}

```

program AA515H;
const
  s = 722.5;

var
  xm, cl, d, cd, cdo, xk, v, h, t, r, xx, ala, cla, w : real;
  infile, outfile : text;
  tt : boolean;
  aaa : integer;
procedure detcdoxk (xm : real;
  var cdo, xk, cla : real);
begin
  if (xm = 9.0) then
    begin
      xk := 0.31;
      cdo := 0.0147191;
      cla := 1.683;
    end;
  if (xm = 10.0) then
    begin
      xk := 0.30;
      cdo := 0.034345;
      cla := 1.734;
    end;
  if (xm = 11.0) then
    begin
      xk := 0.285;
      cdo := 0.039222;
      cla := 1.753;
    end;
  if (xm = 12.0) then
    begin
      xk := 0.28;
      cdo := 0.039493;
      cla := 1.722;
    end;
  end;
begin
  reset(infile, 'Papers\data1');
  showtext;

```

```

rewrite(outfile, 'Hani.out5');
tt := false;
while not tt do
begin
  writeln('input W,h,t,r');
  readln(w);
  readln(h);
  readln(t);
  readln(r);
  writeln(outfile, 'w = ', w : 1 : 2, ' lbs');
  writeln('w = ', w : 1 : 2, ' lbs');
  xm := 9.0;
  while (xm <= 12.0) do
  begin
    v := xm * sqrt(1.4 * t * 1716) / (1e01);
    cl := 2 * (w) / r / s / (v * v);
    detcdoxk(xm, cdo, xk, cla);
    cd := cdo * 1.1 + (xk * cl * cl);
    d := cd * s * (v * v) * r * 0.5;
    xm := xm / 1e01;
    xx := cl / cd;
    ala := cl / (cla * pi) * 180.0;
    write(outfile, h : 1 : 1, ' ', xm : 1 : 1, ' ', v : 1 : 3, ' ', cl : 1 : 5, ' ');
    writeln(outfile, cd : 1 : 5, ' ', xx : 1 : 5, ' ', d : 1 : 2, ' ', ala : 1 : 2);
  {write(outfile);}
    write(h : 1 : 1, ' ', xm : 1 : 1, ' ', v : 1 : 3, ' ', cl : 1 : 5, ' ');
    writeln(cd : 1 : 5, ' ', xx : 1 : 5, ' ', d : 1 : 2, ' ', ala : 1 : 2);
  {writeln;}
    xm := xm * 1e01;
    xm := xm + 1.0;
  end;
  writeln('Hit 1 to exit');
  readln(aaa);
  if aaa = 1 then
    tt := true;
  end;
end.

```

CALCULATIONS FOR THE SUPERSONIC AND HYPERSONIC REIGONS}

```

program AAE515H;
const
  s = 722.5;
  pi = 3.141593;

var
  xm, cl, d, cd, cdo, xk, v, xx, ala, cla, h, t, r, W : real;
  infile, outfile : text;
  tt : boolean;
  asa : integer;
procedure detcdoxk (xm : real;
var cdo, xk : real;);
begin
end;

begin
  reset(infile, 'Papers:data1');
  showtext;
  rewrite(outfile, 'Hani:out6');
  tt := false;
  while not tt do
    begin
      writeln('input W,h,t,r');
      readln(w);
      readln(h);
      readln(t);
      readln(r);
      writeln(outfile, 'w = ', w : 1 : 2, ' lbs');
      writeln('w = ', w : 1 : 2, ' lbs');
      xm := 15.0;

      while (xm <= 100.0) do
        begin
          v := xm * sqrt(1.4 * t * 1716) / (1e01);
          cl := 2 * (w) / r / s / (v * v);
          detcdoxk(xm, cdo, xk);
          if (xm = 15.0) then
            begin
              xk := 0.35;
              cdo := 1.3 * 0.037375;
            end
          end
        end
      end
    end
  end

```

```
    cla := 2.2355;  
end;  
if (xm = 20.0) then  
  begin  
    xk := 0.430;  
    cdo := 1.3 * 0.028804;  
    cla := 2.092;  
  end;  
if (xm = 25.0) then  
  begin  
    xk := 0.5210;  
    cdo := 1.3 * 0.025900;  
    cla := 1.9193;  
  end;  
if (xm = 30.0) then  
  begin  
    xk := 0.602;  
    cdo := 1.3 * 0.02420;  
    cla := 1.662;  
  end;  
if (xm = 35.0) then  
  begin  
    xk := 0.7294;  
    cdo := 1.3 * 0.022705;  
    cla := 1.371;  
  end;  
if (xm = 40.0) then  
  begin  
    xk := 0.8802;  
    cdo := 1.3 * 0.21767;  
    cla := 1.1361;  
  end;  
if (xm = 45.0) then  
  begin  
    xk := 1.02;  
    cdo := 1.3 * 0.02077;  
    cla := 0.980;  
  end;  
if (xm = 50.0) then  
  begin  
    xk := 1.161;  
    cdo := 1.3 * 0.020104;  
    cla := 0.8614;
```

```
end;  
if (xm = 55.0) then  
begin  
  xk := 1.294;  
  cdo := 1.3 * 0.019427;  
  cla := 0.773;  
end;  
if (xm = 60.0) then  
begin  
  xk := 1.422;  
  cdo := 1.3 * 0.018758;  
  cla := 0.703;  
end;  
if (xm = 65.0) then  
begin  
  xk := 1.55;  
  cdo := 1.3 * 0.0183272;  
  cla := 0.645;  
end;  
if (xm = 70.0) then  
begin  
  xk := 1.672;  
  cdo := 1.3 * 0.0176583;  
  cla := 0.598;  
end;  
if (xm = 75.0) then  
begin  
  xk := 1.799;  
  cdo := 1.3 * 0.017373;  
  cla := 0.556;  
end;  
if (xm = 80.0) then  
begin  
  xk := 1.922;  
  cdo := 1.3 * 0.017012;  
  cla := 0.5203;  
end;  
if (xm = 85.0) then  
begin  
  xk := 2.049;  
  cdo := 1.3 * 0.0166643;  
  cla := 0.488;  
end;
```



```

if (xm = 90.0) then
  begin
    xk := 2.183;
    cdo := 1.3 * 0.01639;
    cla := 0.458;
  end;
if (xm = 95.0) then
  begin
    xk := 2.32;
    cdo := 1.3 * 0.016125;
    cla := 0.431;
  end;
if (xm = 100.0) then
  begin
    xk := 2.457;
    cdo := 1.3 * 0.015517;
    cla := 0.407;
  end;
cd := cdo / 1.3 * 1.25 + (xk * cl * cl);
d := cd * s * (v * v) * r * 0.5;
xm := xm / (1e01);
xx := cl / cd;
ala := cl / (cla * pi) * 180.0;
write(outfile, h: 1: 1, ' ', xm: 1: 1, ' ', v: 1: 3, ' ', cl: 1: 5, ' ');
writeln(outfile, cd: 1: 5, ' ', xx: 1: 5, ' ', d: 1: 2, ' ', ala: 1: 2);
write(outfile);
write(h: 1: 1, ' ', xm: 1: 1, ' ', v: 1: 3, ' ', cl: 1: 5, ' ');
writeln(cd: 1: 5, ' ', xx: 1: 5, ' ', d: 1: 2, ' ', ala: 1: 2);
writeln;
xm := xm * 1e01;
xm := xm + 5.0;
end;
writeln('Hit 1 to exit');
readln(aaa);
if aaa = 1 then
  tt := true;
end;
end.

```

Appendix

C

```

program INLETAREA
dimension H(30),D(30),T(30),MACH(30),VEL(30),BLD(30)
dimension HM(30),DM(30),TM(30),W1R(30),AREA(30),BAREA(30)
real MACH,Q
open(unit=1,file='INLETAREA.DAT')

```

```

ALT=35000.
do I=1,13
    ALT=ALT+5000.
    H(I)=ALT
    T(I)=389.99

```

```

end do

```

```

T(10)=394.69
T(11)=402.48
T(12)=410.64
T(13)=418.79

```

```

D(1)=.00058727
D(2)=.00046227
D(3)=.00036391
D(4)=.00028652
D(5)=.00022561
D(6)=.00017767
D(7)=.00013993
D(8)=.00011022
D(9)=.00008683
D(10)=.00006771
D(11)=.00005253
D(12)=.00004097
D(13)=.00003211

```

```

J=0.

```

```

write(6,5)

```

```

format('-----')

```

```

write(6,20)

```

```

write(6,30)

```

```

write(6,5)

```

```

write(1,5)

```

```

write(1,20)

```

```

write(1,30)

```

```

write(1,5)

```

```

format(' Mach #',5X,'Altitude',6X,'Mass flow',7X,'Area',6X

```

```

, 'Corrected Area',8X,'Y')

```

```

format(14X,'(ft)',8X,'(lb/sec)',7X,'(ft**2)',7X,'(ft**2)',9X,'(ft**2)')

```

```

do I=1,13

```

```

    J=J+1

```

```

    write(6,*) 'Enter Mach #, W1R, % bleed at ',H(I),' ft'

```

```

    read(5,*) MACH(J),W1R(J),BLD(J)

```

```

    HM(J)=H(I)

```

```

    DM(J)=D(I)

```

```

    TM(J)=T(I)

```

```

    VEL(J)=MACH(J)*SQRT(1.4*1716*TM(J))

```

```

    AREA(J)=W1R(J)/(32.2*DM(J)*VEL(J))

```

```

    BAREA(J)=AREA(J)*BLD(J)+AREA(J)

```

```

    Y=BAREA(J)/7.

```

```

write(6,40) MACH(J),HM(J),W1R(J),AREA(J),BAREA(J),Y

```

```

write(1,40) MACH(J),HM(J),W1R(J),AREA(J),BAREA(J),Y

```

ORIGINAL PAGE IS
OF POOR QUALITY

```
40      format(1X,F4.2,8X,F8.1,5X,F6.1,10X,F6.3,8X,F6.3,10X,F5.3)
      write(6,*) 'Enter 1 to enter another Mach# at same altitude else 2'
      read(5,*) Q
      if(Q.eq.1) goto 10
      end do
      close(1)
      stop
      end
```

```

program INLETANGLEM6
dimension M(15),MN(15),BET(15),THET(15),XT(15),POR(15)
real M,MN
open(unit=1,file='INLANGM6.DAT')
write(6,*) 'Enter Theta, M1, NR'
read(5,*) THETA,M(1),NR
M(1)=6.
NR=8
THET(1)=THETA*3.141592654/180.
BET(1)=BETA*3.141592654/180.
TT=TAN(THET(1))/2.

do 30 I=1,NR
write(6,*) 'Enter Theta for M1=6 and NR=8',I
read(5,*) THETA
BETA=THETA+3.
THET(I)=THETA*3.141592654/180.
BET(I)=BETA*3.141592654/180.
TT=TAN(THET(I))/2.
TB=0.
if(ABS(TT-TB).lt..00001) goto 20
BET(I)=BET(I)+(TT-TB)*1.7
A=(M(I)**2.*(1.4+COS(2.*BET(I)))+2.)*TAN(BET(I))
TB=(M(I)**2.*SIN(BET(I))**2.-1.)/A
goto 10

XT(I)=4./TAN(BET(I))
MN(I)=M(I)*SIN(BET(I))
MN(I+1)=SQRT((MN(I)**2.+2./4)/(2.8/.4*MN(I)**2.-1))
M(I+1)=MN(I+1)/(SIN(BET(I)-THET(I)))
B=(1.166666666667*MN(I)**2.-.166666666667)**-2.5
POR(I)=(1.2*MN(I)**2./(1.+2*MN(I)**2.))**3.5*B
THET(I+1)=THET(I)
BET(I+1)=BET(I)
continue

write(6,50)
format(' THETA',4X,'BETA',7X,'M(I)',7X,'M(I+1)',5X,'POR',8X,'XT')
write(1,50)
TPOR=1.
do 40 I=1,NR
BETA=BET(I)/3.141592654*180.
THETA=THET(I)/3.141592654*180.
write(6,60) THETA,BETA,M(I),M(I+1),POR(I),XT(I)
format(1X,F5.2,5X,F5.2,5X,F6.3,5X,F6.3,5X,F6.5,5X,F5.2)
write(1,60) THETA,BETA,M(I),M(I+1),POR(I),XT(I)
TPOR=POR(I)*TPOR
continue
C=(1.166666666667*M(NR+1)**2.-.166666666667)**-2.5
TPTR=(1.2*M(NR+1)**2./(1.+2*M(NR+1)**2.))**3.5*C*TPOR
write(6,70)
format(/,' TPOR',7X,'TPTR')
write(6,80) TPOR,TPTR
format(1X,F6.5,6X,F6.5)
write(6,*)
write(1,70)
write(1,80) TPOR,TPTR
write(1,*)
goto 1
close(1)
stop
end

```

THETA	BETA	M(I)	M(I+1)	POR	XT
5.00	13.16	6.000	5.315	.96624	17.11
6.00	15.20	5.315	4.647	.95987	14.73
7.25	17.79	4.647	3.997	.95305	12.46
8.75	21.13	3.997	3.372	.94735	10.35
10.25	25.28	3.372	2.790	.94763	8.47
12.00	30.92	2.790	2.240	.94947	6.68
13.25	38.60	2.240	1.730	.95887	5.01
12.25	49.40	1.730	1.290	.97690	3.43

TPOR	TPTR
.70576	.69241

THETA	BETA	M(I)	M(I+1)	POR	XT
5.25	13.36	6.000	5.282	.96146	16.84
6.25	15.47	5.282	4.594	.95595	14.45
7.25	17.94	4.594	3.956	.95443	12.36
8.50	21.07	3.956	3.357	.95252	10.38
9.75	24.91	3.357	2.806	.95462	8.61
11.00	29.82	2.806	2.299	.95932	6.98
12.25	36.63	2.299	1.822	.96497	5.38
13.75	48.54	1.822	1.323	.96644	3.53

TPOR	TPTR
.71362	.69591

THETA	BETA	M(I)	M(I+1)	POR	XT
5.25	13.36	6.000	5.282	.96146	16.84
6.25	15.47	5.282	4.594	.95595	14.45
7.25	17.94	4.594	3.956	.95443	12.36
8.50	21.07	3.956	3.357	.95252	10.38
9.75	24.91	3.357	2.806	.95462	8.61
11.00	29.82	2.806	2.299	.95932	6.98
13.75	38.25	2.299	1.761	.95222	5.07
12.25	48.32	1.761	1.322	.97668	3.56

TPOR	TPTR
.71165	.69410

THETA	BETA	M(I)	M(I+1)	POR	XT
5.25	13.36	6.000	5.282	.96146	16.84
6.25	15.47	5.282	4.594	.95595	14.45
7.25	17.94	4.594	3.956	.95443	12.36
8.50	21.07	3.956	3.357	.95252	10.38
9.75	24.91	3.357	2.806	.95462	8.61
11.00	29.82	2.806	2.299	.95932	6.98
13.00	37.43	2.299	1.791	.95888	5.23
13.00	48.41	1.791	1.323	.97189	3.55

TPOR	TPTR
.71311	.69540

THETA	BETA	M(I)	M(I+1)	POR	XT
5.00	13.16	6.000	5.315	.96624	17.11
5.00	14.39	5.315	4.756	.97563	15.59
5.00	15.67	4.756	4.288	.98195	14.26
5.00	17.02	4.288	3.888	.98635	13.07
5.00	18.45	3.888	3.540	.98950	11.99
8.33	22.72	3.540	3.035	.96600	9.55
8.33	25.65	3.035	2.617	.97687	8.33
8.33	29.10	2.617	2.257	.98384	7.19

TPOR	TPTR
.83877	.50516

THETA	BETA	M(I)	M(I+1)	POR	XT
6.00	13.98	6.000	5.182	.94491	16.06
6.00	15.47	5.182	4.541	.96247	14.45
6.00	17.05	4.541	4.020	.97355	13.04
6.00	18.74	4.020	3.585	.98085	11.79
6.00	20.56	3.585	3.213	.98583	10.66
10.00	25.97	3.213	2.677	.95641	8.21
10.00	30.03	2.677	2.237	.97180	6.92
10.00	35.22	2.237	1.856	.98102	5.67

TPOR	TPTR
.78061	.61478

THETA	BETA	M(I)	M(I+1)	POR	XT
7.00	14.84	6.000	5.048	.91779	15.10
7.00	16.60	5.048	4.334	.94705	13.42
7.00	18.49	4.334	3.769	.96435	11.96
7.00	20.55	3.769	3.306	.97519	10.67
7.00	22.82	3.306	2.916	.98231	9.51
11.67	29.56	2.916	2.356	.94801	7.05
11.67	35.24	2.356	1.894	.96771	5.66
11.67	43.62	1.894	1.478	.97815	4.20

TPOR	TPTR
.72053	.67477

THETA	BETA	M(I)	M(I+1)	POR	XT
8.00	15.73	6.000	4.915	.88528	14.21
8.00	17.77	4.915	4.133	.92986	12.48
8.00	19.99	4.133	3.533	.95484	10.99
8.00	22.46	3.533	3.050	.96972	9.67
8.00	25.27	3.050	2.645	.97909	8.48
13.33	33.59	2.645	2.063	.94092	6.02
13.33	41.84	2.063	1.571	.96390	4.47
13.33	60.88	1.571	1.019	.96474	2.23

TPOR	TPTR
.65296	.65296

THETA	BETA	M(I)	M(I+1)	POR	XT
7.00	14.84	6.000	5.048	.91779	15.10
7.00	16.60	5.048	4.334	.94705	13.42
7.00	18.49	4.334	3.769	.96435	11.96
7.00	20.55	3.769	3.306	.97519	10.67
7.00	22.82	3.306	2.916	.98231	9.51
10.00	28.01	2.916	2.436	.96550	7.52
11.00	33.56	2.436	1.990	.97045	6.03
14.00	44.26	1.990	1.477	.96094	4.10

TPOR TPTR
.72295 .67730

THETA	BETA	M(I)	M(I+1)	POR	XT
5.00	13.16	6.000	5.315	.96624	17.11
6.00	15.20	5.315	4.647	.95987	14.73
7.00	17.58	4.647	4.019	.95725	12.62
8.00	20.40	4.019	3.443	.95793	10.76
9.00	23.79	3.443	2.917	.96100	9.07
10.00	28.00	2.917	2.437	.96547	7.52
11.50	34.04	2.437	1.970	.96663	5.92
13.50	44.09	1.970	1.479	.96520	4.13

TPOR TPTR
.73621 .68940

THETA	BETA	M(I)	M(I+1)	POR	XT
5.00	13.16	6.000	5.315	.96624	17.11
5.75	14.99	5.315	4.674	.96424	14.94
6.50	17.09	4.674	4.085	.96446	13.01
7.50	19.74	4.085	3.531	.96313	11.15
8.75	23.12	3.531	3.003	.96147	9.37
10.00	27.36	3.003	2.507	.96299	7.73
10.75	32.49	2.507	2.061	.97042	6.28
11.25	39.49	2.061	1.650	.97748	4.85

TPOR TPTR
.76009 .66590

THETA	BETA	M(I)	M(I+1)	POR	XT
4.00	12.37	6.000	5.450	.98180	18.24
6.00	14.93	5.450	4.754	.95715	15.00
8.00	18.16	4.754	4.012	.93553	12.19
10.00	22.19	4.012	3.295	.92489	9.81
12.00	27.34	3.295	2.633	.92552	7.74
10.00	30.46	2.633	2.199	.97287	6.80
13.00	38.97	2.199	1.706	.96226	4.94
17.00	62.94	1.706	.966	.92369	2.04

TPOR TPTR
.65075 .65078

THETA	BETA	M(I)	M(I+1)	POR	XT
5.00	13.16	6.000	5.315	.96624	17.11
6.00	15.20	5.315	4.647	.95987	14.73
7.25	17.79	4.647	3.997	.95305	12.46
8.75	21.13	3.997	3.372	.94735	10.35
10.25	25.28	3.372	2.790	.94763	8.47
13.00	31.90	2.790	2.193	.93773	6.43
12.00	37.98	2.193	1.739	.96983	5.12
12.75	49.86	1.739	1.278	.97389	3.37

TPOR TPTR
.70283 .69083

THETA	BETA	M(I)	M(I+1)	POR	XT
4.00	12.37	6.000	5.450	.98180	18.24
5.00	14.12	5.450	4.867	.97393	15.90
6.00	16.19	4.867	4.287	.96819	13.78
7.00	18.64	4.287	3.731	.96534	11.86
8.00	21.55	3.731	3.211	.96521	10.13
8.00	24.22	3.211	2.782	.97622	8.89
10.00	29.10	2.782	2.325	.96917	7.19
12.00	36.01	2.325	1.854	.96611	5.50

TPOR	TPTR
.78848	.62173

THETA	BETA	M(I)	M(I+1)	POR	XT
5.00	13.16	6.000	5.315	.96624	17.11
6.00	15.20	5.315	4.647	.95987	14.73
7.00	17.58	4.647	4.019	.95725	12.62
8.00	20.40	4.019	3.443	.95793	10.76
9.00	23.79	3.443	2.917	.96100	9.07
9.00	27.10	2.917	2.485	.97407	7.82
12.00	33.98	2.485	1.989	.96098	5.94
14.00	44.27	1.989	1.477	.96095	4.10

TPOR	TPTR
.73517	.68881

THETA	BETA	M(I)	M(I+1)	POR	XT
5.00	13.16	6.000	5.315	.96624	17.11
5.00	14.39	5.315	4.756	.97563	15.59
6.00	16.47	4.756	4.196	.97008	13.53
6.00	18.12	4.196	3.733	.97854	12.23
7.00	20.70	3.733	3.276	.97580	10.58
7.00	22.99	3.276	2.891	.98271	9.43
10.00	28.20	2.891	2.415	.96622	7.46
12.00	34.82	2.415	1.931	.96329	5.75

TPOR	TPTR
.79869	.60150

THETA	BETA	M(I)	M(I+1)	POR	XT
4.00	12.37	6.000	5.450	.98180	18.24
5.00	14.12	5.450	4.867	.97393	15.90
7.00	17.02	4.867	4.193	.95183	13.07
8.00	19.79	4.193	3.580	.95315	11.12
10.00	23.99	3.580	2.967	.94318	8.99
10.00	27.62	2.967	2.478	.96405	7.64
11.00	33.07	2.478	2.025	.96933	6.14
13.00	42.23	2.025	1.550	.96733	4.41

TPOR	TPTR
.73964	.67549

THETA	BETA	M(I)	M(I+1)	POR	XT
4.50	12.76	6.000	5.383	.97473	17.66
5.50	14.65	5.383	4.756	.96723	15.30
6.50	16.88	4.756	4.151	.96281	13.18
7.50	19.51	4.151	3.584	.96159	11.29
8.50	22.65	3.584	3.061	.96301	9.59
9.50	26.51	3.061	2.580	.96625	8.02
10.50	31.47	2.580	2.133	.97044	6.53
12.50	39.56	2.133	1.666	.96797	4.84

TPOR	TPTR
.76295	.66337

THETA	BETA	M(I)	M(I+1)	POR	XT
4.50	12.76	6.000	5.383	.97473	17.66
5.50	14.65	5.383	4.756	.96723	15.30
7.00	17.30	4.756	4.105	.95462	12.84
8.50	20.52	4.105	3.474	.94785	10.68
11.00	25.43	3.474	2.825	.93239	8.41
11.50	30.13	2.825	2.291	.95349	6.89
12.00	36.48	2.291	1.825	.96709	5.41
13.00	47.32	1.825	1.358	.97145	3.69

TPOR	TPTR
.71250	.68975

THETA	BETA	M(I)	M(I+1)	POR	XT
4.50	12.76	6.000	5.383	.97473	17.66
5.00	14.25	5.383	4.812	.97479	15.75
5.75	16.13	4.812	4.265	.97255	13.84
6.75	18.50	4.265	3.733	.96901	11.95
8.00	21.54	3.733	3.212	.96517	10.13
9.25	25.30	3.212	2.717	.96464	8.46
9.50	29.21	2.717	2.293	.97464	7.15
11.25	35.69	2.293	1.856	.97237	5.57

TPOR	TPTR
.79010	.62228

THETA	BETA	M(I)	M(I+1)	POR	XT
4.50	12.76	6.000	5.383	.97473	17.66
6.00	15.06	5.383	4.700	.95853	14.86
7.50	17.86	4.700	4.017	.94711	12.41
9.50	21.72	4.017	3.334	.93396	10.04
11.00	26.18	3.334	2.718	.93874	8.14
12.00	31.56	2.718	2.182	.95236	6.51
12.50	38.71	2.182	1.710	.96659	4.99
14.00	53.30	1.710	1.188	.96515	2.98

TPOR	TPTR
.68928	.68509

THETA	BETA	M(I)	M(I+1)	POR	XT
4.50	12.76	6.000	5.383	.97473	17.66
5.00	14.25	5.383	4.812	.97479	15.75
6.00	16.33	4.812	4.242	.96914	13.65
8.00	19.63	4.242	3.618	.95175	11.21
10.00	23.81	3.618	2.996	.94169	9.06
10.00	27.41	2.996	2.502	.96319	7.71
11.00	32.79	2.502	2.046	.96867	6.21
12.50	41.21	2.046	1.588	.97021	4.57

TPOR	TPTR
.74709	.67212

THETA	BETA	M(I)	M(I+1)	POR	XT
5.00	13.16	6.000	5.315	.96624	17.11
6.00	15.20	5.315	4.647	.95987	14.73
7.25	17.79	4.647	3.997	.95305	12.46
8.75	21.13	3.997	3.372	.94735	10.35
10.25	25.28	3.372	2.790	.94763	8.47
11.00	29.96	2.790	2.286	.95987	6.94
12.00	36.56	2.286	1.820	.96726	5.39
14.25	49.37	1.820	1.300	.96275	3.43

TPOR	TPTR
.70931	.69469

THETA	BETA	M(I)	M(I+1)	POR	XT
5.50	13.57	6.000	5.250	.95633	16.58
6.50	15.74	5.250	4.542	.95188	14.19
8.25	18.94	4.542	3.830	.93774	11.66
9.75	22.67	3.830	3.175	.93721	9.58
11.25	27.36	3.175	2.581	.94224	7.73
12.75	33.66	2.581	2.037	.95020	6.01
14.00	43.20	2.037	1.521	.95954	4.26
14.50	*****	1.521	2.059	*****	-7.26

TPOR	TPTR
.71993	.49905

THETA	BETA	M(I)	M(I+1)	POR	XT
5.50	13.57	6.000	5.250	.95633	16.58
6.50	15.74	5.250	4.542	.95188	14.19
7.50	18.29	4.542	3.894	.95157	12.10
8.50	21.31	3.894	3.309	.95437	10.26
9.50	24.96	3.309	2.781	.95915	8.59
10.50	29.56	2.781	2.301	.96483	7.05
12.50	36.86	2.301	1.814	.96292	5.34
14.50	49.99	1.814	1.282	.96087	3.36

TPOR	TPTR
.70784	.69535

THETA	BETA	M(I)	M(I+1)	POR	XT
5.00	13.16	6.000	5.315	.96624	17.11
6.50	15.61	5.315	4.593	.95030	14.32
7.50	18.15	4.593	3.934	.95016	12.20
8.50	21.15	3.934	3.340	.95318	10.34
9.50	24.78	3.340	2.806	.95819	8.66
10.25	29.12	2.806	2.334	.96633	7.18
12.25	36.14	2.334	1.851	.96388	5.48
14.50	48.73	1.851	1.322	.96031	3.51

TPOR	TPTR
.71273	.69523

THETA	BETA	M(I)	M(I+1)	POR	XT
6.00	13.98	6.000	5.182	.94491	16.06
7.00	16.31	5.182	4.437	.94336	13.67
8.00	19.03	4.437	3.770	.94589	11.60
9.00	22.25	3.770	3.177	.95104	9.78
10.00	26.19	3.177	2.649	.95757	8.13
12.00	32.22	2.649	2.125	.95507	6.35
13.00	40.26	2.125	1.640	.96456	4.72
15.00	60.49	1.640	1.022	.95115	2.26

TPOR	TPTR
.67280	.67279

```

program INLETANGLE
dimension M(15),MN(15),BET(15),THET(15),XT(15),POR(15)
dimension PR(15),TR(15),DR(15)
real M,MN,MNT
open(unit=1,file='INLANG2.DAT')
write(6,*) 'Enter M1, NR'
read(5,*) M(1),NR

do 30 I=1,NR
write(6,*) 'Enter Theta for M1 and NR',I
read(5,*) THETA
BETA=THETA*3.
THET(I)=THETA*3.141592654/180.
BET(I)=BETA*3.141592654/180.
TT=TAN(THET(I))/2.
TB=0.
if(ABS(TT-TB).lt..00001) goto 20
BET(I)=BET(I)+(TT-TB)*1.7
A=(M(I)**2.*(1.4+COS(2.*BET(I)))+2.)*TAN(BET(I))
TB=(M(I)**2.*SIN(BET(I))**2.-1.)/A
goto 10

XT(I)=3.5/TAN(BET(I))
MN(I)=M(I)*SIN(BET(I))
MN(I+1)=SQRT((MN(I)**2.+2./4.)/(2.8/4.*MN(I)**2.-1))
M(I+1)=MN(I+1)/(SIN(BET(I)-THET(I)))
B=(1.166666666667*MN(I)**2.-.166666666667)**-2.5
PR(I)=1.166666666667*MN(I)**2.-.166666666667
DR(I)=(2.4*MN(I)**2.)/(4.*MN(I)**2.+2.)
TR(I)=PR(I)/DR(I)
POR(I)=(1.2*MN(I)**2./(1.+2.*MN(I)**2.))*3.5*B
continue

write(6,12) M(1)
write(1,12) M(1)
format(30X,'Mach # = ',F5.2)
write(6,15)
format('_____')
write(6,50)
write(6,15)
format(' THETA',3X,'BETA',6X,'M(I)',6X,'M(I+1)',4X,'POR',7X,'PR',
,9X,'TR',9X,'XT')
write(1,15)
write(1,50)
write(1,15)
TPOR=1.
TPR=1.
TTR=1.
TDR=1.
do 40 I=1,NR
BETA=BET(I)/3.141592654*180.
THETA=THET(I)/3.141592654*180.
write(6,60) THETA,BETA,M(I),M(I+1),POR(I),PR(I),TR(I),XT(I)
format(1X,F5.2,4X,F5.2,4X,F6.3,4X,F6.3,4X,F6.5,4X,F7.4,4X,F7.4,4X,F5.2)
write(1,60) THETA,BETA,M(I),M(I+1),POR(I),PR(I),TR(I),XT(I)
TPOR=POR(I)*TPOR
TPR=PR(I)*TPR
TDR=DR(I)*TDR
TTR=TR(I)*TTR
continue

```

```

C=(1.16666666667*M(NR+1)**2.-.166666666667)**-2.5
MNT=SQRT((M(NR+1)**2.+2./4)/(2.8/4*M(NR+1)**2.-1))
TPOTR=(1.2*M(NR+1)**2./(1.+2*M(NR+1)**2.))*3.5*C*TPOR
TPTR=(1.16666666667*M(NR+1)**2.-.166666666667)*TPR
TDTR=(2.4*M(NR+1)**2.)/(4*M(NR+1)**2.+2.)*TDR
TTTR=TPTR/TDTR
write(6,17)
format('-----' , '*****')
write(6,70)
format(' TPOR',6X,'TPR',8X,'TTR',11X,'TPOTR',7X,'TPTR',8X,'TTTR',8X,'MN
write(6,80) TPOR,TPR,TTR,TPOTR,TPTR,TTTR,MNT
format(1X,F6.5,3X,F8.4,4X,F7.4,7X,F6.5,6X,F8.4,4X,F7.4,4X,F6.4)
write(1,17)
write(1,70)
write(1,80) TPOR,TPR,TTR,TPOTR,TPTR,TTTR,MNT
write(6,*)
write(1,*)
goto 1
close(1)
stop
end

```

FOR MACH #'S M=5.0 & M=6.0

```
program INLETLNGTH
dimension M,BET,THET
real M1,MN1,M2,MN2,M3,MN3,M4,MN4,M5,MN5,M6,MN6,M7,MN7,MNN2
real MNN3,MNN4,MNN5,MNN6,MNN7
XPI=3.141593/180.
write(6,*) ' ENTER THE VALUES FOR THETA1 AND M1 '
read(5,*) THETA,M1
write(6,*) 'ENTER THE VALUE OF Y AND L1-L5 '
read(5,*) Y,XL1,XL2,XL3,XL4,XL5
M1=5.0
THETA=5.25
Y=3.5
XL1=7.270
XL2=3.08523
XL3=1.7036117
XL4=1.10302
XL5=1.6
THETA=8.0
```

THESE ARE VARYING LENGTHES

```
XL1=7.081008
XL2=2.04934137
XL3=1.09605
XL4=0.714048
P1=1.0
BETA=THETA+3.
THET1=THETA*XPI
BET1=BETA*XPI
TT=TAN(THET1)/2.
TB=0.
if(ABS(TT-TB).lt..00001) goto 20
BET1=BET1+(TT-TB)*1.7
A=(M1**2*(1.4+COS(2.*BET1))+2.)*TAN(BET1)
XXX=(SIN(BET1))**2
TB=(M1**2*((SIN(BET1))**2)-1.)/A
goto 10
```

```
write(6,*) 'BET1 =',BET1
MN1=M1*SIN(BET1)
write(6,*) 'MN1 = ',MN1
MN2=SQRT((MN1**2+5)/(7*MN1**2-1))
write(6,*) ' MN2 =',MN2
write(6,*) BET1,THET1
M2=MN2/(SIN(BET1-THET1))
P2=P1*(1+(2.8/2.4)*(MN1**2-1))
PO1=P1*((1+0.2*M1**2))**3.5
PO2=P2*((1+0.2*M2**2))**3.5
write(6,*) M2
continue
```

```
do 40 I=1,NR
  BETA=BET(I)/3.141592654*180.
  THETA=THET(I)/3.141592654*180.
  write(6,*) BETA,THETA,XT(I),M(I),M(I+1)
  continue
BETA=BET1/XPI
write(6,*) ' BETA = ',BETA
BETA=BETA*XPI
```

ORIGINAL PAGE IS
OF POOR QUALITY

```

X=Y/TAN(BETA)
X1=XL1*COS(THET1)
Y1=XL1*SIN(THET1)
BETA2=ATAN((Y-Y1)/(X-X1))-THET1
BETA2=BETA2/XPI
write(6,50) X,Y
format(10X,'X = ',F6.3,3X,'Y = ',F6.3)
write(6,60) BETA2,X1,Y1
format(10X,'BETA2=',F6.2,3X,'X1=',F6.3,3X,'Y1=',F6.3)
BETA2=BETA2*XPI
read(5,*)
A1=((2/TAN(BETA2)*(M2**2.*(SIN(BETA2))**2-1.)))
THET2=ATAN(A1/(M2**2.*(1.4+COS(2*BETA2))+2))
MNN2=M2*SIN(BETA2)
write(6,*) 'MNN2 = ',MNN2
MN3=SQRT((MNN2**2+5)/(7*MNN2**2-1))
M3=MN3/(SIN(BETA2-THET2))
P3=P2*(1+(2.8/2.4)*(MNN2**2-1))
PO3=P3*((1+0.2*M3**2))**3.5
THETT2=THET2/XPI
write(6,70) THETT2,MN3,M3
format(1X,'THET2 = ',F6.2,3X,'MN3 = ',F6.3,3X,'M3=',F6.3)
read(5,*)
X2=XL2*COS(THET2+THET1)
Y2=XL2*SIN(THET2+THET1)
write(6,61) X2,Y2
format(10X,'X2=',F6.3,3X,'Y2=',F6.3)
BETA3=ATAN((Y-Y1-Y2)/(X-X1-X2))-THET1-THET2
A2=((2/TAN(BETA3)*(M3**2.*(SIN(BETA3))**2-1.)))
THET3=ATAN(A2/(M3**2.*(1.4+COS(2*BETA3))+2))
MNN3=M3*SIN(BETA3)
MN4=SQRT((MNN3**2+5)/(7*MNN3**2-1))
M4=MN4/(SIN(BETA3-THET3))
P4=P3*(1+(2.8/2.4)*(MNN3**2-1))
PO4=P4*((1+0.2*M4**2))**3.5
THETT3=THET3/XPI

write(6,80) THETT3,MN4,M4
format(1X,'THET3 = ',F6.2,3X,'MN4 = ',F6.3,3X,'M4=',F6.3)
BETA3=BETA3/XPI
write(6,*) 'BETA3 = ',BETA3
BETA3=BETA3*XPI
read(5,*)
X3=XL3*COS(THET3+THET2+THET1)
Y3=XL3*SIN(THET3+THET1+THET2)
write(6,62) X3,Y3
format(10X,'X3=',F6.3,3X,'Y3=',F6.3)
BETA4=ATAN((Y-Y1-Y2-Y3)/(X-X1-X2-X3))-THET1-THET2-THET3
A3=((2/TAN(BETA4)*(M4**2.*(SIN(BETA4))**2-1.)))
THET4=ATAN(A3/(M4**2.*(1.4+COS(2*BETA4))+2))
MNN4=M4*SIN(BETA4)
MN5=SQRT((MNN4**2+5)/(7*MNN4**2-1))
M5=MN5/(SIN(BETA4-THET4))
P5=P4*(1+(2.8/2.4)*(MNN4**2-1))
PO5=P5*((1+0.2*M5**2))**3.5
THETT4=THET4/XPI
write(6,90) THETT4,MN5,M5
format(1X,'THET4 = ',F6.2,3X,'MN5 = ',F6.3,3X,'M5=',F6.3)
BETA4=BETA4/XPI
write(6,*) 'BETA4 = ',BETA4
BETA4=BETA4*XPI
read(5,*)
X4=XL4*COS(THET4+THET1+THET2+THET3)
Y4=XL4*SIN(THET4+THET1+THET2+THET3)
write(6,63) X4,Y4

```

ORIGINAL PAGE IS
OF POOR QUALITY

```

10 format(10X, 'X4=',F6.3,3X, 'Y4=',F6.3)
BETA5=ATAN((Y-Y1-Y2-Y3-Y4)/(X-X1-X2-X3-X4))
BETA5=BETA5-THET1-THET2-THET3-THET4
A4=((2/TAN(BETA5))*(M5**2.*(SIN(BETA5))**2-1.)))
THET5=ATAN(A4/(M5**2.*(1.4+COS(2*BETA5))+2))
MNN5=M5*SIN(BETA5)
MN6=SQRT((MNN5**2+5)/(7*MNN5**2-1))
M6=MN6/(SIN(BETA5-THET5))
P6=P5*(1+(2.8/2.4)*(MNN5**2-1))
PQ6=P6*((1+0.2*M6**2))**3.5
THETT5=THET5/XPI
write(6,91) THETT5,MN6,M6
format(1X, 'THET5 = ',F6.2,3X, 'MN6 = ',F6.3,3X, 'M6=',F6.3)
BETA5=BETA5/XPI
write(6,*) ' BETA5 = ',BETA5
BETA5=BETA5*XPI
TOTPD=PQ6/P01
PD=P6/P1
write(6,*) ' THE TOTAL PRESSURE DRPUT QBLIQ1.FOROP IS ',TOTPD
write(6,*) ' THE PRESSURE RISE IS ',PD
read(5,*)
stop
end

```


MACH # 4

```
program INLETLLENGTH
dimension M,BET,THET
real M1,MN1,M2,MN2,M3,MN3,M4,MN4,M5,MN5,M6,MN6,M7,MN7,MNN2
real MNN3,MNN4,MNN5,MNN6,MNN7
XPI=3.141593/180.
write(6,*) ' ENTER THE VALUES FOR THETA1 AND M1 '
read(5,*) THETA,M1
write(6,*) 'ENTER THE VALUE OF Y AND L1-L5 '
read(5,*) Y,XL1,XL2,XL3,XL4,XL5
M1=3.0
THETA=8.00
Y=3.5
XL1=7.081008
XL2=2.04934137
L3=1.70362
L4=1.10302
XL3=1.09605
XL4=1.10302
P1=1.0
BETA=THETA+3.
THET1=THETA*XPI
BET1=BETA*XPI
TT=TAN(THET1)/2.
TB=0.
if(ABS(TT-TB).lt..00001) goto 20
BET1=BET1+(TT-TB)*1.7
A=(M1**2*(1.4+COS(2.*BET1))+2.)*TAN(BET1)
XXX=(SIN(BET1))**2
TB=(M1**2*((SIN(BET1))**2)-1.)/A
goto 10

write(6,*) 'BET1 = ',BET1
MN1=M1*SIN(BET1)
write(6,*) 'MN1 = ',MN1
MN2=SQRT((MN1**2+5)/(7*MN1**2-1))
write(6,*) ' MN2 = ',MN2
write(6,*) BET1,THET1
M2=MN2/(SIN(BET1-THET1))
P2=P1*(1+(2.8/2.4)*(MN1**2-1))
P01=P1*((1+0.2*M1**2))**3.5
P02=P2*((1+0.2*M2**2))**3.5
write(6,*) M2
continue
BETA=BET1/XPI
write(6,*) ' BETA = ',BETA
BETA=BETA*XPI
X=Y/TAN(BETA)
X1=XL1*COS(THET1)
Y1=XL1*SIN(THET1)
BETA2=ATAN((Y-Y1)/(X-X1))-THET1
BETA2=BETA2/XPI
write(6,50) X,Y
format(10X,'X = ',F6.3,3X,'Y = ',F6.3)
write(6,60) BETA2,X1,Y1
format(10X,'BETA2=',F6.2,3X,'X1=',F6.3,3X,'Y1=',F6.3)
BETA2=BETA2*XPI
read(5,*)
A1=((2/TAN(BETA2)*(M2**2.*(SIN(BETA2))**2-1.)))
THET2=ATAN(A1/(M2**2.*(1.4+COS(2*BETA2))+2))
MNN3=M1*SIN(THET2)
```

```

MNN2=SQRT((MNN2**2+5)/(7*MNN2**2-1))
M3=MNN2/(SIN(BETA2-THET2))
P3=P2*(1+(2.8/2.4)*(MNN2**2-1))
PO3=P3*((1+0.2*M3**2)**3.5)
THETT2=THET2/XPI
write(6,70) THETT2,MN3,M3
format(1X,'THET2 = ',F6.2,3X,'MN3 = ',F6.3,3X,'M3= ',F6.3)
read(5,*)
X2=XL2*COS(THET2+THET1)
Y2=XL2*SIN(THET2+THET1)
write(6,61) X2,Y2
format(10X,'X2= ',F6.3,3X,'Y2= ',F6.3)
BETA3=ATAN((Y-Y1-Y2)/(X-X1-X2))-THET1-THET2
A2=((2/TAN(BETA3))*(M3**2*(SIN(BETA3)**2-1.)))
THET3=ATAN(A2/(M3**2*(1.4+COS(2*BETA3))+2))
MNN3=M3*SIN(BETA3)
MN4=SQRT((MNN3**2+5)/(7*MNN3**2-1))
M4=MN4/(SIN(BETA3-THET3))
P4=P3*(1+(2.8/2.4)*(MNN3**2-1))
PO4=P4*((1+0.2*M4**2)**3.5)
THETT3=THET3/XPI

write(6,80) THETT3,MN4,M4
format(1X,'THET3 = ',F6.2,3X,'MN4 = ',F6.3,3X,'M4= ',F6.3)
BETA3=BETA3/XPI
write(6,*) ' BETA3 = ',BETA3
BETA3=BETA3*XPI
read(5,*)
TOTPD=PO4/PO1
PD=P4/P1
write(6,*) ' THE TOTAL PRESSURE DROP IS ',TOTPD
write(6,*) ' THE PRESSURE RISE IS ',PD
read(5,*)
stop
end

```

MACH # 3 AND MACH # 2

```
program INLETLLENGTH
dimension M,BET,THET
real M1,MN1,M2,MN2,M3,MN3,M4,MN4,M5,MN5,M6,MN6,M7,MN7,MNN2
real MNN3,MNN4,MNN5,MNN6,MNN7
XPI=3.141593/180.
write(6,*) ' ENTER THE VALUES FOR THETA1 AND M1'
read(5,*) THETA,M1
write(6,*) 'ENTER THE VALUE OF Y AND L1-L5 '
read(5,*) Y,XL1,XL2,XL3,XL4,XL5
M1=3.0
THETA=8.00
Y=3.5
```

```
FOR MACH # 3
XL1=6.0
```

```
FOR MACH 2
XL1=3.0
XL1=9.13034937
XL2=2.04934137
L3=1.70362
L4=1.10302
XL3=1.09605
XL4=1.10302
P1=1.0
BETA=THETA+3.
THET1=THETA*XPI
BET1=BETA*XPI
TT=TAN(THET1)/2.
TB=0.
if(ABS(TT-TB).lt..00001) goto 20
BET1=BET1+(TT-TB)*1.7
A=(M1**2*(1.4+COS(2.*BET1))+2.)*TAN(BET1)
XXX=(SIN(BET1))**2
TB=(M1**2*((SIN(BET1))**2)-1.)/A
goto 10
```

```
write(6,*) 'BET1 =',BET1
MN1=M1*SIN(BET1)
write(6,*) 'MN1 = ',MN1
MN2=SQRT((MN1**2+5)/(7*MN1**2-1))
write(6,*) ' MN2 =',MN2
write(6,*) BET1,THET1
M2=MN2/(SIN(BET1-THET1))
P2=P1*(1+(2.8/2.4)*(MN1**2-1))
P01=P1*((1+0.2*M1**2))**3.5
P02=P2*((1+0.2*M2**2))**3.5
write(6,*) M2
continue
BETA=BET1/XPI
write(6,*) ' BETA = ',BETA
BETA=BETA*XPI
X=Y/TAN(BETA)
X1=XL1*COS(THET1)
Y1=XL1*SIN(THET1)
BETA2=ATAN((Y-Y1)/(X-X1))-THET1
BETA2=BETA2/XPI
write(6,50) X,Y
```

```

format(10X,'X1=',F6.3,3X,'Y1=',F6.3)
write(6,60) BETA2,X1,Y1
format(10X,'BETA2=',F6.2,3X,'X1=',F6.3,3X,'Y1=',F6.3)
BETA2=BETA2*XPI
read(5,*)
A1=((2/TAN(BETA2))*(M2**2.*(SIN(BETA2))**2-1.)))
THET2=ATAN(A1/(M2**2.*(1.4+COS(2*BETA2))+2))
MNN2=M2*SIN(BETA2)
write(6,*) ' MNN2 = ',MNN2
MN3=SQRT((MNN2**2+5)/(7*MNN2**2-1))
M3=MN3/(SIN(BETA2-THET2))
P3=P2*(1+(2.8/2.4)*(MNN2**2-1))
P03=P3*((1+0.2*M3**2))**3.5
THETT2=THET2/XPI
write(6,70) THETT2,MN3,M3
format(1X,'THET2 = ',F6.2,3X,'MN3 = ',F6.3,3X,'M3=',F6.3)
read(5,*)
TOTPD=P03/P01
PD=P3/P1
write(6,*) ' THE TOTAL PRESSURE DROP IS ',TOTPD
write(6,*) ' THE PRESSURE RISE IS ',PD
read(5,*)
stop
end

```

Appendix

D

```

Pba1 LAMBD,MHU,N,MACHI,LAEF,LEF
RHOIN=0.000032114
RHOAT=0.002367
VELIN=9813.2
RADN=0.5
LAMBD=69.53
ALPHA=0.0
ANOFA=0.0
MHU=0.0000093
N=0.00
MACHI=10.0
BETA=0.0
RADLE=0.02083
EMISS=0.89
STEFB=.000000001714
GAMMA=1.34
TNOT=7538.2
HOLAM= 0.1055*(RHOIN/RHOAT)**.5*(VELIN/10**4)**1.16
HOTUR=0.437*(RHOIN/RHOAT)**.78*(VELIN/10**4)**1.54
HNOSE=HOLAM/RADN**.5
LAEF=SIN(LAMBD)*COS(ALPHA)
LEF=ASIN(LAEF)
PF1=(1.33*MACHI**2+2.5)*((COS(LEF))**2+0.0019)
PF2=1.33*(MACHI*(COS(LEF)))**2+1
PF=PF2/PF1
HL1=HOLAM*(PF/RADLE)**.5
HL2=0.72*(COS(LEF))**1.15+.04*SIN(LEF)
HLSTAG=HL1*HL2
dø 10 J0=1,106
    XX=J0/2.0
    XDIS=J0*1.0
    RN=RHOIN*VELIN*XDIS/MHU
    if (RN.lt.3.5E5) then
        HLAM1=HOLAM*(PF*(1+2*N)/(3.*XDIS))**.5
        HLAM2=1.75*SIN(BETA)-.86*((SIN(BETA))**2)
        HLAM3=0.036/((MACHI*SIN(BETA))**2+1.0)
        HLAM=HLAM1*(HLAM2+HLAM3)
        UE=VELIN*SIN(LEF)
        TAW=TNOT-(1-.15)*UE**2/12012.0
        goto 20
    endif
    HTURB1=HOTUR*(XDIS/10.0)**(-2.0)*((1.0+1.25*N)/(2.25*XDIS))**0.2
    HTURB2=PF**0.8*(2.9*(SIN(1.5*BETA))-1.6*((SIN(BETA))**0.3))
    HTURB3=0.02/((MACHI*SIN(BETA))**2+1.0)
    HTURB=HTURB1*(HTURB2+HTURB3)
    TAW=TNOT-0.1*VELIN**2*((SIN(LEF))**2)/12012.0
    HWU=HTURB
    goto 80
    HWU=HLAM
    do 90 J=1,1E4,10
        TT=J*1.0
        A=TT**4+HWU*TT/(EMISS*STEFB)
        B=HWU*TAW/(EMISS*STEFB)
        AB=A-B
        if (AB.gt.1.0E-6) then
            goto 110
        endif
        if (AB.lt.-1.0E-6) then
            TT=TT+10.0
            goto 111
        endif
        goto 40
    continue
    write (6,100) HWU,TT*20,XDIS/2

```

ORIGINAL PAGE IS
OF POOR QUALITY

144-A

Appendix

E

LIST OF ENERGY STATE FORTRAN PROGRAMS
Bob Stonebraker

PROGRAM HECONST - Computes lines of constant He (ft.).

PROGRAM FSCNST - Computes contours of constant Fs (ft./lb.)
for phase 1 of the mission.

PROGRAM FSCNST2 - Computes contours of constant Fs (ft./lb.)
for Phase 2 of the mission.

PROGRAM PHASE1 - Computes fuel consumption, elapsed time and
range for Phase 1.

PROGRAM PHASE2 - Computes fuel consumption, elapsed time and
range for Phase 2.

SUBROUTINE ATMOSFR (ALT,T,RO,P) - Computes standard atmospheric
variables as a function of altitude.

SUBROUTINE TFRMJT (M,ALT,FN,SFC) - Computes net thrust and sfc
from given data as a function of Mach number
and altitude. (based on economic sfc)

SUBROUTINE SCRMJT (M,ALT,FN,SFC) - Computes net thrust and sfc
from given data as a function of Mach number
and altitude. (based on equivalent fuel/air
ratio of 0.8)

SUBROUTINE DRAG (M,ALT,D) - Computes drag from given data as a
function of Mach number and altitude.

SUBROUTINE SPLINE (X,F,XF,FN,N) - Interpolates between points
(X,F) for point (XF,FN).


```

      PROGRAM HECONST
C      ROBERT STONEBRAKER
C      COMPUTES VALUES OF CONSTANT He (ft.)
      IMPLICIT REAL(A-H,O-Z)
      REAL M
      OPEN(5,FILE='HECONST.DAT')
      R=1715.621
      G=32.1578
      HE=2.E4
      DO 200 I=1,10
      HG=0.
100  CALL ATMOSFR(HG,T,RO,P)
      M=SQRT((HE-HG)*2.*G/(1.4*R*T))
      WRITE(5,*) M,HG,HE
      WRITE(*,*) M,HG,HE
      HG=HG+4000.
      IF(HG.GT.110000.) GOTO 200
      IF(HG.LT.HE) GOTO 100
200  HE=HE+2.0E4
      CONTINUE
      STOP
      END

```

```

C      PROGRAM FSCONST
C      ROBERT STONEBRAKER
C      COMPUTES VALUES OF CONSTANT  $F_s$  (ft/lb) OVER PHASE 1
C      WITH NET THRUST, SFC, AND DRAG AS FUNCTIONS OF
C      ALTITUDE AND MACH NO.
C
      IMPLICIT REAL(A-H,O-Z)
      REAL M
      OPEN(5,FILE='FSCONST.DAT')
      WRITE(*,*) 'ENTER INITIAL VEHICLE WIEGHT IN LBS.'
      READ(*,*) W
      M=.8
      R=1715.621
C      MACH NO. LOOP
      DO 100 I=1,27
      ALT=40000.
C      ALTITUDE LOOP
      DO 200 J=1,30
      CALL ATMOSFR(ALT,T,RO,P)
      A=3600*SQRT(1.4*R*T)
C
      CALL TFRMJT(ALT,M,FN,SFC)
      IF(FN.EQ.0.) GOTO 200
      IF(SFC.EQ.0.) GOTO 200
C
      CALL DRAG(ALT,M,D)

      FS=M*A*(FN-D)/(FN*SFC*W)
      IF(FS.LT.0.) THEN
        FS=0.
      ENDIF
      WRITE(*,10) M,ALT,FN,D,SFC,FS
10  FORMAT(F5.2,3X,F8.1,3X,F10.1,3X,F10.1,3X,F6.3,3X,F7.1)
      WRITE(5,20) M,ALT,FS
20  FORMAT(F5.2,3X,F8.0,3X,F7.1)
200 ALT=ALT+2000.
      W=W-100.
100 M=M+.200000
      STOP
      END

```

```

C      PROGRAM FSCNST2
C      ROBERT STONEBRAKER
C      COMPUTES VALUES OF CONSTANT Fs (ft/lb) OVER PHASE 2
C      WITH NET THRUST, SFC, AND DRAG AS FUNCTIONS OF
C      ALTITUDE AND MACH NO.
C
C      IMPLICIT REAL(A-H,O-Z)
C      REAL M
C      OPEN(5,FILE='FSCNST2.DAT')
C      WRITE(*,*) 'ENTER INITIAL VEHICLE WIEGHT IN LBS.'
C      READ(*,*) W
C      M=6.
C      R=1715.621
C      MACH NO. LOOP
C      DO 100 I=1,41
C      ALT=70000.
C      ALTITUDE LOOP
C      DO 200 J=1,16
C      SPEED OF SOUND (ft/sec)
C      CALL ATMOSFR(ALT,T,RO,P)
C      A=SQRT(1.4*R*T)
C      Q=.5*RO*1.4*R*T*M**2
C      IF(Q.GE.1800) THEN
C      FS=0
C      GOTO 300
C      ENDIF
C
C      CALL SCRMJT(ALT,M,FN,SFC)
C      FN=4*FN
C      SFC=SFC/3600
C      IF(FN.EQ.0.) GOTO 200
C
C      CALL DRAG(ALT,M,D)
C
C      FS=M*A*(FN-D)/(FN*SFC*W)
C      WRITE(*,10) M,ALT,FN,D,SFC,FS
C      10 FORMAT(F4.1,3X,F7.0,3X,F10.1,3X,F10.1,3X,F9.6,3X,E12.5)
C      300 WRITE(5,20) M,ALT,FS
C      20 FORMAT(F4.1,3X,F7.0,3X,F12.3)
C      200 ALT=ALT+2000.
C      W=W-147.
C      100 M=M+.10
C      STOP
C      END

```

```

PROGRAM PHASE1
C  ROBERT STONEBRAKER
C  COMPUTES THE FUEL CONSUMED ALONG PREDETERMINED FLIGHT PATH
C  FROM (M=.8 AT 40,000' TO M=6 AT 76,000')
IMPLICIT REAL(A-H,O-Z)
REAL M
OPEN(5,FILE='PHASE1.DAT')
OPEN(6,FILE='PHASE11.DAT')
WRITE(*,*) 'ENTER INITIAL VEHICLE WEIGHT'
READ(*,*) W
WRITE(*,*) 'ENTER MACH NO. STEP SIZE'
READ(*,*) DM
R=1715.621
G=32.1578
M=.8
HG=40000.
HGO=40000.
A=968.1
C  COMPUTE INITIAL HE AND F=1/FS AT M=.8 AND ALT(HG)=40000
HE1=49326.186
CALL TFRMJT(HG,M,FN,SFC)
SFC=SFC/3600.
CALL DRAG(HG,M,D)
P1=W/(M*A*(FN-D))
F1=FN*SFC*P1
C
N=5.2/DM+1
DO 100 I=1,N
M=M+DM
CALL FLTPTH(M,HG)
CALL ATMOSFR(HG,T,RO,P)
CALL TFRMJT(HG,M,FN,SFC)
CALL DRAG(HG,M,D)
SFC=SFC/3600.
A=SQRT(1.4*R*T)
HE2=HG+.5*(1.4*R*T*M**2)/G
TR=FN-D
IF(TR.EQ.0) GOTO 100
P2=W/(M*A*(FN-D))
F2=FN*SFC*P2
DTIME=(HE2-HE1)*.5*(P2+P1)
DFUEL=(HE2-HE1)*.5*(F2+F1)
W=W-DFUEL
TIME=TIME+DTIME
ACC=DM/(M*DTIME)
RNG=RNG+SQRT((M*A*DTIME)**2-(HG-HGO)**2)/5280.
HGO=HG
FUEL=FUEL+DFUEL
ELT=TIME/60
WRITE(*,10) ELT,RNG,M,HG,FN,D,W
WRITE(5,10) ELT,RNG,M,HG,FN,D,W
10FORMAT(F7.3,2X,F8.1,2X,F6.2,2X,F8.0,2X,F8.0,2X,F8.0,2X,F8.0)
WRITE(6,20) RNG,M,HG,ACC,FUEL
20 FORMAT(F8.1,2X,F6.2,2X,F8.0,2X,F7.4,2X,F7.0)

```

```
HE1=HE2
P1=P2
100 F1=F2
TIME=TIME/60
WRITE(*,*) 'M =',M,' ALT =',HG,'ft.'
WRITE(*,*) 'T =',TIME,'min. W fuel =',FUEL,'lbs.'
```

```

PROGRAM PHASE2
C  ROBERT STONEBRAKER
C  COMPUTES FUEL CONSUMED ALONG PREDETERMINED FLIGHT PATH
C  FROM (M=6 AT 76,000' TO M=10 AT 100,000')
  IMPLICIT REAL (A-H,O-Z)
  REAL M
  OPEN(5,FILE='PHASE2.DAT')
  OPEN(6,FILE='PHASE22.DAT')
  WRITE(*,*) 'ENTER INITIAL VEHICLE WEIGHT'
  READ(*,*) W
  WRITE(*,*) 'ENTER MACH NO. STEP SIZE'
  READ(*,*) DM
  WRITE(*,*) 'ENTER NO. OF SCRAMJETS'
  READ(*,*) K
  R=1715.621
  G=32.1578
  M=6
  HG=75835.
  HGO=75835.
  A=968.1
C  COMPUTE INITIAL HE AND F=1/FS AT M=6
  HE1=600433.
  CALL SCRMJT(HG,M,FN,SFC)
  FN=K*FN
  SFC=SFC/3600.
  CALL DRAG(HG,M,D)
  P1=W/(M*A*(FN-D))
  F1=FN*SFC*P1
C
  N=4./DM+30
  DO 100 I=1,N
    M=M+DM
C
C  FLIGHT PATH ALONG Q=1800
  IF(M.GE.10.) THEN
    M=10.
    HG=HG+300.
    IF(HG.GE.100000.) GOTO 500
    GOTO 50
  ENDIF
  HG=-7.35005*M**4+262.753*M**3-3749.61*M**2+29936.5*M-16027.
C
50  CALL ATMOSFR(HG,T,RO,P)
  CALL SCRMJT(HG,M,FN,SFC)
  FN=K*FN
  SFC=SFC/3600.
  CALL DRAG(HG,M,D)
  A=SQRT(1.4*R*T)
  HE2=HG+.5*(1.4*R*T*M**2)/G
  TR=FN-D
  IF(TR.EQ.0) GOTO 100
  P2=W/(M*A*(FN-D))
  F2=FN*SFC*P2
  DTIME=(HE2-HE1)*.5*(P2+P1)

```

```

DFUEL=(HE2-HE1)*.5*(F2+F1)
W=W-DFUEL
TIME=TIME+DTIME
ACC=DM/(M*DTIME)
RNG=RNG+SQRT((M*A*DTIME)**2-(HG-HGO)**2)/5280.
HGO=HG
ELT=TIME/60
FUEL=FUEL+DFUEL
WRITE(*,10) ELT,RNG,M,HG,FN,D,W
WRITE(5,10) ELT,RNG,M,HG,FN,D,W
10FORMAT(F7.3,2X,F8.1,2X,F6.2,2X,F8.0,2X,F8.0,2X,F8.0,2X,F8.0)
WRITE(6,20) RNG,M,HG,ACC,FUEL
20 FORMAT(F7.3,2X,F6.2,2X,F8.0,2X,F7.4,2X,F7.0)
HE1=HE2
P1=P2
100 F1=F2
500 WRITE(*,*) 'FUEL =',FUEL
STOP
END

```

```

SUBROUTINE ATMOSFR(HG,T,RO,P)
C   ROBERT STONEBRAKER
C   COMPUTES TEMPERATURE, DENSITY, AND PRESSURE GIVEN A
C   GEOMETRIC ALTITUDE HG.
  IMPLICIT REAL(A-H,O-Z)
  RE=2.086466E7
  H=HG*RE/(RE+HG)
C
  IF(H.LT.36000.) THEN
    H0=0.
    T0=518.69
    RO0=2.3769E-3
    P0=2116.2
    A=-3.56627E-3
    T=TEMP(T0,A,H,H0)
    RO=ROSLOP(RO0,T,T0,A)
    P=PSLOP(P0,T,T0,A)
    GOTO 500
  ENDIF
C
  IF(H.LT.82000.) THEN
    H0=36000
    T=389.99
    RO0=7.0858E-4
    P0=474.7098
    RO=ROLNR(RO0,T,H,H0)
    P=PLNR(P0,T,H,H0)
    GOTO 500
  ENDIF
C
  IF(H.LT.154000.) THEN
    H0=82000
    T=389.99
    RO0=7.7664E-5
    P0=52.03
    A=1.64355E-3
    T=TEMP(T0,A,H,H0)
    RO=ROSLOP(RO0,T,T0,A)
    P=PSLOP(P0,T,T0,A)
    GOTO 500
  ENDIF
500 RETURN
END
C
FUNCTION TEMP(T0,A,H,H0)
  TEMP=T0+A*(H-H0)
  RETURN
END
FUNCTION ROSLOP(RO0,T,T0,A)
  ROSLOP=RO0*((T/T0)**(-(32.1578/(A*1715.621)+1.)))
  RETURN
END
FUNCTION PSLOP(P0,T,T0,A)
  PSLOP=P0*((T/T0)**(-32.1578/(A*1715.621)))

```



```
RETURN
END
FUNCTION ROLNR(ROO,T,H,H0)
ROLNR=ROO*EXP(-32.1578/(1715.621*T)*(H-H0))
RETURN
END
FUNCTION PLNR(P0,T,H,H0)
PLNR=P0*EXP(-32.1578/(1715.621*T)*(H-H0))
RETURN
END
```

```

SUBROUTINE TFRMJT(HG,M,FN,SFC)
C   ROBERT STONEBRAKER
C   COMPUTES THE NET THRUST AND SFC OF THE FULL SCALE
C   TURBOFAN-RAMJET AS A FUNCTION OF ALTITUDE AND MACH NO.
C   BASED ON CURVE FIT POLYNOMIALS AND NATURAL CUBIC SPLINES.
C
  IMPLICIT REAL (A-H,O-Z)
  REAL M
  DIMENSION HGA(15),FNA(15),SFCA(15)
C
  IF(M.LT.0.8) THEN
    FN=0
    SFC=0
    GOTO 500
  ENDIF
  IF(M.GT.6.0) THEN
    FN=0
    SFC=0
    GOTO 500
  ENDIF
C
  K=7
C *** 0.8 TO 3.5
  HGA(1)=40000
  FNA(1)=-2879.52*M**5+28051.4*M**4-101019.*M**3+172092.*M**2
  * -112116.*M+37378.7
  SFCA(1)=-.0430727*M**6+.570346*M**5-3.00762*M**4+8.02043*M**3
  * -11.2762*M**2+7.86021*M-1.40087
C
C *** 2.0 TO 4.5
  HGA(2)=50000
  FNA(2)=2569.33*M**3-15206.7*M**2+53954.5*M-37169.1
  IF(M.LE.3.5) THEN
    SFCA(2)=.0640001*M**3-.492*M**2+1.316*M-.424001
    GOTO 60
  ENDIF
  SFCA(2)=.034*M**2-.237*M+1.312
C
C *** 2.5 TO 6.0
  60 HGA(3)=60000
  FNA(3)=-905.152*M**4+14058.4*M**3-72866.3*M**2+174728.*M-139344.
  IF(M.LT.3.5) THEN
    SFCA(3)=.0880001*M**2-.422*M+1.299
    GOTO 70
  ENDIF
  SFCA(3)= -.0020003*M**3+.0522861*M**2-.28693*M+1.34922
C
C *** 3.0 TO 6.0
  70 HGA(4)=70000
  FNA(4)=-1287.11*M**4+22021.3*M**3-134968.*M**2+371824.*M-369131.

```

```

      SFCA(4)=.0103333*M**3-.130929*M**2+.613024*M-.1077
C
C *** 4.0 TO 6.0
      HGA(5)=80000
      FNA(5)=-2007.67*M**3+30631.5*M**2-137628.*M+212654.
      SFCA(5)=.00866667*M**3-.105*M**2+.486334*M+.0959986
C
C *** 4.0 TO 6.0
      HGA(6)=90000
      FNA(6)=-1233.33*M**3+18722.*M**2-83600.7*M+128444.
      SFCA(6)=.0076661*M**3-.0854991*M**2+.372829*M+.311008
C
C *** 4.0 TO 6.0
      HGA(7)=100000
      FNA(7)=-683.667*M**3+10277.5*M**2-44661.8*M+66948.
      SFCA(7)=.024*M**3-.320001*M**2+1.476*M-1.37301
C
      CALL SPLINE(HGA,FNA,HG, FN,K)
      IF(FN.LT.0.) THEN
        FN=0
      ENDIF
      CALL SPLINE(HGA,SFCA,HG,SFC,K)
      IF(SFC.LT.0.) THEN
        SFC=0
      ENDIF
500 RETURN
      END

```

```

SUBROUTINE SCRMJT(HG,M,FN,SFC)
C  ROBERT STONEBRAKER
C  COMPUTES FG(lbsf), FN(lbsf), ISP(sec), SFC(lbsm/lbsf/hr)
C  AS FUNCTION OF ALT. AND MACH NO.
C  CURVE FIT EQUATIONS BASED ON FUEL/AIR RATIO OF 0.8
  IMPLICIT REAL (A-H,O-Z)
  IMPLICIT REAL (M,I)
  DIMENSION MA(15),F(15)

C
  DATA MA(1),MA(2),MA(3)/5.0,7.5,10.0/
  N=3

C
C  *** FG ***
C    F(1)=-4.92613E-10*HG**3+1.45585E-4*HG**2-14.8904*HG+534062
C    F(2)=-4.91975E-10*HG**3+1.71206E-4*HG**2-20.4451*HG+845486
C    F(3)=-4.99582E-10*HG**3+1.95693E-4*HG**2-26.1568*HG+1201470
C    CALL SPLINE(MA,F,M,FG,N)
C
C  *** FN ***
C    F(1)=-1.61294E-10*HG**3+4.71692E-5*HG**2-4.77752*HG+169622
C    F(2)=-1.04412E-10*HG**3+3.57416E-5*HG**2-4.20399*HG+171214
C    F(3)=-4.13576E-11*HG**3+1.7587E-5*HG**2-2.52803*HG+123291
C    CALL SPLINE(MA,F,M,FN,N)
C
C  *** ISP ***
C
F(1)=-5.79888E-12*HG**3+1.19854E-6*HG**2-8.53466E-2*HG+5398.13
F(2)=-9.88777E-12*HG**3+2.55155E-6*HG**2-0.22344*HG+9142.38
F(3)=-7.61882E-12*HG**3+1.98524E-6*HG**2-0.174684*HG+7093.69
  CALL SPLINE(MA,F,M,ISP,N)
C
  SFC=3600./ISP
  RETURN
  END

```

```

SUBROUTINE DRAG(HG,M,D)
C   ROBERT STONEBRAKER
C   COMPUTES DRAG OF 515H VEHICLE DESIGN AS A FUNCTION OF
ALTITUDE
C   AND MACH NO. BASED ON CURVE FIT POLYNOMIALS OF GIVEN DATA.
IMPLICIT REAL(A-H,O-Z)
REAL M
DIMENSION HGAA(15),DA(15)
C
K=13
HGAA(1)=40000
DA(1)=981.718*M**2+10219.2*M-5885.21
HGAA(2)=45000
DA(2)=777.411*M**2+7952.26*M-4088.61
HGAA(3)=50000
DA(3)=617.958*M**2+6144.13*M-2528.24
HGAA(4)=55000
DA(4)=494.109*M**2+4690.13*M-1114.06
HGAA(5)=60000
DA(5)=398.678*M**2+3505.97*M+235.57
HGAA(6)=65000
DA(6)=326.16*M**2+2523.4*M+1598.03
HGAA(7)=70000
DA(7)=272.36*M**2+1685.99*M+3051.45
HGAA(8)=75000
DA(8)=234.18*M**2+945.452*M+4678.9
HGAA(9)=80000
DA(9)=209.415*M**2+259.422*M+6572
HGAA(10)=85000
DA(10)=196.64*M**2-409.555*M+8834.34
C   **NOTE**LAST THREE EQUATIONS ARE NOT VALID FOR M < 4
IF(M.LT.4.0) THEN
K=10
GOTO 500
ENDIF
HGAA(11)=90000
DA(11)=-59.1967*M**3+1483.62*M**2-10103.1*M+31674.9
HGAA(12)=95000
DA(12)=-69.7467*M**3+1732.75*M**2-12589.8*M+39067.1
HGAA(13)=100000
DA(13)=-83.6275*M**3+2064.89*M**2-15665.8*M+48294.5
C
500 CALL SPLINE(HGAA,DA,HG,D,K)
D=1.1*D
RETURN
END

```

```

SUBROUTINE SPLINE(X,F,XN,FX,N)
C   ROBERT STONEBRAKER 4/10/90
C   COMPUTES VALUES OF AN UNKNOWN FUNCTION FROM UNEVENLY SPACED
C   DATA USING A NATURAL CUBIC SPLINE.
      IMPLICIT REAL (A-H,O-Z)
      DIMENSION X(15),F(15),A(15),B(15),C(15),G(15),R(15)
C
C   DETERMINES WHICH INTERVAL OF THE DOMAIN HOLDS X
      DO 100 I=2,N
        IF(XN.LE.X(I)) THEN
          J=I-1
          GOTO 200
        ENDIF
      100 CONTINUE
C
C   DEFINES MATRIX COEFFICIENTS
      200 DO 300 I=1,N
        DELX=X(I+1)-X(I)
        A(I)=(X(I)-X(I-1))/DELX
        B(I)=2*(X(I+1)-X(I-1))/DELX
        C(I)=1
        R(I)=6*(F(I+1)-F(I))/(DELX**2)
        *-6*(F(I)-F(I-1))/(DELX*(X(I)-X(I-1)))
      300 CONTINUE
        A(1)=0.
        C(N)=0.
C
C   THOMAS ALGORITHM FOR G(i)
      DO 400 I=2,N
        FACTOR=A(I)/B(I-1)
        B(I)=B(I)-FACTOR*C(I-1)
      400 R(I)=R(I)-FACTOR*R(I-1)
        G(N)=R(N)/B(N)
        DO 500 I=2,N
          NI=N-I+1
      500 G(NI)=(R(NI)-C(NI)*G(NI+1))/B(NI)
        G(1)=0.
        G(N)=0.
C
C   DELX=X(J+1)-X(J)
      FX=G(J)*(((X(J+1)-XN)**3)/DELX-DELX*(X(J+1)-XN))/6
      *+G(J+1)*(((XN-X(J))**3)/DELX-DELX*(XN-X(J)))/6
      *+F(J)*(X(J+1)-XN)/DELX+F(J+1)*(XN-X(J))/DELX
C
      RETURN
      END

```